NASA CR-66253

IITRI Project No. G6006

CHARACTERIZATION OF CERAMIC MATERIALS FOR MICROELECTRONIC APPLICATIONS

National Aeronautics
and Space Administration
Langley Research Center
Hampton, Virginia 23365

NASA CR-66253

IIT RESEARCH INSTITUTE
10 West 35th Street
Chicago, Illinois 60616

Contract No. NAS1-4870
IITRI Project No. G6006

CHARACTERIZATION OF CERAMIC MATERIALS FOR MICROELECTRONIC APPLICATIONS

IITRI G6006-12
Summary Report No. 1
for the period
November 23, 1965 to November 23, 1966

Prepared by

A. J. Mountvala

Prepared for

National Aeronautics and Space Administration
Langley Research Center
Hampton, Virginia 23365

November 23, 1966

CHARACTERIZATION OF CERAMIC MATERIALS FOR MICROELECTRONIC APPLICATIONS

ABSTRACT

The methods for characterizing ceramic materials for microelectronic applications have been considered. The two methods recommended have been identified as "direct" and "mechanistic" and although they differ in their approach, they are interrelated in devising a meaningful characterization.

The major emphasis in this investigation has been on the characterization of $BaTiO_3$ ceramics. Work has been done to understand the intrarelationship between the dielectric behavior of the boundary phase and the bulk phase as a function of microstructure. Both grain size and stoichiometry are significant parameters that effect the dielectric properties of polycrystalline $BaTiO_3$. However, the concentration and distribution of the various types of defects and secondary phases may vary differently in the bulk of the grain and along grain boundaries and, therefore, grain size and stoichiometry effects must be considered relative to each other. In addition, we have theoretically estimated the effect of a grain size dependent dielectric constant of the boundary phase on the effective dielectric constant of the $BaTiO_3$ ceramic. A model has been proposed to support the experimental evidence for a high resistivity surface layer on $BaTiO_3$ grains. The major experimental work has been on the change in the dielectric behavior of $BaTiO_3$ during the controlled conversion of compacted high-purity powders to increasingly densified and bonded ceramics. The frequency dispersions of the dielectric constant, loss tangent, and conductivity have been obtained and relaxation time constants evaluated. The experimental data indicates different high frequency and low frequency relaxation processes characteristic of the microstructure of the ceramic material. The effects of adsorbed water on the dielectric properties of $BaTiO_3$ and possible surface layer mechanisms have been evaluated. The characterization of the bulk and

boundary phase properties has been attempted in terms of an equivalent circuit. The circuit consists of a capacitance and parallel resistance representing the bulk of the grain, in series with a capacitance and parallel resistance representing the boundary phase. This can be modified by a frequency dependent shunt resistance to account for adsorbed surface layer properties due to exposures to specific atmospheres.

CONTENTS

ILLUSTRATIONS

ILLUSTRATIONS (cont'd)

ILLUSTRATIONS (cont'd)

TABLES

CHARACTERIZATION OF CERAMIC MATERIALS FOR MICROELECTRONIC APPLICATIONS

I. SUMMARY

The major emphasis in this investigation has been on the characterization of $BaTiO_3$ ceramics for microelectronic applications. A phenomenological approach has been used correlating over bulk and boundary phase properties.

To be able to effectively characterize $BaTiO_3$ ceramics for microelectronic applications, it is mandatory to understand the intrarelationship between the dielectric behavior of the boundary phase and the bulk phase as a function of microstructure. Both grain size and stoichiometry are significant parameters that effect the dielectric properties of polycrystalline $BaTiO_3$. However, the concentration and distribution of the various types of defects vary differently in the bulk of the grain and along grain boundaries and, therefore, grain size and stoichiometry effects must be considered relative to each other.

We have attempted to estimate, theoretically, the effect of a grain size dependent dielectric constant of the boundary phase on the effective dielectric constant of a dense, pore-free $BaTiO_3$ ceramic on the basis of a modified Bruggeman equation.

A model has been formulated to support the experimental evidence for a high resistivity surface layer on $BaTiO_3$ grains. The essential features of this model are that the cation vacancies created by the process of cationic migration to the surface represent acceptor states which may trap electrons from energy levels above the trap state. This would drastically reduce the number of available electrons and the resistivity of the depletion layer would rise by several orders of magnitude.

An equivalent circuit has been used to characterize polycrystalline $BaTiO_3$. The circuit consists of a capacitance and parallel resistance representing the bulk of the grain, in series with a capacitance and parallel resistance representing the boundary

layer. The major experimental emphasis, to date, in our work, has been on the manner in which the properties of high-purity $BaTiO_3$ powders are related to those of the fired ceramic. The change in the dielectric behavior as a function of frequency, temperature, and environment have been measured during the controlled conversion of the compacted powders to increasingly densified and bonded ceramics.

Results obtained on porous cold-compacted samples, stored and evaluated in vacuum, indicate that water vapor from exposure to atmosphere can significantly increase the ac conductivity of $BaTiO_3$ by adsorption of $(OH)^-$ molecules. No such significant effect was observed with dense, fired, ceramic material. The observed surface effect on porous material is critical to the fabrication of such bodies. This effect should be differentiated from the high resistivity barrier layer on $BaTiO_3$ ceramics which is intrinsic to the material.

The experimental data indicates different high frequency and low frequency relaxation processes, characteristic of the microstructure of the ceramic material.

Further experimental results will substantiate the extent to which $BaTiO_3$ ceramics can be characterized by an equivalent circuit model and the manner in which such a circuit is altered by microstructural and environmental effects.

On the basis of the work done, it is possible to answer in the affirmative that $BaTiO_3$ ceramics can be effectively characterized for microelectronic applications. It has been demonstrated that by evaluation of selected dielectric properties meaningful information can be obtained to characterize the material in terms of an equivalent circuit, representing the properties of the bulk grain, boundary phases, and other types of surface phenomena, such as adsorbed layer effects.

II. INTRODUCTION

Technical ceramics, unlike a number of other areas which have developed into sound scientific groupings, is still somewhat empirical. The ceramist could say that it is so because nature has made ceramic materials particularly hard to understand and inordinately complex for simple theory; and while the physicist often works with high-purity single crystals, the ceramist must work with multicrystalline, polyphase materials, and select for high purity and stoichiometry. However, the fact that ceramic materials cannot be prepared, as yet, with the high degree of purity of elemental materials does not preclude their scientific development. We shall see that there are other significant parameters such as stoichiometry and grain boundary-to-grain phase distributions that play a critical role in the understanding of ceramic materials.

The question that comes to mind next is what to do with the extremely large, potentially usable area of polycrystalline ceramics. Are single crystals the only recourse for electronic use, or is there a methodical, logical attack on the vagaries of polycrystalline materials? An electronic engineer in semiconductor work can specify, for example, that he wants a single crystal of silicon; knowing its direction of growth and cut and its resistivity, he can, from application of p-n junction phenomena, effectively design this crystal into a usable device. This, unfortunately, is not possible with polycrystalline materials.

How, then, can one go from this stage of reliability of a single crystal to an area of unknowns in polycrystalline ceramics? The key approach to the solution is characterization.

The current program is aimed specifically at a meaningful characterization of barium titanate ceramics, which have significant applications in microelectronics. The interest in barium titanate and similar perovskite type structures stems from their high dielectric

constants, as well as, in some cases, from their piezoelectric properties. Since the dielectric behavior of dense, polycrystalline $BaTiO_3$ depends on its electrical properties as well as on the topotactical arrangement of both the bulk phase and the grain boundary phase, it is necessary to investigate the nature and distribution of these phases.

In the current program, on the experimental characterization of $BaTiO_3$ ceramics, the properties of the surface layer on $BaTiO_3$ grains have been studied by evaluating the frequency dispersion of the conductivity and dielectric losses. An equivalent circuit model has been used to represent the barium titanate grains carrying a surface layer. The circuit essentially consists of a capacitance and parallel resistance representing the bulk of the grain, in series with a capacitance and parallel resistance representing the surface and/or boundary layer. Other surface effects, such as adsorbed layers in specific atmospheres, would, of course, tend to modify this simple equivalent circuit. The characterization of ceramic materials for microelectronic applications, by way of an equivalent circuit, is useful as it can be translated for designing electronic devices.

In the case of single crystal silicon, characterization made the significant difference in its application for semiconductor devices. However, the complex nature of ceramic materials, as compared with silicon, makes characterization more difficult, but not impossible. Although impurities play an important role in the properties of ceramic materials, stoichiometry, in some instances, is much more significant. Undoubtedly, we would like to characterize ceramic materials that are free of all trace impurities. But, unlike in elemental semiconductor type materials, such as silicon, the purification of ceramics causes some problems. Because of the need for preparing high purity materials, a number of relatively novel methods have been used, such as plasma arc with induction coupling and the decomposition of organo - metallics. These methods do consistently produce fine particle powders of ceramic materials, but not necessarily of a better purity than some of the other

techniques. In fact, quite often small particle size refractory oxides have been obtained at the expense of stoichiometry. Even the removal of trace impurities by thermal and/or chemical techniques quite often causes problems in stoichiometry. Therefore, the requirements for high purity must be considered along with the significance of stoichiometry. The role of impurities will be evaluated by "finger-printing" the extent of the trace impurities and their effects on the dielectric behavior of $BaTiO_3$. Major emphasis has been placed on both stoichiometry and purity, in selecting the specially prepared materials to be investigated in this program. The purity level of these ceramics is an order of magnitude superior to what is commercially available for $BaTiO_3$ ceramics. Therefore, although it is not possible, at this stage, to work with $BaTiO_3$ ceramics comparable to the "ultra-high purity" silicon materials, the very significant improvements in purity, and the fact that we have been able to obtain $BaTiO_3$ powders of exact stoichiometry, justifies their use and makes the interpretation possible.

The overall objectives of this program make it mandatory to answer the following questions:

1. Is it possible to characterize a typical electronic ceramic, such as $BaTiO_3$, in terms that are meaningful for the applications?
2. If so, what methods and approaches provide the most effective characterization?

A phenomenological approach has been taken in characterizing polycrystalline ceramics, correlating the bulk properties and boundary phase properties. The physical behavior of ceramic materials can be described by the following functional relationship:

$$y_i = f\,(y_i^{SC},\ y_i^{GB})$$

where y_i is a certain property of the polycrystalline material, which depends on y_i^{SC}, the same property of the single crystal and

y_i^{GB}, the behavior of boundary phases with respect to property y_i. The averaging of single crystal and boundary phase properties, indicated by the functional sign f, is usually complex and frequently of semi-empirical nature, or derived under simplifying assumptions.

If two properties of the polycrystalline ceramic, y_1 and y_2, which cannot be expressed explicitly by an equation of the above type, are affected predominantly by one particular grain boundary process, a direct relationship exists between y_1 and y_2 which may be used to characterize the material with respect to y_1 or y_2. Such a characterization is useful if one of the properties is difficult to measure directly, while the other property can be evaluated with ease or determined accurately by some mechanistic approach.

The significant differences between the electronic properties of single-crystal and polycrystalline materials is undoubtedly due to the contribution of the presence of grain boundaries in the latter. The grain-boundary phase possesses a defect structure and usually has electrical properties different from those of the bulk phase. Therefore, in the characterization of $BaTiO_3$ ceramics, major emphasis has been placed in correlating the bulk properties with the surface or grain-boundary properties, taking into consideration the effects of grain size variation and deviations from stoichiometry.

A useful characterization of electronic ceramic materials such as $BaTiO_3$ must contain the answers to these questions:

1. What are the electrical properties of the boundary phase in polycrystalline ceramics and their relationship to grain size and pressure?
2. What are the properties of the surface defect layer of a powder particle, and how do they change with grain size, temperature, and oxygen partial pressure?

3. What is the correlation between the properties of the defect surface layer of the powder particles and the properties of the boundary phase in the ceramic?

III. THE CONCEPTS OF CHARACTERIZING POLYCRYSTALLINE MATERIALS

The research effort that has been expended in the study of ionic compounds is illustrated in Fig. 1. This chart indicates not only the particular areas that have been investigated, but also indicates, qualitatively, the amount of work carried out in a particular field.

The alkali halides have been studied for a long time, theoretically as well as experimentally. Single crystals of these compounds are easily obtained and, more important, one may assume that the bonding between the ions in the alkali halides is nearly 100% ionic. The Pauli principle, then, forbids appreciable electronic overlap, and a theoretical treatment on the basis of a Slater determinant formed from Bloch functions can be applied. Single crystals of the high-melting oxides, in sizes and of a chemical purity as required for physical property measurements, became available only recently. Furthermore, the oxides constitute a special class of ionic compounds insofar as they exhibit a considerable amount of covalent bonding in addition to the ionic bond. In alumina, the covalent contribution amounts to about 40% of the total bond between cations and anions. The sharing of electrons in addition to electron-exchange is difficult to approach theoretically.

The surface and volume properties of single crystal oxides have been given much attention. Relatively little work has been done on the high-temperature charge and heat transport in single crystals of high purity. The high-temperature heat transport mechanism in ionic crystals predicted by Peierls in 1931 has not been verified experimentally in the intervening years to date, although of importance for the evaluation of electron-phonon interactions at high temperatures. Little attempt has been made, on the other hand, to correlate surface studies on single crystal oxides with grain-boundary effects in polycrystalline materials.

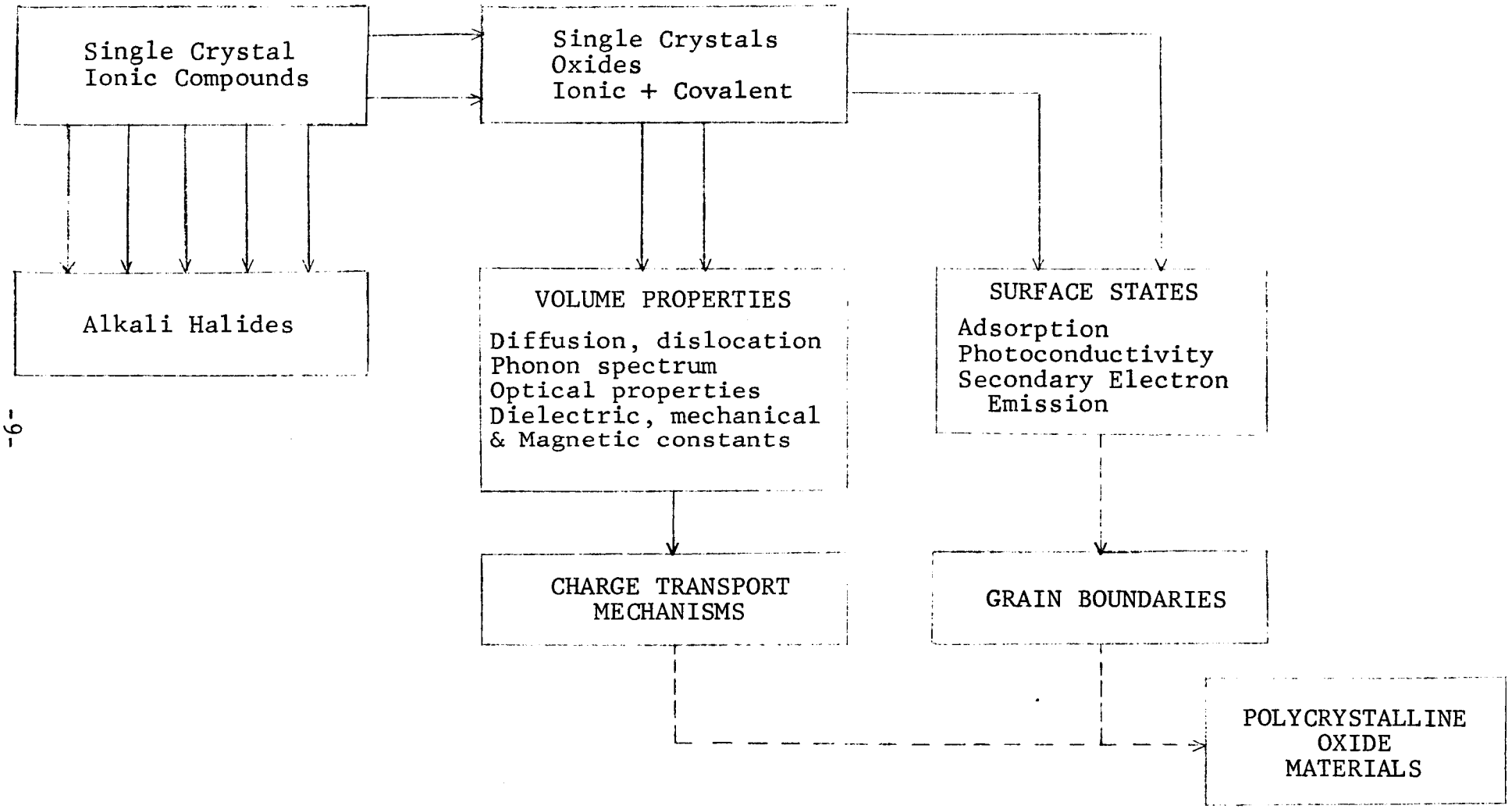

Fig. 1 - RESEARCH EFFORT IN THE FIELD OF IONIC COMPOUNDS

The number of arrows is a rough indication of the extent of research in the particular field, broken lines indicate very little work.

Many methods have been tried to characterize ceramic materials and, for the most part, they have not been successful in achieving this goal. They have succeeded in many cases in the identification of ceramics and have also advanced the understanding of mechanisms such as fracture, strength improvement, and corrosion resistance. Undoubtedly, some of the difficulty has been due to the orientation of the "characterizer." The nondestructive testing groups have worked with ceramics, but they are method rather than materials oriented. Materials experts have looked at individual mechanisms and appear to have overlooked their totality.

The question then arises as to what methods can be used for characterization. The two methods which should be used simultaneously can be identified as "direct" and "mechanistic." Although these two methods differ in approach, they are interrelated in devising a complete characterization of a ceramic for a particular application. The end-application for which a ceramic has to be characterized is critical in the selection of those properties or parameters which will best characterize it.

The characterization of ceramic materials by the "direct" method alone merely enables us to identify certain physical, chemical, thermal, and electrical properties of a specimen and, to some extent, relate them to the processing parameters. Undoubtedly, this approach is essential for determining the reproducibility of one piece of ceramic hardware compared to another for a particular forming or processing cycle. However, when this approach of characterization is utilized alone, it does not permit us to generically characterize a ceramic within certain predetermined "selectivity limits" (such as is possible with a silicon crystal of specified doping limit and orientation) and thereby evaluate its suitability for a specific application. Our present inability to do this with ceramic materials is largely due to a lack of knowledge of the relationships between the inherent properties of the material and its functional characteristics.

In the second method the mechanistic property or properties that are most suitable for characterizing a ceramic material should be of first-order importance; by this we mean that they should be predominantly (if not entirely) a function of the pertinent microstructural and atomistic aspects that one wants to characterize for a particular application and should not be masked by other effects. This is essential if we are to systematically define and devise property evaluations to correlate the relationships that can effectively characterize a ceramic material.

The intrarelationships which exist between certain significant atomic and microstructural aspects and "first-order" properties, in ceramic materials, and which merit further investigation are shown in Fig. 2.

Let us consider grain size. The characterization of grain size by the first approach is what the definition of the method implies--a direct assessment of the grain size. This can be carried out by microscopic techniques. But no matter how sophisticated and refined a measuring technique may be, it cannot characterize the volumetric or bulk effects of the grain size. In addition, there are secondary effects of potential interfacial barriers, dispersed phases, etc., all of which must be considered. Therefore, a direct evaluation of the grain size has to be carried out along with an associative approach. This second approach, in the case of the grain size, can take into consideration any one of the first-order properties shown in Fig. 2.

Interfacial barriers, which are responsible for a number of variations in the electrical properties of ceramics, can also be characterized by a number of "first-order" properties, as shown in Fig. 2. Stoichiometry effects with related "first-order" properties have also been shown in the same figure.

GRAIN SIZE

Piezoelectrics, titanates	k_p (piezoelectric response)
Ferroelectrics, titanates	TC of Dielectric constant
Most ceramics	I-E characteristics
Capacitor materials, titanates	TC of electrical resistivity

INTERFACIAL "ELECTRONIC" BARRIERS

Most ceramics	I-E characteristics
Oxides, titanates	Dielectric constant (at high and low freq)
Oxides, titanates	Capacitance (at high and low freq)
Most ceramics	Open circuit emf
Carbides, borides, silicides	Work function
Oxides, carbides	TC of electrical resistivity

STOICHIOMETRIC EFFECTS (cation/anion ratio; oxygen content)

Most ceramics	Open circuit emf
Oxides, titanates, carbides	TC of electrical resistivity
Most ceramics	Electrical resistivity
Carbides, borides, silicides	Work function
Carbides	Hardness
Carbides	Magnetic susceptibility
Titanates	Dielectric constant
Titanates, semiconducting oxides	Color centers

Fig. 2 - INTRARELATIONSHIPS BETWEEN FIRST-ORDER PROPERTIES OF CERAMIC MATERIALS BY THE "MECHANISTIC" METHOD

IV. CHARACTERIZATION OF BARIUM TITANATE

A. Introduction

Although this study is concerned with the characterization of $BaTiO_3$ ceramics, it is part of a broader effort to contribute to the closing of the gap between the two centers of interest, indicated in Fig. 1: the field of single crystal ionic compounds, which is of high scientific but limited technical interest, and the field of polycrystalline sintered oxides, which seems to attract lesser scientific attention but is of the highest technical interest.

In the case of barium titanate, the properties of interest are dielectric constant, dielectric loss, saturation polarization, coercive field, conductivity, breakdown field, switching time, piezoelectric coupling, Curie temperature, and the temperature coefficients of these properties. The task of characterizing $BaTiO_3$ ceramics consists then in finding the correlations between these properties and certain features of polycrystalline materials such as, grain size, porosity, impurities and internal stresses. The issue has been further complicated by experimental observations that:

1. $BaTiO_3$ ceramics of comparable grain size and porosity, impurity, and stress-levels do not necessarily have identical dielectric properties.
2. Partially as a consequence of (1), there is little known about the change in dielectric behavior of $BaTiO_3$ ceramics with a change in the four parameters, grain size, porosity, impurity content, and internal stress. Only a few empirically established trends are known, which do not allow prediction of the properties of $BaTiO_3$ ceramics with the degree of reliability and precision needed for microelectronic applications of this material.

It is necessary, therefore, to depart from the conventional way of characterizing polycrystalline $BaTiO_3$ in terms of grain size, porosity, impurity level, and stress, and to study in detail the effect of other parameters. This approach is illustrated in Fig. 3.

The obvious effect of grain size variation on the dielectric properties of $BaTiO_3$ ceramics concerns the corresponding change in the amount of grain boundary phase present. Still another effect may arise from a dependence of the properties of the boundary phase on grain size. Such a dependence is to be expected for a powder particle small enough that its surface free energy becomes an appreciable part of its total energy. Under these circumstances, domain wall formation and surface conductivity will be particle size dependent.

On the other hand, the grain size effect on the dielectric constant of sintered $BaTiO_3$ does not necessarily result from an intrinsic property of the bulk grains. Finer particles usually yield higher densities in sintering. Higher densities, in turn, may cause a larger compressive strain in the material upon cooling through the cubic-tetragonal transformation temperature. Several investigators have found an increasing amount of cubic phase in sintered $BaTiO_3$ with decreasing grain size. The increase in dielectric constant of sintered $BaTiO_3$ with decreasing grain size could then be explained by the increasing amount of cubic phase present--that is, by the increase in internal strain rather than by a direct grain size effect.

A discussion of the effects of deviation from stoichiometry on the electrical properties of barium titanate should distinguish between several types of nonstoichiometry which may affect these properties in different ways: chemical impurities, cationic doping, oxygen deficiency, and TiO_2 excess or deficiency. The situation is complicated by the fact that the concentration of different types of deviation from stoichiometry in the bulk of the grain and along grain boundaries may vary in a different

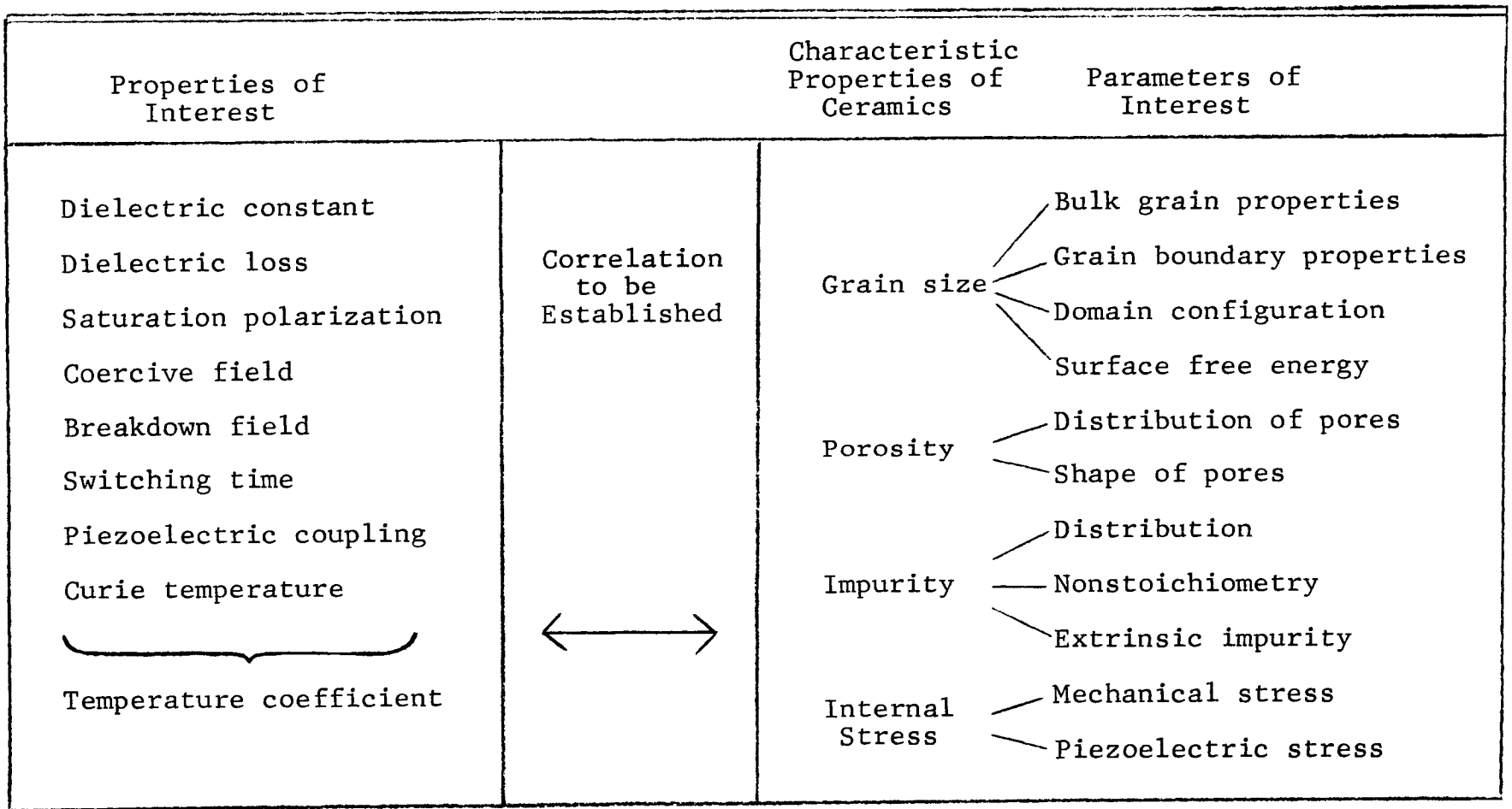

Fig. 3 - CORRELATION APPROACH TO CHARACTERIZATION OF BARIUM TITANATE

manner. Thus, grain size and stoichiometry effects cannot be considered to be independent of each other and it is sometimes difficult to evaluate the importance of studies of stoichiometry effects if they are lacking information on grain sizes.

B. Analysis of Literature on Surface Layer Concepts On $BaTiO_3$

In order to establish effective trend-lines for characterization of $BaTiO_3$ ceramics, we have attempted to analyze some significant contributions from the published literature on barium titanate. The main emphasis in our literature analysis has been on the various surface layer concepts that have been proposed. The effects of stoichiometry and secondary phases have also been considered.

The literature on ferroelectrics is extensive and increasing at a high rate. Probably the most comprehensive review of all available data published before 1961 is given in Ferroelectric Crystals by F. Jona and G. Shirane.[1] Equally important for the work under this program is the compilation of data on grain boundary defect layers by J. Volger.[2] In the following we attempt to present significant contributions to the investigation of grain size and stoichiometric effects on the ferroelectric and dielectric properties of barium titanate ceramics which have been published recently, including some of the important earlier work.

Useful data for a meaningful characterization of polycrystalline barium titanate are relatively scarce compared to the wealth of information available on single crystal $BaTiO_3$. Credit for the first successful attempt to derive the dielectric and elastic properties of polycrystalline, tetragonal $BaTiO_3$ from single crystal properties must be given to Marutake[3,4] who corrected the original Bruggeman equation[5] for the dielectric constant of aggregates by taking into account piezoelectric stresses for the case of tetragonal $BaTiO_3$. While the Bruggeman equation yields permittivity values in the order of 2500 for polycrystalline $BaTiO_3$, assuming a dielectric constant along the c-axis (K_c) of 225 and

along the a-axis (K_a) of 4400, for a single crystal, Marutake arrived at an average value K of 1600 under essentially the same assumptions for K_c and K_a, in much better agreement with the experimentally observed value of 1500.

Marutake's work has been criticized for he is assuming spherical crystallites as opposed to the laminar domain structure observed in $BaTiO_3$. According to Bruggeman[6] the permittivity of laminar aggregates may not differ appreciably from that of spherical aggregates. Marutake's calculation refers to dense ceramics with grains in the order of 10μ or larger and is not applicable to the anomalies observed for smaller grain sizes.

Correction formulae which account for the effect of porosity on the dielectric constant have been reported by Rushman and Strivens.[7] Their equation is based on the Clausius-Mossotti relation and has the form, for two-phase mixtures where spheres of phase 1 (index 1) are embedded in a matrix phase 2 (index 2):

$$\frac{K_2 - K_m}{K_m + 2K_2} = V_1 \frac{K_2 - K_1}{K_1 + 2K_2}$$

where, V_1 is the volume fraction of dispersed phase 1, K_1 and K_2 are the dielectric constants of the two phases, and K_m effective dielectric constant of the mixture. The equation appears to give correct results for volume fractions of closed pores in $BaTiO_3$ up to 0.3. Rushman and Strivens believe that there might be a smooth transition of the form factor from $2K_2$ to $2K_1$ upon phase inversion. This has not been proven experimentally, however, and is in doubt. The problem is similar to that of calculating the strength of porous ceramics with porosity larger than about 30% (volume fraction of pores >0.3), where the logarithm of the contact area is no longer a linear function of the porosity, or, in other words, where "open porosity" starts to appear in addition to "closed porosity".

A model is currently being worked out by Stadelmaier[8] which takes into account the effects of both porosity and grain boundary depolarization on the dielectric constant of porous

$BaTiO_3$. Although this model neglects piezoelectric stresses, it might provide a substantially improved basis for the calculation of the dielectric constant compared to the approach taken by Rushman and Strivens.[7]

W. Känzig introduced in 1955 the concept of a surface layer on $BaTiO_3$ ceramics,[9] and since then numerous investigators have studied this subject. Subbarao et al.[10] found a larger number of c-domains at the surface of $BaTiO_3$ crystals than could result from random orientation and believe that this is due to a strong electric field in the surface layer which switches the polar axis of the surface domains into the direction of the field. Irradiation effects support this explanation. A surface field in the order of 10^5 to 10^6 V/cm over a depth of about 10^{-5}cm could be expected for a Schottky-type depletion layer on $BaTiO_3$ crystals, assuming a donor concentration on the order of $10^{16}/cm^3$ and a density of states of $10^{22}/cm^3$ (identical with the concentration of Ti atoms).

Fatuzzo and Merz[11] compare the two surface layer models developed by Merz[12] and by Drougard and Landauer[13] with respect to their capability of explaining (a) the thickness dependence of the activation field for switching, (b) the thickness dependence of the coercive field, (c) the thickness dependence of the switching time for very large fields, (d) the field dependence of the switching time, and (e) domain wall motion.

The essential difference between the two models is this: Merz assumes a space charge type surface layer with a high voltage drop across it, which reduces the voltage across the bulk of the grain. The surface voltage drop is field dependent and always a certain fraction of the applied field. Drougard and Landauer, on the other hand, assume a very thin and lossy, chemical type defect layer, with a field independent voltage drop across. In reality, a third model for the surface layer is required which may combine certain features of both models along with new ones. In the approach taken by Merz, the $BaTiO_3$ grain is treated as a series

combination of two capacitors, one representing the surface layer with a low dielectric constant in the order of 5 and with high capacitive resistance, and the second one corresponding to the bulk of the grain with high dielectric constant. He estimates the thickness of the surface layer to be more than 0.5×10^{-4} but less than 1.5×10^{-4} cm. Merz explains the low dielectric constant of the surface layer by the high local field and by the mechanical clamping of the boundary layer to the bulk of the grain.

While both models are in agreement with several experimentally observed effects, they predict a decrease in switching time for large fields with increasing thickness of the crystal in contradiction to experimental facts. In addition, the Merz model leads to a decrease of the dielectric constant with decreasing thickness of the crystal, while the Drougard-Landauer model postulates a thickness independent dielectric constant. There do not seem to be enough experimental data available to decide in favor or against one of the models in this respect.

The observation of Kniepkamp and Heywang[14] that the dielectric constant of $BaTiO_3$ ceramics with grains of 1μ or less is much larger than that of coarse-grained material, reaching values of the permittivity in the neighborhood of 4000, is probably a strain effect which is not accounted for in the above-discussed single crystal surface layer-models. The finer particles yield a higher densification upon firing and, presumably, a larger extent of strain on cooling through the cubic-tetragonal transformation region which may result in smaller c/a values than usually observed for coarse-grain ceramics. Smaller c/a values, in turn, would mean higher K_c values and thus a higher average permittivity for fine-grain material.

The work of Minomura[15] on the pressure dependence of the cubic-tetragonal transformation in $BaTiO_3$ shows a linear decrease of the Curie temperature with pressure. At a pressure of 10 kilobars, for instance, the cubic-tetragonal transformation is shifted to a temperature of about 70°C.

It is conceivable that in dense ceramics of very fine grains an appreciable number of particles retain a c/a ratio of essentially 1.000 even at room temperature, which would explain the higher dielectric constant of this material. This has been observed, in fact, by Jonker and Noorlander[16] whose work will be discussed in more detail in subsequent paragraphs.

Gerthsen and Hardtl[17] have described a method to detect high-resistivity boundary layers in $BaTiO_3$ ceramics utilizing the fact that strong fields across boundary layers stray and give rise to an attraction of dielectric particles. Barrier heights in the order of 1 eV may result in a potential drop of about 1V over a depth of about 10^{-5} cm at the surface of the grains, thus generating fields on the order of 10^5 V/cm. Colloidal TiO_2 powder of a grain size of 1μ and smaller, immersed in silicone oil, was successfully used to mark the high-resistance layers of metallographic cross-sections of $BaTiO_3$ ceramics.

A significant contribution to the study of the relation between electrical properties and microstructure of barium titanate ceramics has been given by Stadelmaier and Derbyshire.[18] In order to show how the square hysteresis loop of a perfect single crystal of $BaTiO_3$ is modified in polycrystalline ceramics, they have developed an equation for the effects of an applied field upon randomly oriented grains switching from negative to positive saturation polarization. The result indicated a 20% decrease in saturation polarization and an increase of the same amount of the coercive field. Furthermore, the effect of unsaturated poles has been treated by an averaging procedure, yielding an equation:

$$P = P_o \left[1 - \exp(-d/d_o\chi)\right]$$

where P is the saturation polarization, P_o the polarization inside the grain, d the average grain size, d_o the grain boundary thickness (not the thickness of the boundary layer), and χ the susceptibility. From measurements of the saturation polarization on $BaTiO_3$ ceramics of 100μ and 1μ average grain size, respectively, the unknown quantities P_o and d_o were determined to be: $P_o = 4 \times 10^{-6}$ C/cm and $d_o = 0.9 \times 10^{-8}$ cm. The equation indicates that the effect

of grain boundary polarization is negligible down to grain sizes of 5μ, while it becomes appreciably large for particles below 0.5μ.

It should be noted that stresses in the polycrystalline material which are neglected in this work could cause considerable reduction of the saturation polarization. The experiment on the coarse and fine grained material (100μ and 1μ grain size) revealed a strong aging effect. The initial susceptibility of the coarse material was 1300 and did not change with time, while the fine-grained specimens had an initial susceptibility of 2500 to 3000 which decreased down to 1300 after several months at room temperature. This effect is difficult to explain since aging effects in $BaTiO_3$ are usually attributed to a relief of stresses which should result in an increase of the susceptibility rather than a decrease.

Several investigators have studied the characteristics of the surface layer on $BaTiO_3$ grains by measuring the frequency dispersion of the ac conductivity and dielectric losses. The interpretation of the results is based on the work of Volger,[2] Fröhlich,[19] Fricke,[20] Reimerov,[21] Muller,[22] and others. Particularly interesting are the studies of Abe,[23] Gerthsen,[17] and Heywang.[24]

Abe investigated the anomalous dispersion of the coercive field at very low frequencies in Rochelle salt and finds that the field dependence of the domain wall velocity can be explained by the existence of a Schottky-type defect layer. Gerthsen uses an equivalent circuit to represent the barium titanate grain carrying a surface layer. The circuit consists of a capacitance and parallel resistance representing the bulk of the grain in series with a capacitance and parallel resistance representing the surface layer. The frequency dispersion of the total impedance of the equivalent circuit is in qualitative agreement with that measured on polycrystalline $BaTiO_3$, doped with 3 at.% La.

The same concept is worked out in more detail by Heywang who studied the resistivity anomaly in doped $BaTiO_3$. He finds that the frequency dispersion of the resistivity and the voltage dependence of the resistivity of $BaTiO_3$ throughout the temperature range -180° to +200°C can be explained qualitatively and quantitatively by the above-described equivalent circuit representation of barium titanate particles, assuming that bulk and surface layer have inherent loss tangents which do not vary appreciably in the frequency range investigated. It is surprising that Heywang finds good agreement with experiments on $BaTiO_3$ ceramics, although his equivalent circuit is valid only for a single particle. His work not only permits the determination of resistivity, dielectric constant, and thickness of the barrier layer, but also may facilitate the calculation of the effective dielectric constant of polycrystalline $BaTiO_3$, including the effect of porosity. Heywang's calculations yield a barrier height of about 0.9 eV and a barrier layer thickness of the order of 10^{-5} cm.

A recent calculation of the barrier layer thickness by Heywang,[25] based on simple assumptions with respect to the depolarization field in individual grains of $BaTiO_3$, is in remarkable agreement with experimental results on the well known ferroelectric anomalies observed on fine-grained barium titanate ceramics. The depolarization field E in a $BaTiO_3$ particle in vacuo with a saturation polarization $P_s \approx 20 \times 10^{-6}$ C/cm^2 is approximately $E = P_s/\epsilon_o\epsilon_c$, where ϵ_o and ϵ_c are the permittivities in vacuo and along the c-axis, respectively. It is essential to realize that because of the high permittivity of barium titanate, the depolarization field goes through the crystal, against the direction of polarization. With $\epsilon_c \approx 200$ in direction of P_s, the potential difference (φ) across the crystal is, $\varphi = Ed$, d being the thickness of the crystal. φ cannot exceed the band gap in $BaTiO_3$ because otherwise electrons from the valence band could enter the conduction band, neutralizing partially the polarization charges $Q = P_s$, and thus reducing the depolarization field. With a band gap of $\Delta = 3$ eV for $BaTiO_3$, one

obtains for the critical thickness d, for which the depolarization field is not reduced by intrinsic charge transport, $d \cong \Delta/E = \Delta\epsilon_o\epsilon_c/P_s \cong 0.03\mu$.

In the polycrystalline ceramic, the medium surrounding a grain is barium titanate instead of vacuum, with an average dielectric constant higher than that of the grain along P_s. Thus, the depolarization field proceeds through the region around the grain rather than through the grain itself, and the critical thickness is now $d = \Delta\epsilon_o\epsilon_a/P_s \cong 0.75\mu$. Therefore, the depolarization in the polycrystalline phase is expected to be weaker than in the particle, in agreement with the observations of Merz[12] and Kanzig.[26]

Indications that the barrier layer properties are affected by adsorption and desorption processes[27] suggest the usefulness of a study of the kinetics of oxygen adsorption at the surface of $BaTiO_3$ particles. Chemisorption or physical adsorption of oxygen could result in a negative surface charge and a depletion layer of a thickness in the order of 10^{-5} cm. In such a layer, field-induced cation diffusion is very likely to occur.

A thorough study of the effect of cationic doping on the electrical properties of $BaTiO_3$ ceramics has been given by Saburi.[28] Substitution of barium or titanium by trivalent or pentavelent ions, respectively, decreased the conductivity, while substitution by monovalent or divalent ions, respectively, increased the conductivity, as expected. It is interesting that Saburi noticed a blue coloration of the samples accompanying the reduction in resistivity. Carnahan and Brittain[29] observed a faint blue coloration in vacuum-reduced titanium oxide, caused by an absorption band centering at 1.2μ wavelength, along with a decrease in resistivity. In both cases, doping with trivalent or pentavalent ions and vacuum reduction introduces relatively shallow donor states which may give rise to a similar absorption in the infrared.

The effect of excess TiO_2 or BaO on the phase structure in $BaTiO_3$ ceramics can be evaluated from the phase diagram worked

out by Rase and Roy.[30] It is well known that a small excess of TiO_2 enhances sintering by the formation of a liquid phase above 1322°C. Less well known is the distribution of $BaTi_3O_7$ or $BaTiO_5$ in ceramics sintered with an excess of TiO_2 and to what extent the dielectric properties are degraded by the presence of these compounds. These effects have been considered by Hellicar and Parnell[31] for surface layer reactions.

An excess of TiO_2 not only enhances sintering but also appears to inhibit grain growth during sintering. This latter effect has been given much attention since Kniepkamp and Heywang[14] had observed that ferroelectric properties are nearly nonexistent in $BaTiO_3$ ceramics with grains predominantly in the submicron range. For many dielectric applications, the ferromagnetic properties of $BaTiO_3$ (that is, the dielectric hysteresis) are a disadvantage. The effect of excess TiO_2 on the grain size and on the dielectric properties of sintered $BaTiO_3$ has been discussed recently by Jonker and Noorlander,[16] and in a recent state-of-the-art review.[32]

The combination of results of studies of the optical and electrical properties of TiO_2 and related oxides with the work discussed above should enable one to develop a barrier layer model which is more realistic than previous ones. The development of such a model is a continuing objective of this program.

C. An Interpretation of the Dielectric Behavior of $BaTiO_3$ Ceramics

To obtain a meaningful characterization of $BaTiO_3$ ceramics, it is essential to determine the properties of the surface layer and grain-boundary phases as a function of grain size, stoichiometry, and any other pertinent microstructural and atomistic parameters. In order to do so, we have attempted to theoretically interpret the possible dependence of the dielectric behavior of the grain-boundary phase on the grain size and stoichiometry, in polycrystalline $BaTiO_3$, in terms of the overall bulk properties.

Such a theoretical approach is essential to the overall question of characterization and will compliment the experimental

work carried out on this program.

The literature on barium titanate ceramics indicates that one has to consider each $BaTiO_3$ grain as consisting of essentially two phases: (1) a bulk phase with properties approximately equal to those of a single crystal and (2) a surface layer phase with lower dielectric constant and higher resistivity due to the state of minimum energy leading to a different configuration of atoms and ions near the surface of the crystallite than that in the bulk. The properties of the grain are, in effect, those of the surface layer if the surface layer thickness is independent of the grain diameter, and the grain diameter is of the same order of magnitude as the surface layer thickness. It should be noted that in considering grain size, the effects of porosity must also be borne in mind and likewise with stoichiometry.

Känzig[26] in his excellent work on $BaTiO_3$ powders did not pay much attention to the effects of porosity on the dielectric measurements because of the unreliability of the porosity corrections. These are unreliable because one can only approximate, mathematically, the intricate shape and distribution of pores present in a real two-phase system. This means, on the other hand, that deviations from theoretical behavior directly reflect the characteristics of the phase distribution in a given system and may provide a useful characterization of such a two-phase system.

Figure 4 shows the dielectric constant of a two-phase mixture as a function of the volume fraction of the material with the lower dielectric constant--calculated on the basis of the equation given, and experimentally tested on porous $BaTiO_3$ by Rushman and Strivens[7] for spherical particles embedded in a continuous matrix phase. For the low dielectric constant material, $K = 3$ has been chosen. Curve A shows the relationship under the assumption that barium titanate is the continuous phase. This assumption certainly no longer holds true for volume fractions of the dispersed phase of 0.5 and larger. Its validity may be

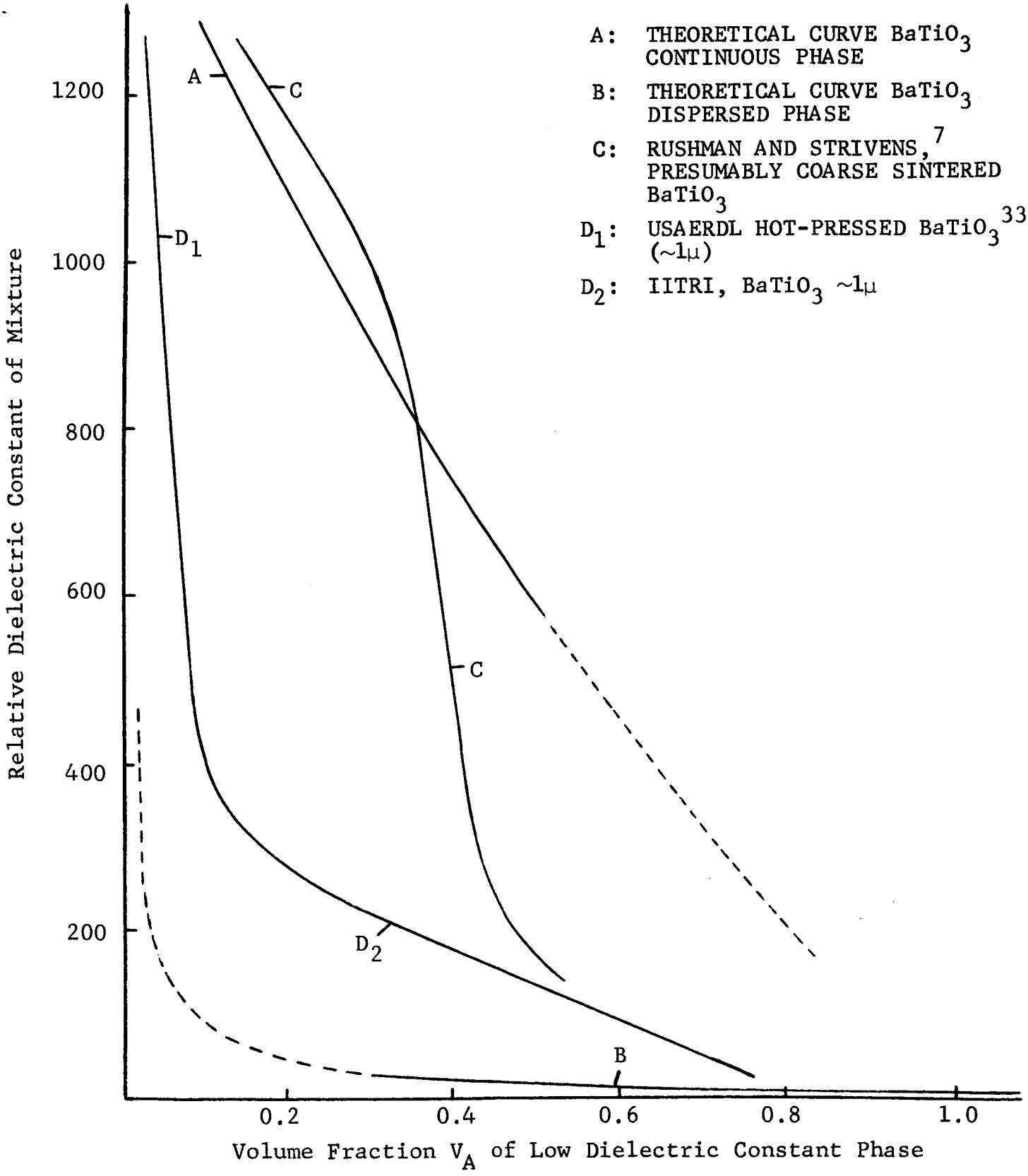

Fig. 4 - DIELECTRIC CONSTANT OF TWO-PHASE SYSTEM

questioned when the volume fraction of the low dielectric constant phase (V_A) is in the range 0.3. Curve B shows the relationship under the assumption that $BaTiO_3$ is the dispersed phase and the second phase of low dielectric constant is continuous. This assumption is probably justified down to a volume fraction of the continuous phase of 0.5. In reality, the behavior of the system changes from curve A to curve B, and the transition region may range from $V_A = 0.2$ to $V_A = 0.8$, depending on the actual shape and grain size distribution of the $BaTiO_3$ particles and the spatial arrangement of the two phases. One must realize that impurities or compounds other than $BaTiO_3$ on the surface of the barium titanate particles, due to an excess of TiO_2 in preparing the material, or physical defect layers on the $BaTiO_3$ grains, have to be treated as a third-phase present.

Curves C and D are experimental ones. C represents data obtained by Rushman and Strivens on cold-pressed and sintered $BaTiO_3$ of a total impurity level below 0.2 wt%.[7] The authors did not give particle sizes; however, since their work was done in 1947, one may assume that they used rather coarse $BaTiO_3$, around 10μ or above. Since they sintered the material below and above the recrystallization temperature, curve C is not representative for a constant particle size distribution.

Curve D_1 is the result obtained on hot-pressing $BaTiO_3$ of particle size 0.1 to 0.2μ.[33] Curve D_2 has been obtained experimentally on $BaTiO_3$ samples with controlled porosity, from work done at IITRI on fine grained specimens. It should be added that extrapolation of curve C to zero porosity leads to a dielectric constant of the dense ceramic of $K \cong 1600$, while extrapolation of curve D to zero porosity yields a K of ~3200, in agreement with the observation that fine particles result in much higher K values than coarse ones. This also supports the assumption that Rushman and Strivens used particles above ~5μ.

It follows that both the transition in behavior from theoretical curve A to theoretical curve B and the slope in the transition region are sensitively dependent on the particle size

of the $BaTiO_3$ and the way in which the continuous $BaTiO_3$ phase is formed or altered upon sintering.

Besides the effect of porosity and grain size on the dielectric properties of $BaTiO_3$ ceramics, an important aspect is the nature of the much discussed surface defect layer on the $BaTiO_3$ grains and its effect on the dielectric properties of the ceramics. Merz[12] assumes a very low dielectric constant for the boundary phase in dense, polycrystalline $BaTiO_3$ on the order of 5 and explains this by a clamping effect due to internal strain.

If the amount of internal strain were indeed responsible for a low dielectric constant of the boundary phase (and only the boundary phase), the dielectric constant of this phase could well be a function of grain size. The amount of internal strain appears to increase with decreasing grain size. Several investigators have found this effect manifested in an approach of the c/a ratio to 1.000. This increasing amount of cubic phase with decreasing grain size may be the reason for the increase of the dielectric constant of the bulk grain phase with decreasing grain size, but nothing is known about the corresponding changes in the boundary phase. The boundary phase does not significantly contribute to the x-ray reflections of a polished or etched surface. We have attempted to estimate the effect of a grain size dependent dielectric constant of the boundary phase on the effective dielectric constant of a dense, pore-free $BaTiO_3$ ceramic on the basis of the Bruggeman equation for a two-phase system.[6] This equation holds for non-piezoelectric, heterogeneous systems only, but probably shows qualitatively the right trend.

$$\frac{K_v - K_m}{K_v - K_b} = (1 - V)\,(K_m/K_b)^{\frac{1}{2}}$$

where K_v,V = dielectric constant and volume fraction of the bulk phase, respectively

K_b = dielectric constant of the boundary phase

K_m = effective dielectric constant of the system

With the introduction of the parameter $a = K_b/K_v$ we have:

$$\left(\frac{1}{1-a}\right)\left(1 - \frac{K_m}{K_v}\right) = (1 - V)\left(\frac{K_m}{aK_v}\right)^{\frac{1}{2}}$$

Figure 5 shows the trend of K_m, for three different values of "a" and under the assumption $K_v = 1000$, as a function of the volume fraction of the bulk grain. The volume fraction V is also translated into grain size assuming a thickness of the boundary phase of 10^{-5} cm = 0.1μ. This assumption and the further assumption that the thickness of the boundary layer does not depend on grain size appears reasonable on the basis of literature data shown in the preceding sections.

It can be hypothesized that the dielectric constant of the boundary phase on the surface layer is grain size dependent and changes from a high value for large grains to a small value for small grains ("a" going from 10 to 10^{-2}, for instance). The effective dielectric constant K_m of the ceramic then would pass through a maximum, increasing first with decreasing grain size, but decreasing with decreasing grain size below a certain critical grain size, probably in the submicron range. The position of the maximum would depend on the parameter "a". Testing this hypothesis would contribute to our knowledge of the nature of the boundary phase in several ways.

In addition to the experimental evidence for a high-resistivity surface layer on $BaTiO_3$ grains[17] we would propose a simple model for such a high-resistivity boundary layer. This has been schematically shown in Fig. 6. A barium titanate grain has very probably a layer of adsorbed oxygen around its surface, the strength of the oxygen bond depending on the energy levels of the available surface states. Since the oxygen atoms or molecules accept electrons from the crystal to form the bond, they represent a negative surface charge. The thickness of the surface depletion layer may be of the order of 10^{-5} cm, typical for a Schottky-type barrier. The electric field across the depletion layer may be on the order of 10^5 V/cm under the assumption that the barrier

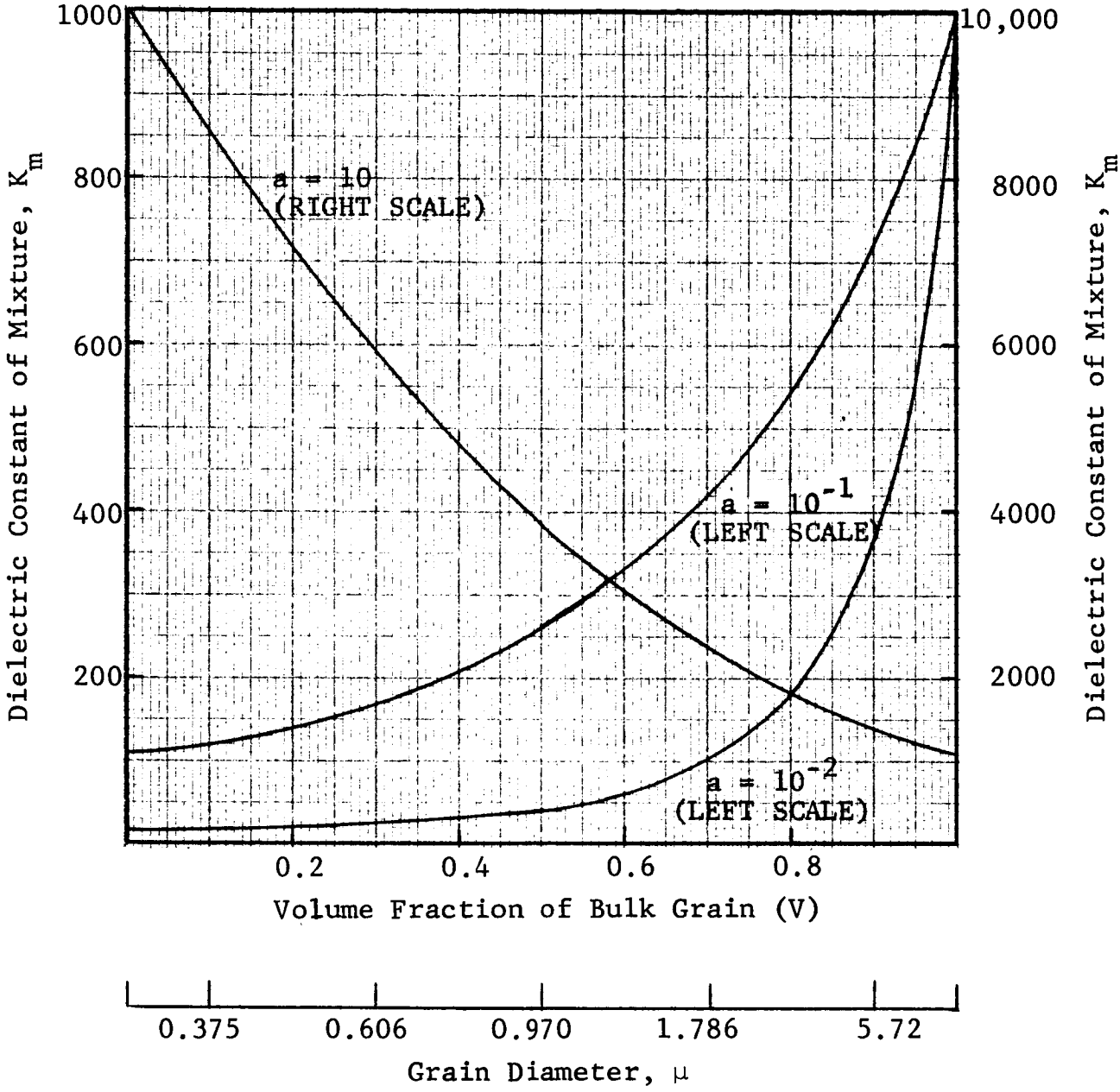

Fig. 5 - EFFECTIVE DIELECTRIC CONSTANT OF $BaTiO_3$ CERAMIC AS A FUNCTION OF GRAIN SIZE (CALC. FROM MODIFIED BRUGGEMAN EQ.)[6]

Where: Surface layer thickness = 0.1μ = constant
$K_b = aK_v$ and $K_v = 1000$

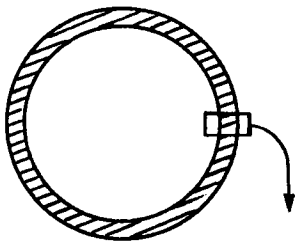

FORMATION OF SURFACE DEFECT LAYER

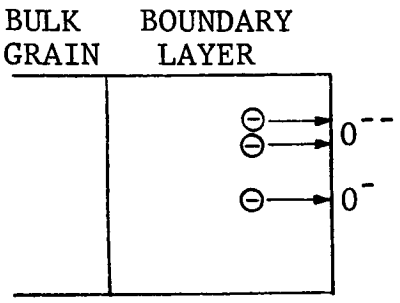

1. Chemically and Physically Adsorbed Oxygen Removes Electrons From Crystal, Creates Negative Surface Charge. Assumption: Surface States Below Fermi Level

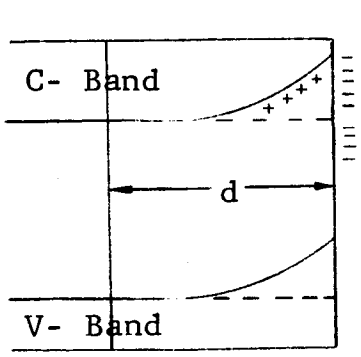

2. Electronic Energy Band Shift Due to Negative Surface Charge.
Magnitude of the Effect:

Barrier Layer Thickness d	$\cong$	10^{-5} cm
Density of States	$\cong$	$10^{17}/cm^3$
Negative Surface Charges	$\cong$	$10^{13}/cm^2$
Barrier Height E_B	$\cong$	1eV
El. Field Across Barrier Layer F_d	$\cong$	10^5 V/cm

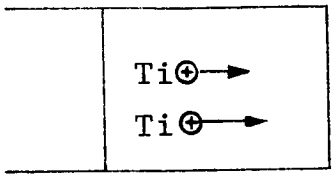

3. Field Induced Cationic Diffusion to Surface. Formation of TiO_x on Surface Extending Lattice

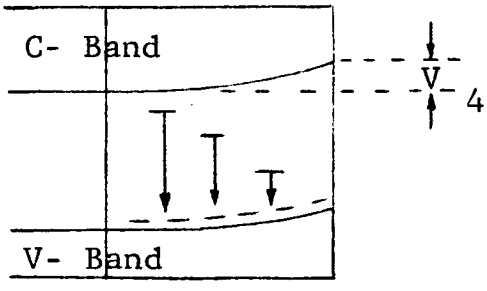

4. Equilibrium Situation, $V < E_B$. Holes in Valence Band Create Acceptor States Which Trap Electrons From Higher States, Increasing Barrier Layer Resistivity.

Fig. 6 - BARRIER LAYER MODEL FOR $BaTiO_3$ GRAIN

potential is of the order of 1 eV. This high electric field is likely to induce cationic migration to the surface, especially since the Ti cation is quite mobile in the $BaTiO_3$ structure. The titanium would probably combine on the surface with oxygen, forming an extremely thin layer of TiO_x, undetectable by x-ray techniques. The neutralization of the adsorbed oxygen by the formation of titanium oxide reduces the negative surface charge and thus the electric field. The field-induced cationic migration to the surface comes to a standstill after a certain portion of movable cations have migrated to the surface.

The essential feature of the proposed model would be that the cation vacancies created by the process of cationic migration to the surface represent acceptor states which may trap electrons from energy levels above the trap state. The number of electrons available for conduction would be drastically reduced by this means, and the resistivity of the depletion layer would rise probably by several orders of magnitude. The principles of the model suggested here are not new at all. Conditions, extensively studied on other materials (for instance, zinc oxide and lithium-doped zinc oxide), are simply translated into the case of barium titanate.

V. EXPERIMENTAL WORK

A. Introduction

The major experimental emphasis to date has been on the manner in which the properties of high-purity barium titanate powders are related to those of the ceramic body. Data are being accumulated on the changes in specific electrical properties (dielectric constant, dissipation factor, and electrical resistivity) as functions of frequency and temperature during the controlled conversion of the compacted powders to increasingly densified and bonded ceramics. Such an approach will enable us to study the nature of the grain-boundary layer relative to the grain and to correlate it with the surface layers of $BaTiO_3$ particles.

B. Characterization of Starting Materials

1. Purity and Stoichiometry

In obtaining $BaTiO_3$ powders from various sources, major emphasis was placed on the stoichiometry and purity levels of the material. A number of the materials used in this program are in the developmental stage and not necessarily available commercially. Although the purity level of these powders is not similar to what has been achieved with elemental semiconductor materials, such as silicon, it is an order of magnitude superior to what is used for commercial $BaTiO_3$ capacitors. Efforts are being continued to obtain sample powders of higher and better purity. The fact that the extent of purity has been "finger-printed" for all our starting materials enables us to determine the possible effects of various impurities.

As pointed out in the preceding discussions, stoichiometry is an important factor in $BaTiO_3$ ceramics. The ratio of Ba/Ti and the presence of other titanates of Ba, must also be taken into consideration. To this extent, we have been able to obtain $BaTiO_3$ powders of exact stoichiometry.

Therefore, although the concept of "ultra-high purity" as defined for silicon has not yet been achieved for $BaTiO_3$, the very significant improvements in the purity and stoichiometry of the $BaTiO_3$ material to be investigated on this program justifies their use and makes the interpretation meaningful.

Barium titanate powders have been received from a number of sources. These include: Eldorado Mining & Refining Ltd., The Glidden Company, National Lead Company, and ITT Laboratories. Tables I and II list data on these powders provided by the manufacturer. In order to supplement these data, measurements of the water content, the pycnometric density, and the grain size distribution of the powders were conducted. Also, the crystallographic structure and the c/a ratio were determined by x-ray technique. Table III shows the results of the x-ray analysis. The variation of the c/a ratio for materials A to D, though small, is expected to result in a noticeable variation of the average dielectric constant of the powders. Material E is obviously cubic barium titanate, as indicated by ITT Laboratories, as the result of a low-temperature production process. The x-ray density of materials A to D was found to be 5.98 g/cm^3 and was higher than the density determined pycnometrically. Deviations of the pynometrically determined density from the x-ray density were inversely proportional to the grain size of the powders, and are thus explained by incomplete wetting of the powders by the pycnometer liquid. The fineness of material B was indicated by a considerable broadening of the x-ray reflections.

A 5g sample of high-purity $BaTiO_3$ powder was also obtained from the AF Materials Laboratory, Wright-Patterson Air Force Base. This material has been prepared by the controlled decomposition of metal alkoxides and is reported to have exact stoichiometry and a particle size of about 240A. The experimental sample is supposed to have been prepared and encapsulated under an inert atmosphere. Due to the limited quantity available, experimentation with this material will be done at a later stage.

Table I

CHARACTERIZATION OF BARIUM TITANATE POWDER SAMPLES
PROVIDED BY THE MANUFACTURERS

Source	Manufacturer's Code	Our Sample Designation	Impurity, Total Content in ppm	Main Impurity	Grain Size	Remarks
Eldorado Mining and Refining Ltd. Ottawa, Canada	3-549-102-5	A	<250	Zn, Sr	6.18μ	Surface area 10 m^2/g K_{20} = 2840 (Pellet) T_C^{20} = 129°C
Glidden Company Baltimore, Md.	186-A-80	B	≤500	Mg, Sr	0.005-0.01μ	Low temp. process not calcined, relatively high water content (~5 wt%)
National Lead Co. Research Lab. South Amboy, N.J.	MP-218	C	≤240	Sb, Si	-100 mesh to submicron range	Calcination of barium titanyl oxalate 3 hrs at 1000°C
National Lead Co. TAM Division Niagara Falls, N.Y.	Lot #311	D	≤8200 $BaO:TiO_2$ = 0.986	P, Zn	Diam. / Cum.% Over: 10.0μ / 4; 5.0 / 29; 3.0 / 56; 2.0 / 72; 1.5 / 80; 1.0 / 88; 0.7 / 94; 0.5 / 97; 0.3 / 99	
ITT Laboratories	Lot #2110-100	E	<250 ≈100 Ba:Ti = 1:1 ± 0.003		0.01-0.1μ	Low temp. process cubic modification

Table II

CHEMICAL ANALYSIS OF $BaTiO_3$ POWDER
PROVIDED BY MANUFACTURER

Material	Weight % D	C[2]	B[1]
B_2O_3	<.005		
SiO_2	<.003	.01	
P_2O_5	<.3		
ZrO_2	.02		.004
Sb_2O_3	<.01	<.01	
HfO_2	<.02		
Al_2O_3	.01	.0005	.005
Fe_2	.005	<.001	
MnO_2	<.0005	Mn <.00005	
PbO	<.005	Pb <.0005	
MgO	.005	Mg <.0005	.027
SnO	<.005	<.0005	
Nb_2O_5	<.01		
WO_3	<.05		
Cr_2O_3	<.002	Cr <.0001	
NiO	<.005	Ni <.0003	
TiO_2[3]	34.4		
MoO_3	<.01		
CaO	.05		.005
V_2O_5	<.003	V .0003	
(Cont'd)			

Table II (Cont'd)

Material	Weight % D	C(2)	B(1)
CuO	<.0001	Cu .0002	
ZnO	<.2		
BaO(3)	65.10		
SrO	.05		.01
Na_2O	.01		
Li_2O	<.005		
K_2O	<.01		
Water Content(4)	.11	.05	2.02
Ignition Loss	.18		

(1) Typical impurity level

(2) Typical spectrographic analysis

(3) Chemical analysis

(4) Determined in this laboratory: 300°C/20 min

Table III

X-RAY ANALYSIS OF $BaTiO_3$ POWDERS

Material	Crystal Structure	c/a[1] [2]
A	Tetragonal $BaTiO_3$	1.0056 ± 0.0008
B	Tetragonal $BaTiO_3$	Line Broadening prevents exact determination of c/a
C	Tetragonal $BaTiO_3$	1.0056 ± 0.0008
D	Tetragonal $BaTiO_3$	1.0088 ± 0.0008
E	Cubic $BaTiO_3$	1.0000 ± 0.0008

(1) Obtained from (200), (002) peaks

(2) Literature values[33] for tetragonal $BaTiO_3$: c/a = 1.0027 - 1.0101 ± 0.0001 - 0.0010

In addition to the materials listed in Table I, we have just received another type of high-purity $BaTiO_3$ powder from the National Lead Co. It is reported by the manufacturer to be tetragonal $BaTiO_3$ with a Ba/Ti ratio of 1:1. These newer materials will now be used for all further experiments.

In determining the water content of the powders listed in Table I, it was noted that after heating at 300°C for about 20 min and cooling to room temperature, the weight of the powder samples increased steadily, approaching a constant value after about 30 min. The weight change was particularly pronounced for material B. The time-weight gain relation appeared to be of the Stark-type indicating readsorption of water or gases on the crystallites of the powders. This effect will be studied further at a later date, since the adsorption of water vapor or oxygen may affect the structure of the particle surface.

It was also noted that all powders discolored upon heating at about 300°C and became white again on cooling. The discoloration into yellow-green was strongest for materials A and D which contain zinc as major impurity, while it was less noticeable for materials B and C. Therefore, it may be possible to characterize the impurity content in these materials by such color changes.

2. Particle Size Analysis

The particle size distribution of the powders shown in Table I has been determined by a Kay Centrifugal Disc Photosedimentometer developed at IITRI. In this process, powder suspensions are passed through the photosedimentometer in which the attenuation of light passing through the settling particles is measured and recorded on a strip chart. The chart data are programmed into a computer for final analysis.

Figures 7 to 11 show the particle size distribution for $BaTiO_3$ powders A, B, C, D, and E. Material E contains extremely fine particles in or below the 100A range, the percentage of which was difficult to determine. This introduces an error in the lower branch of the curve of Fig. 11 of probably 1 to 2%. Figure 12

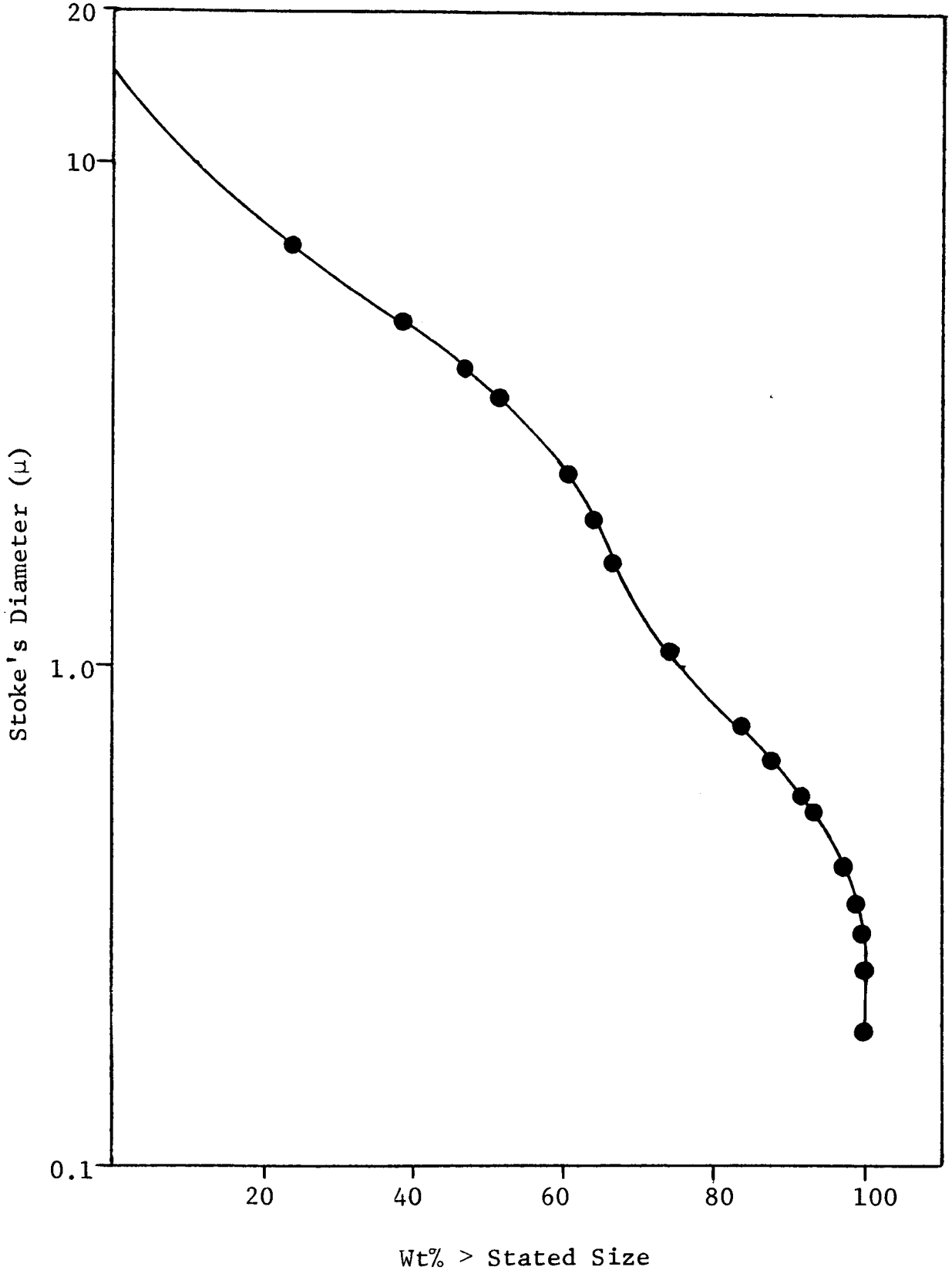

Fig. 7 - PARTICLE SIZE DISTRIBUTION OF $BaTiO_3$ POWDER - MATERIAL A

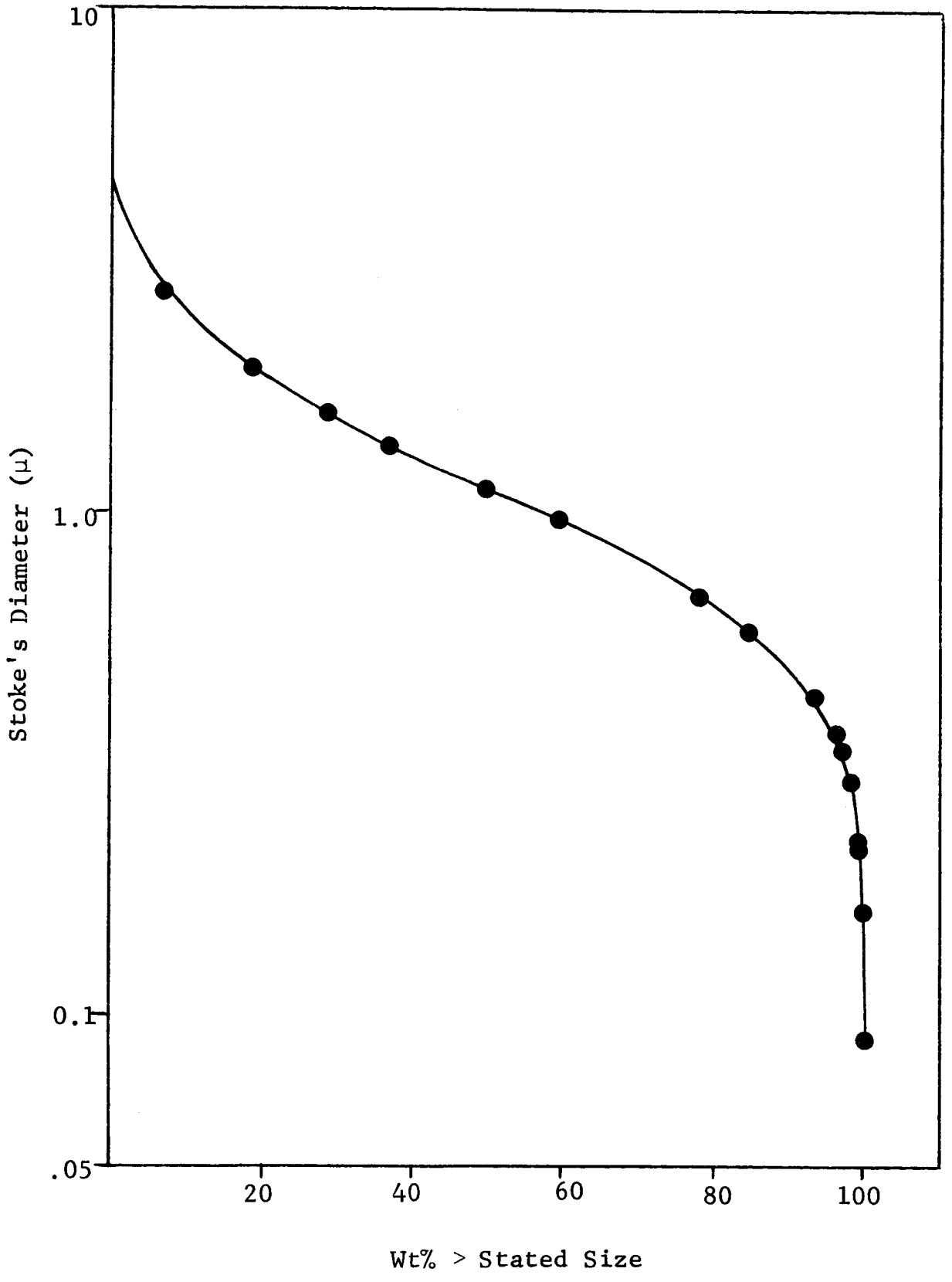

Fig. 8 - PARTICLE SIZE DISTRIBUTION OF $BaTiO_3$ POWDER - MATERIAL B

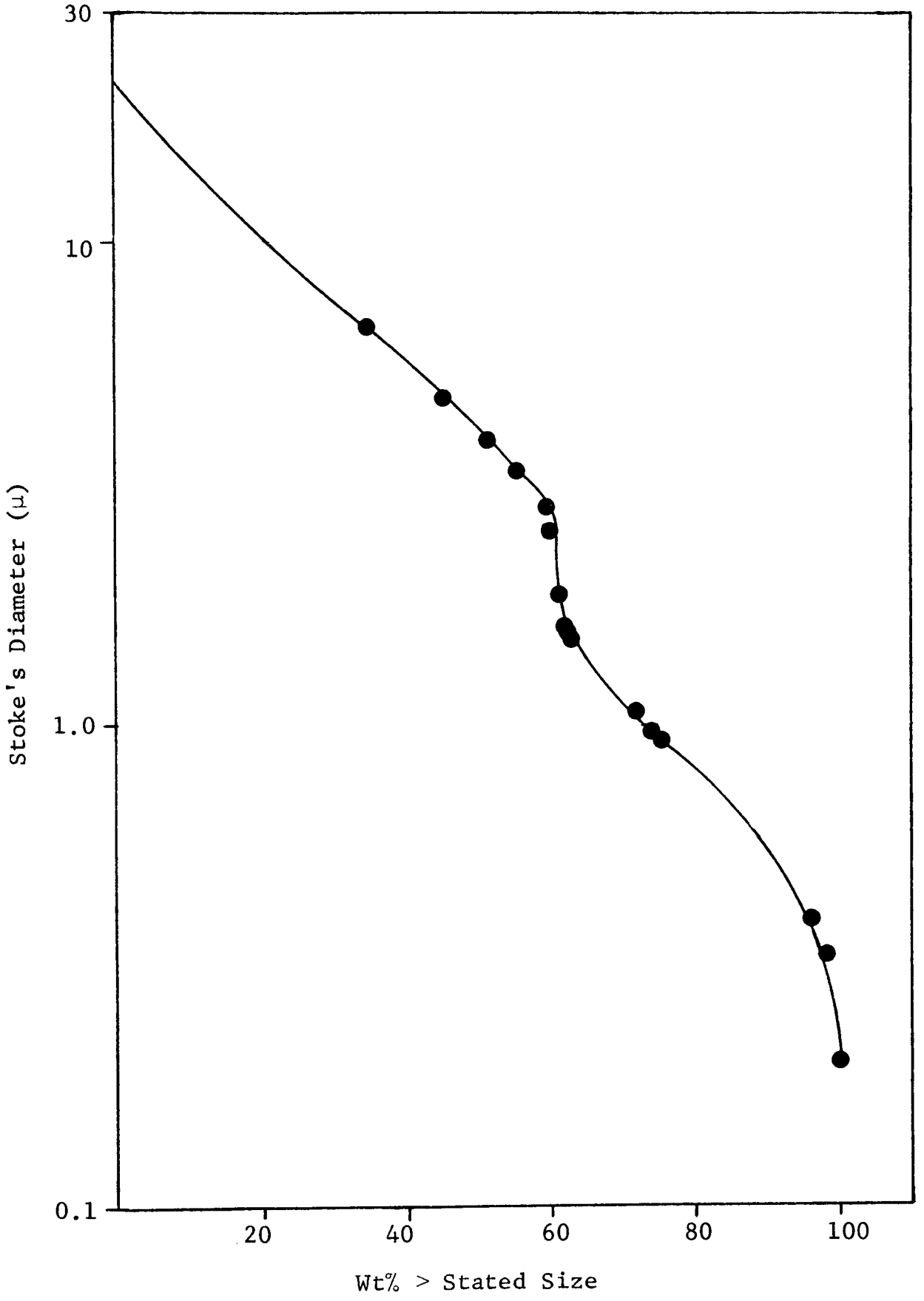

Fig. 9 - PARTICLE SIZE DISTRIBUTION OF $BaTiO_3$ POWDER - MATERIAL C

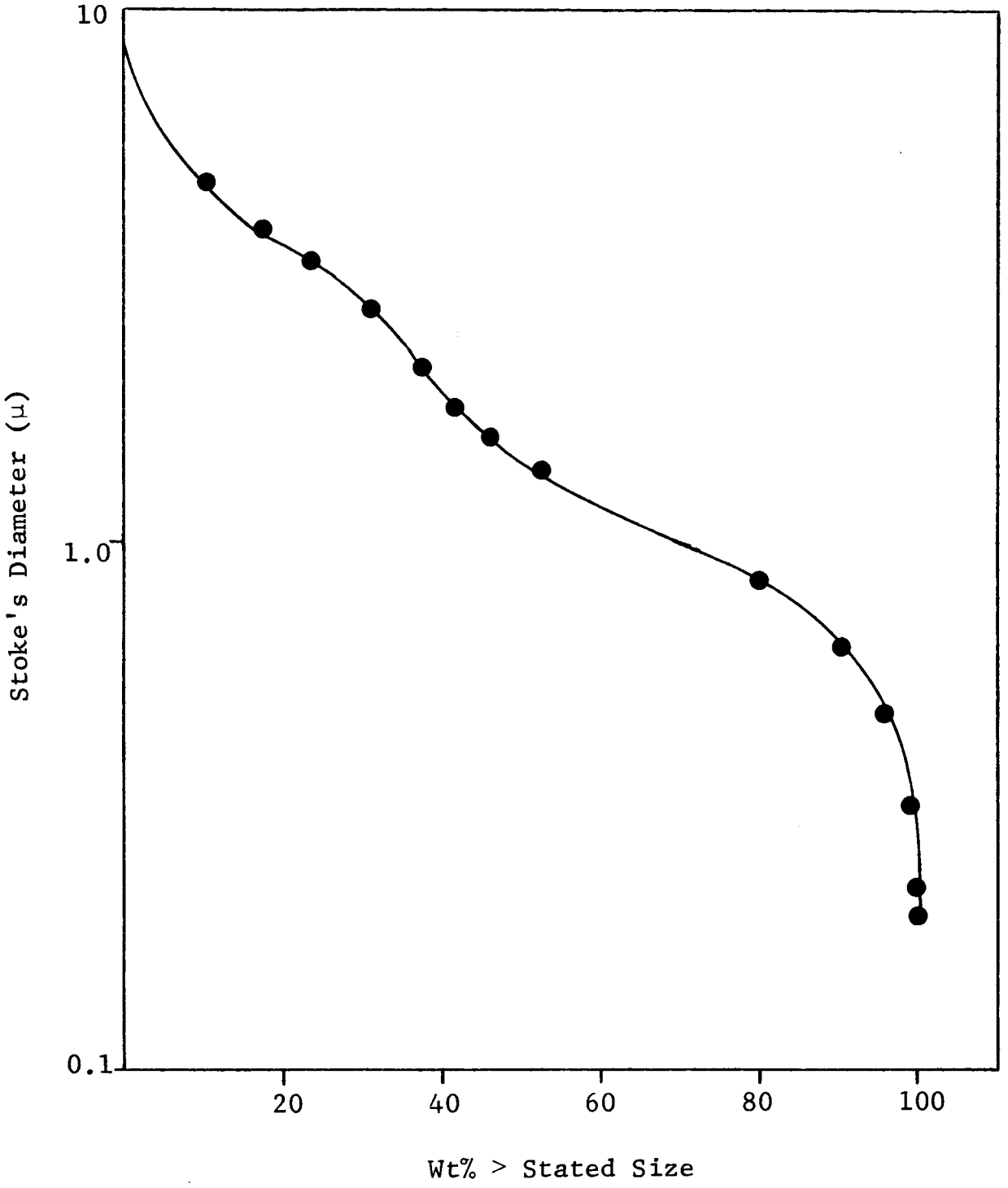

Fig. 10 - PARTICLE SIZE DISTRIBUTION OF $BaTiO_3$ POWDER - MATERIAL D

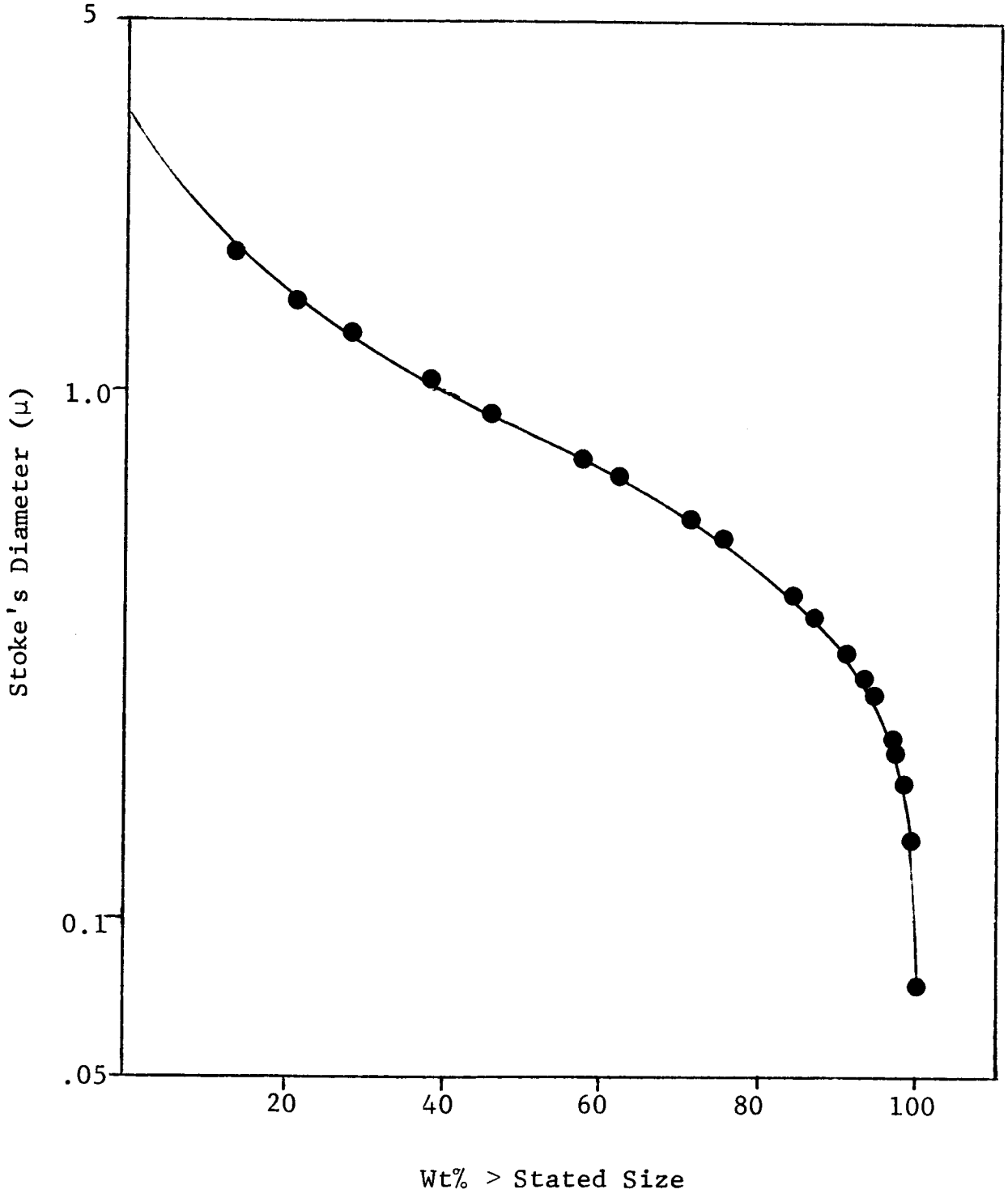

Fig. 11 - PARTICLE SIZE DISTRIBUTION OF $BaTiO_3$ POWDER - MATERIAL E

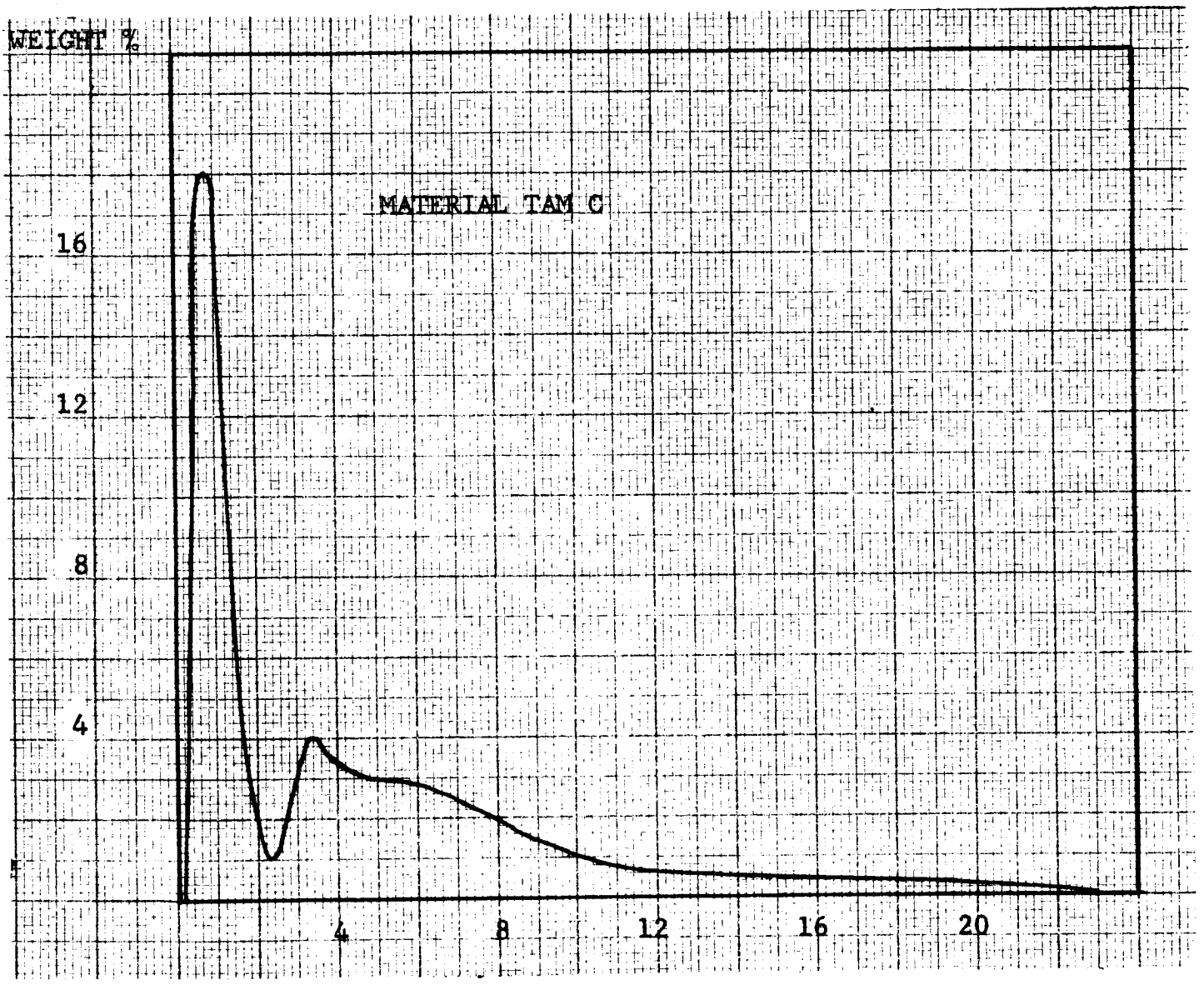

Fig. 12 - PARTICLE SIZE DISTRIBUTION FOR TAM-$BaTiO_3$ MATERIAL C, FOR .5 MICRON INTERVALS

shows the distribution for material C, for 0.5μ intervals.

Figures 13 and 14 show electron micrographs of the high-purity barium titanate powder from the Glidden Company, designated as material B. The manufacturer specifies the average grain size as being 50-100A on the basis of electron-micrographic analysis. The photosedimentometer curve, shown in Fig. 11, indicates a large portion of fine particles below 0.5μ but showed also a large fraction of particles around 1μ. Figures 13 and 14 explain the discrepancy: the individual particles do, indeed, have diameters of the order of 100A but agglomerate surprisingly uniformly into clusters of 0.05 to 0.5μ in diameter. These apparently did not disperse into their individual constituents in the photosedimentometer measurements. Similarly, there are also larger agglomerates with diameters near 1μ, which account for the wide distribution curve presented earlier.

Figures 15 and 16 show electron micrographs of the powder from TAM designated as material D. Figure 15 gives clear evidence for the spread in grain size present in this material. This wide distribution is somewhat obscured in the photosedimentometer curve since this curve is based on weight percent fractions rather than on number of particles.

C. Preparation of Samples

1. General Procedure

The steps in preparation of the samples were as follows:

(a) Addition of organic binder to the as-received powder. The binder chosen was 1.5% cellulose acetate plus 6% dibutyl phthalate in acetone.

(b) Cold pressing of discs in steel dies--5.4 cm (2 1/8 in.) diameter, 1-3 mm thick--at 10,000 psi.

(c) Burning out of the organic binder--650°C for about ½ hr.

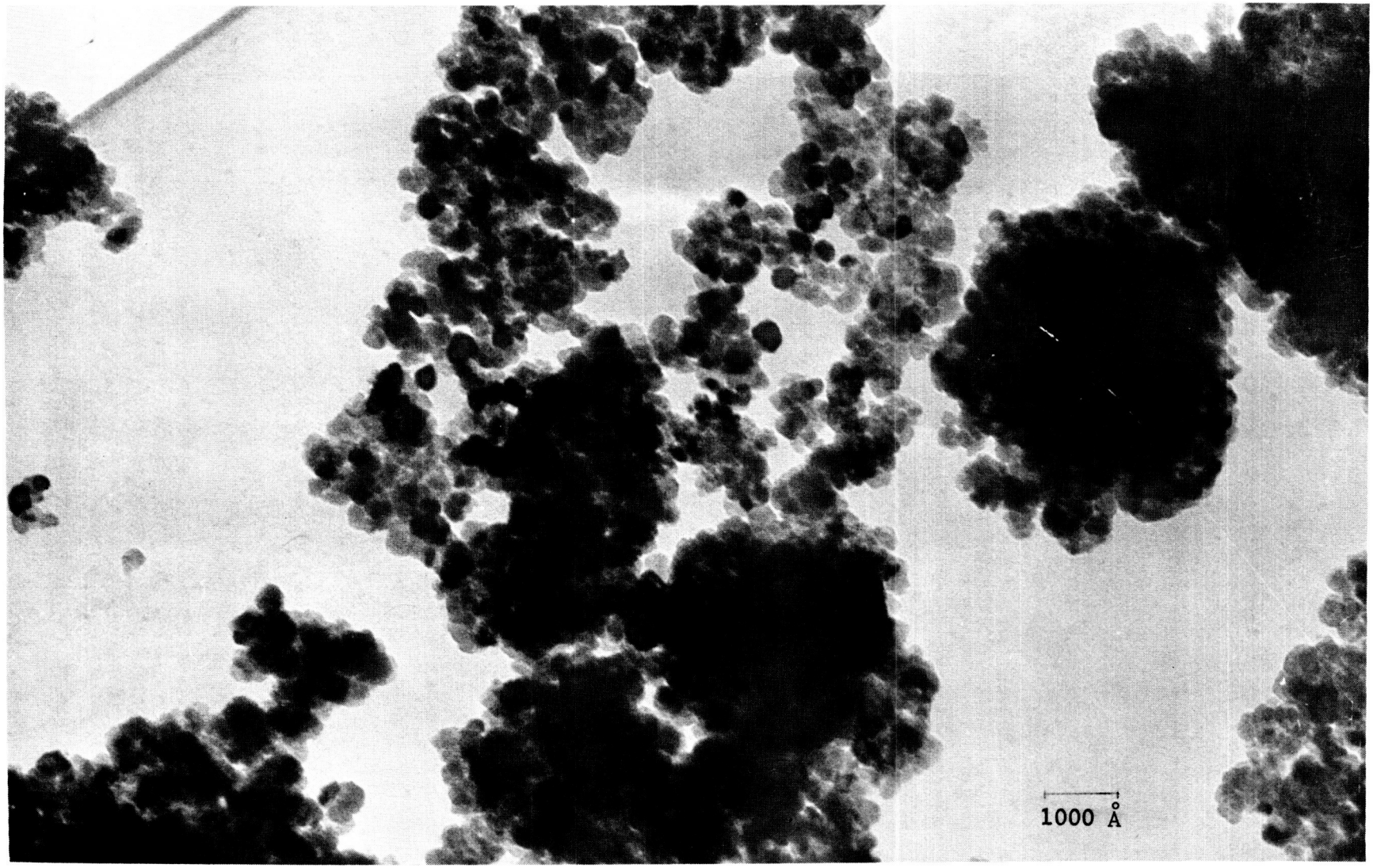

Fig. 13 - ELECTRON MICROGRAPH OF $BaTiO_3$ POWDER B, MAGNIFICATION 135,000

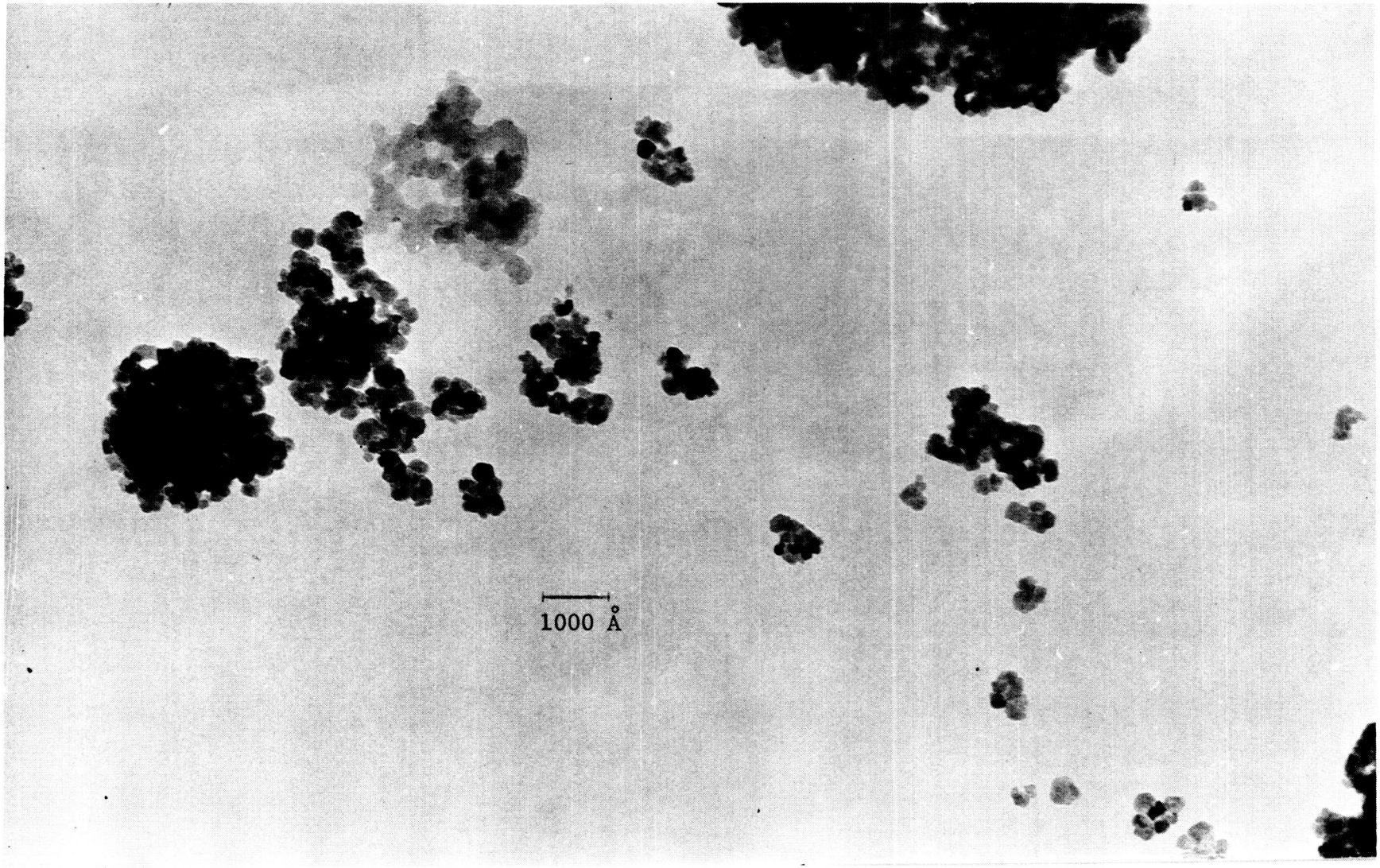

Fig. 14 - ELECTRON MICROGRAPH OF $BaTiO_3$ POWDER B, MAGNIFICATION 114,000

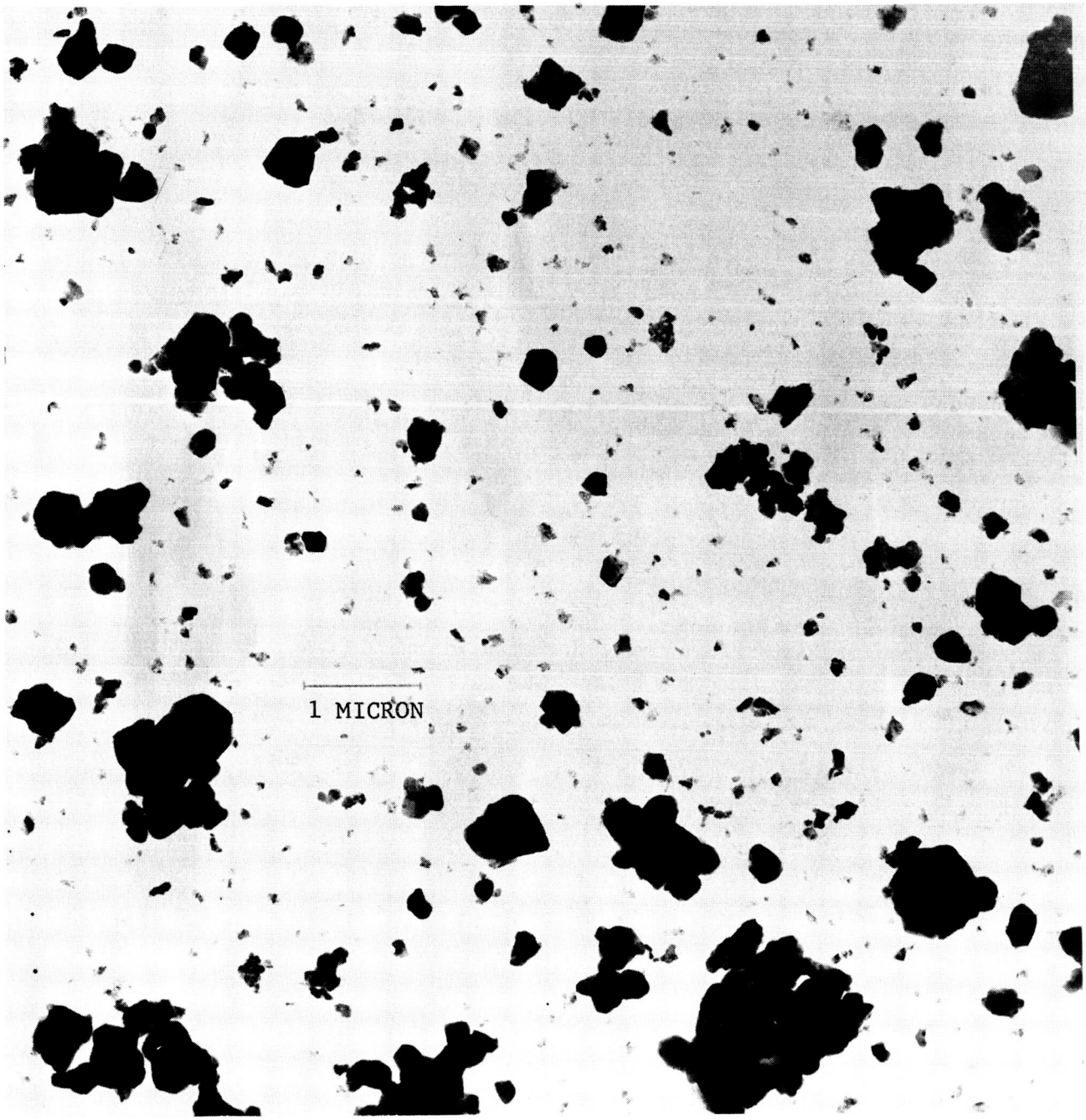

Fig. 15 - ELECTRON MICROGRAPH OF $BaTiO_3$ POWDER D, MAGNIFICATION 20,000

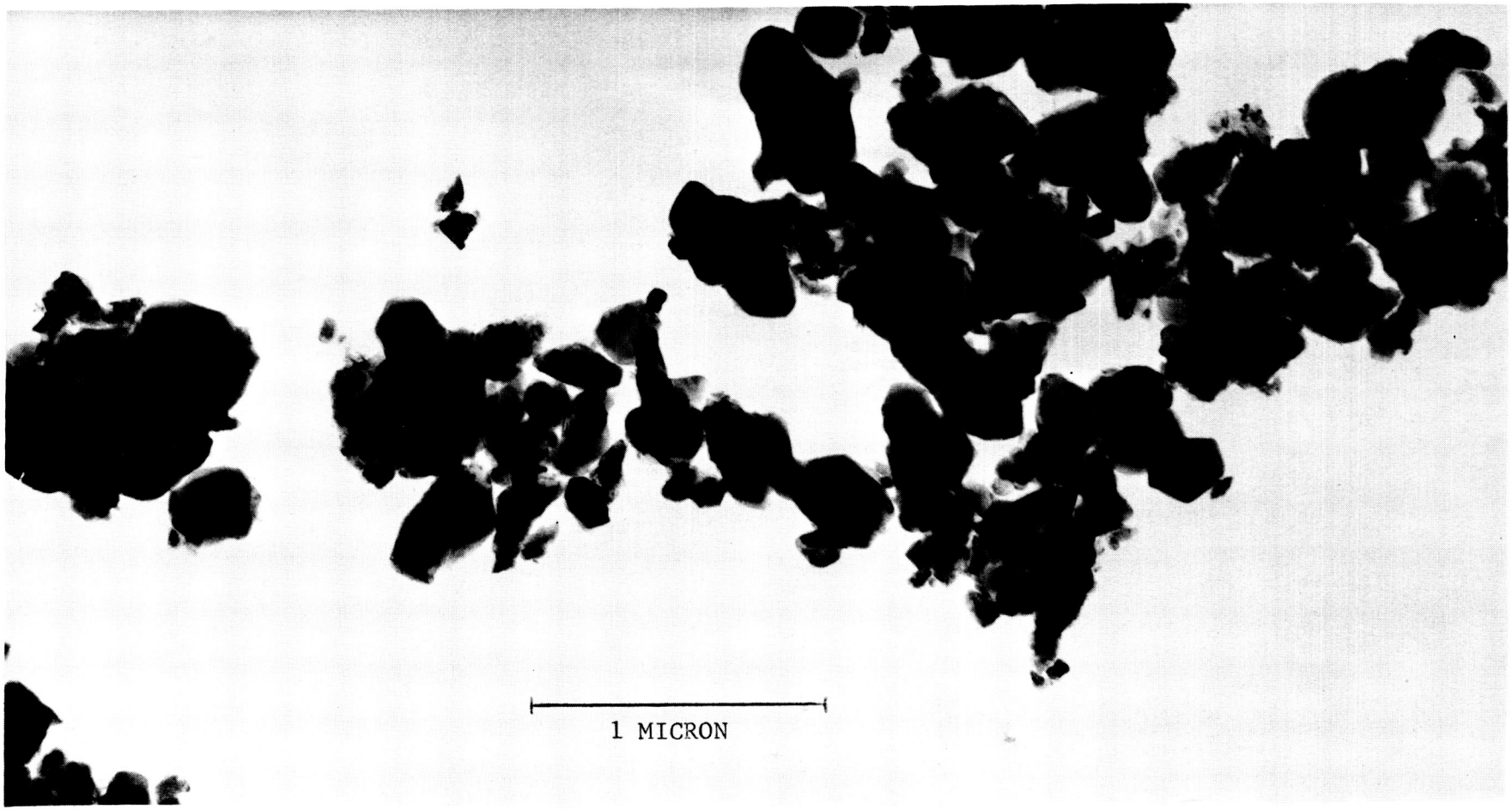

Fig. 16 - ELECTRON MICROGRAPH OF $BaTiO_3$ POWDER D, MAGNIFICATION 50,000

(d) Sintering of the samples at various temperatures. The heating rate was ~250°C/hr. The sintering atmosphere was air with oxygen fed in at a low rate. Other sintering atmospheres will also be investigated.

(e) Application of electrodes: a number of different electrode materials, such as gold, platinum, and silver, applied by vapor deposition and in the form of a paint, have been used.

2. Cold-Compaction Characteristics

In studying the dielectric behavior of $BaTiO_3$ samples, as the material is converted from powder compacts to sintered ceramics, it is important to standardize those parameters that influence the particle interaction. Therefore, the compaction mechanisms for the three materials selected for our experiments were evaluated.

The materials selected were material B, which has an average particle size of ~100A, and materials C and D, which have a particle size distribution around 1μ.

Figure 17 shows the compaction characteristics of materials B, D, and a mixture of 60D + 40B (wt%). The extremely fine powder B almost always laminated when the pressure exceeded about 10,000 psi. The curve, however, was extrapolated as a dotted line to 20,000 psi. The lamination of the fine powder was most probably due to the comparatively large amount of adsorbed gas present in this material. No attempts were made at this time to evacuate the system during pressing since sufficiently high green densities were obtained with corresponding high densities upon sintering.

Figure 18 shows a logarithmic plot of compaction vs pressure. The initial compaction mechanism is different for the three materials, but above about 10,000 psi the slope of the three curves becomes very nearly identical. This indicated that at pressures above 10,000 psi the elastic compression of the powder compacts, which must be the same for all three materials, became a significant

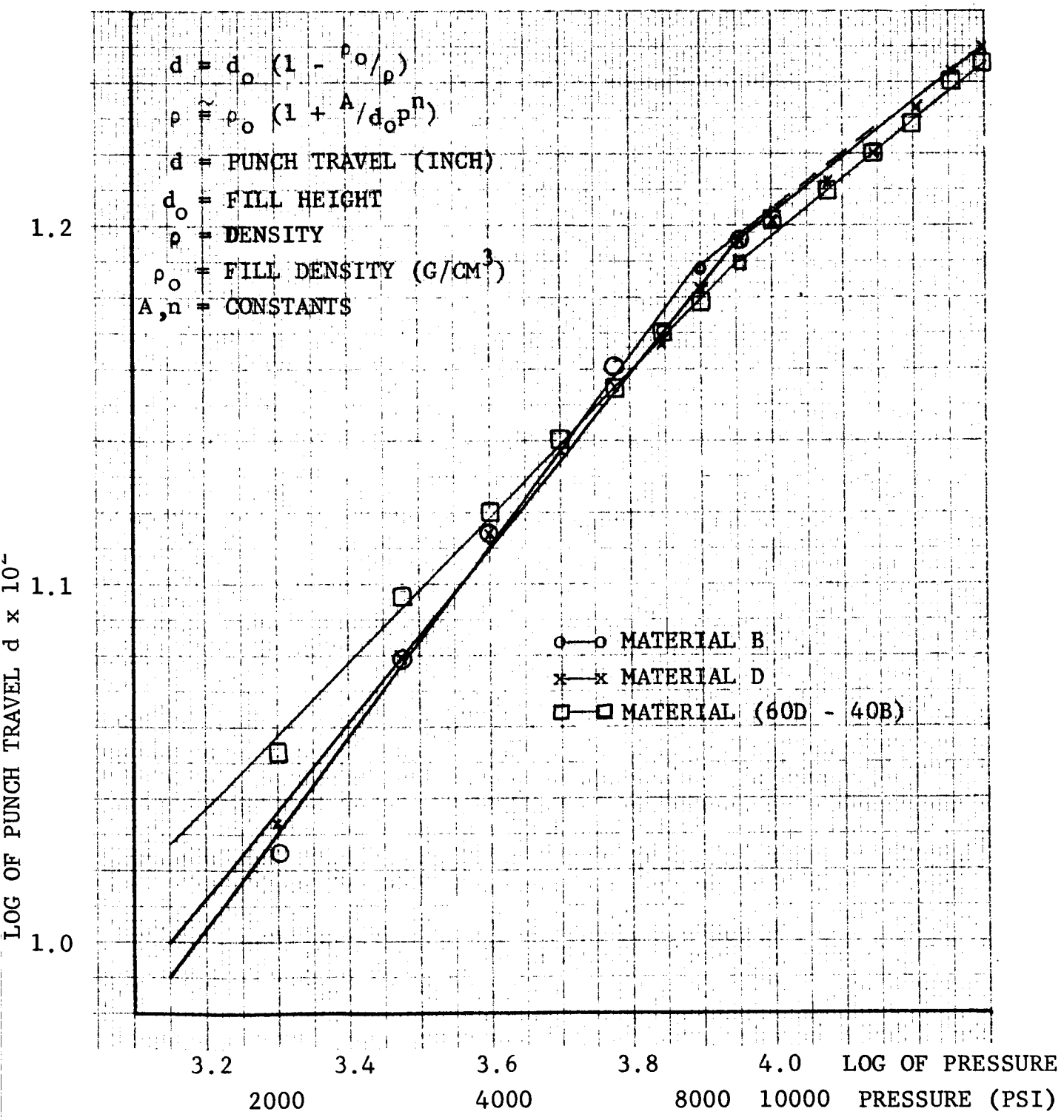

Fig. 17 - COLD COMPACTION CHARACTERISTICS OF BARIUM TITANATE POWDERS OF DIFFERENT PARTICLE SIZE

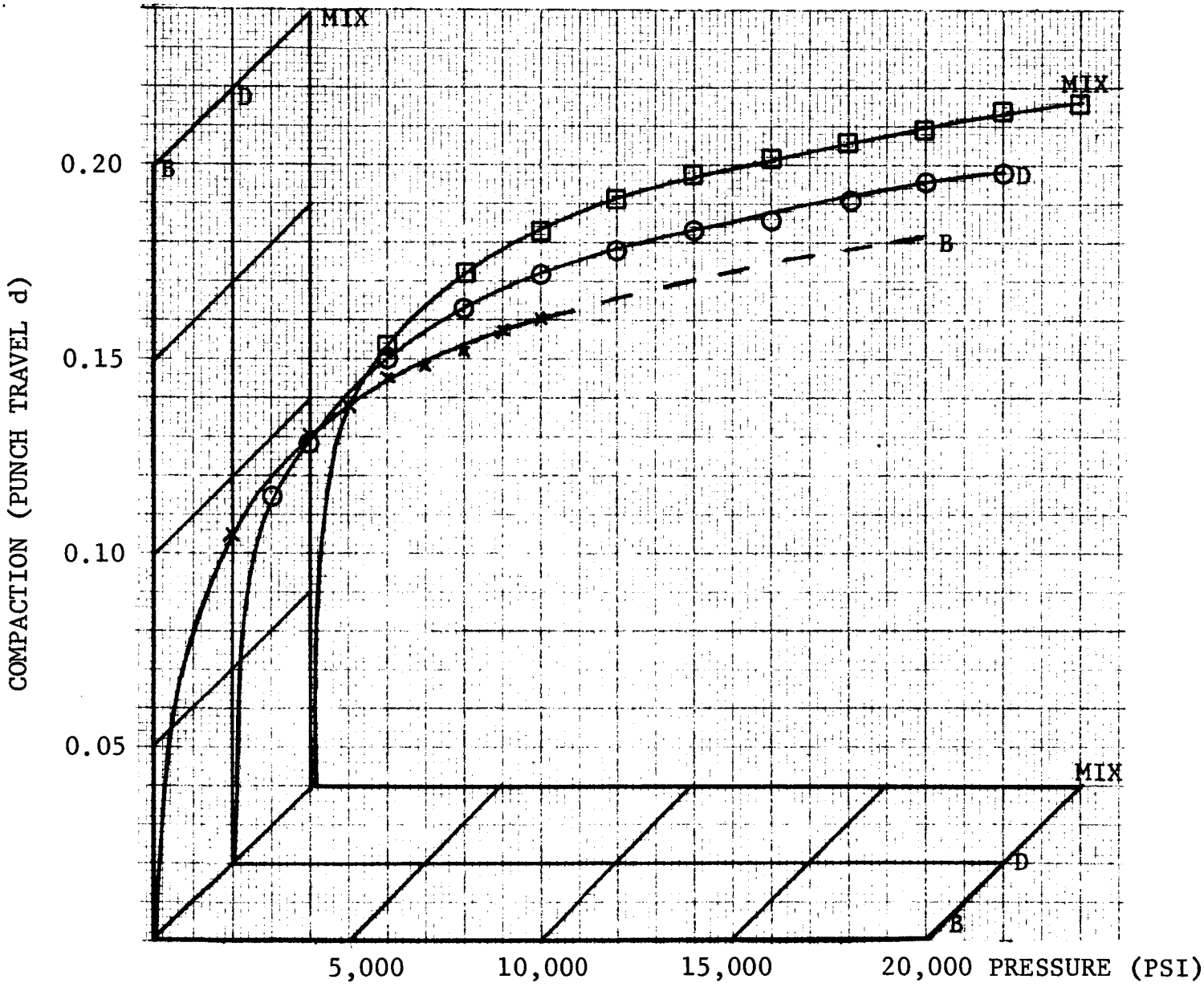

Fig. 18 - COLD COMPACTION OF BARIUM TITANATE OF VARIOUS DIFFERENT PARTICLE SIZES (MATERIALS: B, D, AND MIX OF 60D-40B)

part of the total compaction. Measurements of the dilation of the powder compacts upon pressure release showed that indeed the major portion of the compaction at pressures above 10,000 psi was due to elastic compression rather than to changes in the arrangement of the powder particles. This means that little is gained in terms of permanent compaction by pressing at much more than 10,000 psi pressure. As a standard compaction pressure we have chosen 15,000 psi.

Best results were obtained by pressing at 1500 psi per minute up to the maximum pressure, with no holding time, and releasing the pressure at about the same rate. This procedure yielded sound samples, free of lamination (even with material B), with very little density variation from sample to sample of the same material in the same batch. Green densities were on the order of 45% of theoretical. The amount of powder in the starting mix and procedures involved in the blending of the binder are critical for a constant green density. By standardizing these parameters, the green density variation for powders from different batches (prepared by a cold compaction pressure of 15,000 psi and a pressing rate of 1,500 psi/min) has been controlled to within 1% for the D and B powders, and within 2% for the mixture of 60% D + 40% B powders.

According to Fig. 18, the compaction of the three powders can be represented by one equation for pressures above 10,000 psi:

$$d = 5.6 \times 10^{-2} \, p^{0.163}$$

and for pressures below 10,000 psi down to 1,000 psi:

$$d = 1.0 \times 10^{-2} \, p^{0.312} \quad \text{for material B}$$

$$d = 1.5 \times 10^{-2} \, p^{0.264} \quad \text{for material D}$$

$$d = 2.4 \times 10^{-2} \, p^{0.208} \quad \text{for mixture 60D-40B}$$

where d = decrease in thickness with pressure

p = pressure.

The term d is related to the density ρ of the powder compact:

$$d = d_o(1 - \frac{\rho_o}{\rho})$$

and

$$\rho = \rho_o(1 - \frac{A}{d_o} p^n)^{-1} \simeq \rho_o (1 + \frac{A}{d_o} p^n)$$

where d_o, ρ_o = fill height and fill density at p = 0

A = a constant, the pre-exponential term given above for the three materials

n = the pressure exponent, listed above for the three materials.

D. Dielectric Properties of $BaTiO_3$ Samples

1. Introduction

The characteristics of a surface layer, such as on $BaTiO_3$ grains, can be studied by measuring the frequency dispersion of the ac conductivity and dielectric losses. The interpretation of the results is based on the work of Volger,[2] Fröhlich,[19] and others.

An equivalent circuit has been used to represent the barium titanate grain carrying a surface layer. The circuit consists of a capacitance and parallel resistance representing the bulk of the grain in series with a capacitance and parallel resistance representing the surface layer. This is shown in Fig. 19.

The dispersion relations given in Fig. 19 refer to the following equations for the static (s) and high frequency (∞) dielectric constant (ϵ) and conductivity (σ) for the case of a two-layer dielectric:

$$\epsilon_s = \frac{(d_b + d_v)(d_b \epsilon_b \rho_b^2 + d_v \epsilon_v \rho_v^2)}{(d_b \rho_b + d_v \rho_v)^2}$$

$$\epsilon_\infty = \frac{d_b + d_v}{d_b/\epsilon_b + d_v/\epsilon_v}$$

FREQUENCY RESPONSE OF
EQUIVALENT CIRCUIT

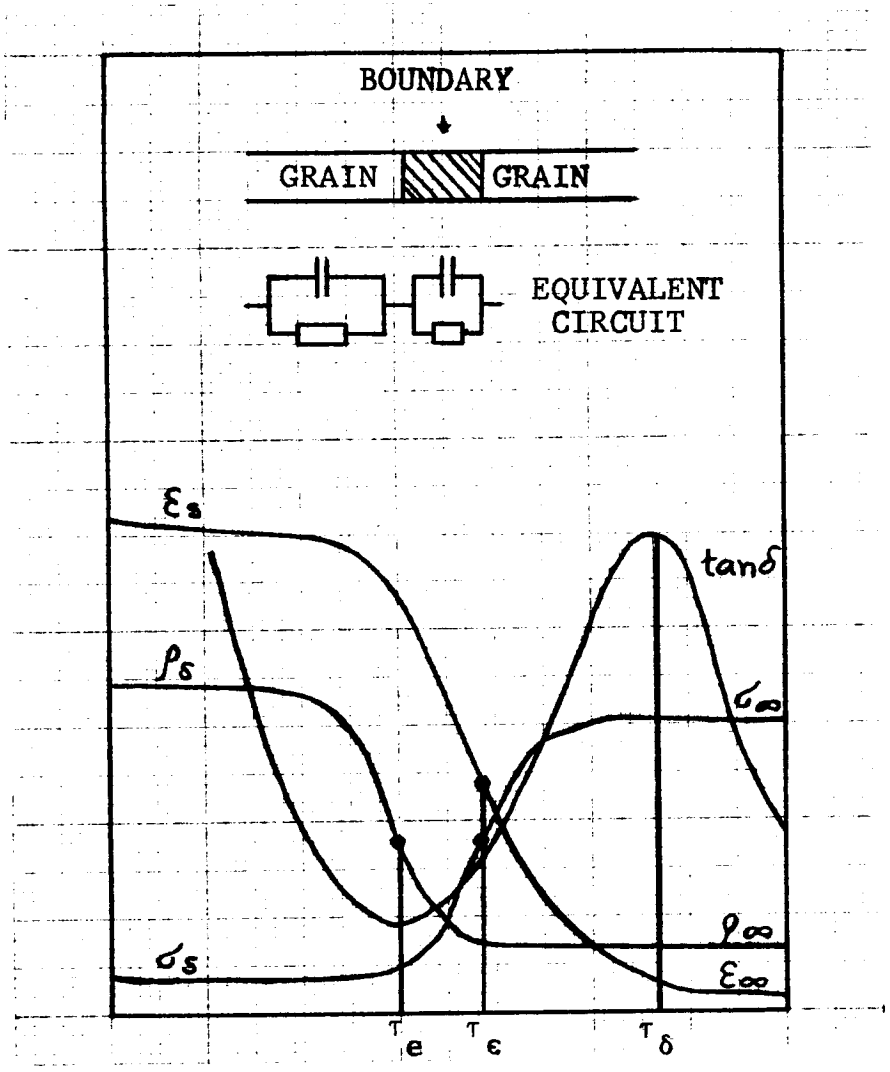

$\omega = 2\pi f$

RELATIONSHIPS FOR EQUIVALENT CIRCUIT

$$\varepsilon = \frac{\varepsilon_s + \varepsilon_\infty \tau_\varepsilon^2 \omega^2}{1+\tau_\varepsilon^2 \omega^2} \qquad \rho = \frac{\rho_s + \rho_\infty \tau_\rho^2 \omega^2}{1+\tau_\rho^2 \omega^2}$$

$$\tan\delta = \frac{\sigma_\infty}{\varepsilon_o \omega \varepsilon_\infty} \frac{(\varepsilon_\infty \sigma_s / \varepsilon_s \sigma_\infty) + \tau_\delta^2 \omega^2}{1+\tau_\delta^2 \omega^2} \qquad \sigma = \frac{\sigma_s + \sigma_\infty \tau_\sigma^2 \omega^2}{1+\tau_s^2 \omega^2}$$

$$\tau_\varepsilon = \tau_\sigma = \varepsilon_o \frac{\varepsilon_s - \varepsilon_\infty}{\sigma_\infty - \sigma_s} = \varepsilon_o \frac{\varepsilon_1 d_2 + \varepsilon_2 d_1}{\sigma_1 d_2 + \sigma_2 d_1}$$

$$\tau_\rho = (\sigma_\infty/\sigma_s)^{\frac{1}{2}} \times \tau_\varepsilon \qquad \tau_\delta = (\varepsilon_\infty/\varepsilon_s)^{\frac{1}{2}} \times \tau_\varepsilon$$

ε = Dielectric Constant, Index s ≡ Static
" ∞ ≡ High Frequency
$\varepsilon_o = 8.86 \times 10^{-14}$ (F/cm)

ρ = Resistivity (ohm-cm)

σ = Conductivity $(\text{ohm-cm})^{-1}$

$\omega = 2\pi f$, f = Frequency (cps)

τ = Relaxation Time

δ = Loss Angle

Fig. 19 - EQUIVALENT CIRCUIT MODEL FOR TWO-LAYER DIELECTRIC, SHOWING QUALITATIVE FREQUENCY DEPENDENCE OF ε, σ, ρ, AND Tan δ AND RELATIONSHIPS BETWEEN THESE QUANTITIES[2]

$$\sigma_s = \frac{d_b + d_v}{d_b/\sigma_b + d_v/\sigma_v}$$

$$\sigma_\infty = \frac{(d_b + d_v)\left(\frac{d_b}{\rho_b^2 \epsilon_b^2} + \frac{d_v}{\rho_v^2 \epsilon_v^2}\right)}{\left(\frac{d_b}{\epsilon_b} + \frac{d_v}{\epsilon_v}\right)^2}$$

The indices b and v refer to grain boundary phase and bulk grain phase, respectively; d is the thickness of the grain or the thickness of the boundary layer, σ is conductivity and ρ is resistivity.

Therefore, it should be possible to obtain valuable information on the dielectric properties and the geometrical configuration of the surface layer phase in $BaTiO_3$ ceramics made from relatively coarse particles with varying additions of extremely fine, submicron grains by treating the ceramic as a two-phase material along the lines discussed above. The treatment of barium titanate ceramics is, however, complicated by the additional effects of ferroelectric domain structures and piezoelectric strains in the tetragonal phase.

2. Results and Analysis on the Dielectric Behavior

In order to evaluate the dielectric properties of $BaTiO_3$ material, through various controlled stages of compaction and bonding, dielectric constant and loss measurements have been carried out.

The results have been obtained by using a General Radio Co., type 1650-A impedance bridge and a type 1690 dielectric sample holder. This bridge has a capacitance accuracy of ± 1%, and dissipation factor accuracy of ± 5%, of measured values, between 20 cps to 20 kcps; for comparative results, this degree of accuracy is sufficient. A General Radio type 1615-A capacitance bridge is available, which has, at 1 kcps, a capacitance accuracy of ± 0.01% + 0.00003 pF and a dissipation factor accuracy of 0.1% + 10^{-5} of measured values. Subsequent dielectric measurements will be done with this instrument.

Dielectric evaluation of $BaTiO_3$ particles was carried out with materials A and B dispersed in paraffin oil. Preliminary results of the effective dielectric constant of the $BaTiO_3$-oil mixtures are shown in Table IV. Figure 20 shows the effective dielectric constant of a two-phase mixture (K_m), consisting of a dispersed phase of $BaTiO_3$ particles of dielectric constant K_1, embedded in a paraffin matrix phase of dielectric constant K_2, for volume fractions (V_1) of the dispersed phase up to 0.3. Calculations are based on the Clausius-Mossotti relation using the Wien form factor for spheres and the correction given by Rushman and Strivens.[7] Rushman and Strivens have shown that their equation for the dielectric constants of two-phase mixtures agrees with experiments on porous $BaTiO_3$ ceramics in the volume fraction range indicated above. The application of Rushman and Strivens' formula to our preliminary results on dispersed $BaTiO_3$ particles yields extremely low dielectric constants for the oil-immersed powders. This may be due to numerous, very small air gaps between the powder particles and the paraffin oil or to a laminar structure of the liquid phase, parallel to the capacitor plates.

The change in the dielectric properties of $BaTiO_3$ material, through various stages of compaction and bonding have been studied for three different types of $BaTiO_3$ powders: material B, material D, and a mixture of 60 wt% D + 40 wt% B. The initial particle size of B and D are significantly different, and their characteristics have been discussed in detail in an earlier section.

Therefore, for each different class of starting powder (D, B, and 60D/40B), we have three different states of packing which implies not only different densities, but also varying contact area between particles and/or grains. Both parameters must be borne in mind when interpreting the results on the dielectric measurements.

The dielectric properties have been measured as a function of frequency and temperature over a range 60 to 10^4 cps and 27°-160°C, respectively. Frequency dispersions of the dielectric constant and

Table IV.

RELATIVE DIELECTRIC CONSTANT OF $BaTiO_3$ PARTICLES EMBEDDED IN PARAFFIN OIL

Material[a]	Volume Fraction of $BaTiO_3$	Dielectric Constant[b] K_m (Mixture)	K_1 ($BaTiO_3$)
P[c]	0	2.02 +	0.01
P + A			
A as received	0.265	2.22	2.91
A calcined 300°C/20 min	0.266	2.20	2.81
P + B			
B as received	0.207	2.35	4.20
B calcined 300°C/20 min	0.203	2.54	6.06

(a) Sample designation as in Table I.

(b) K_m measured at 1 kc; K_1 calculated from Rushman and Striven's equation.[7]

(c) Paraffin oil, Fisher Scientific Co., Cat. No. 0-119, Lot No. 773249.

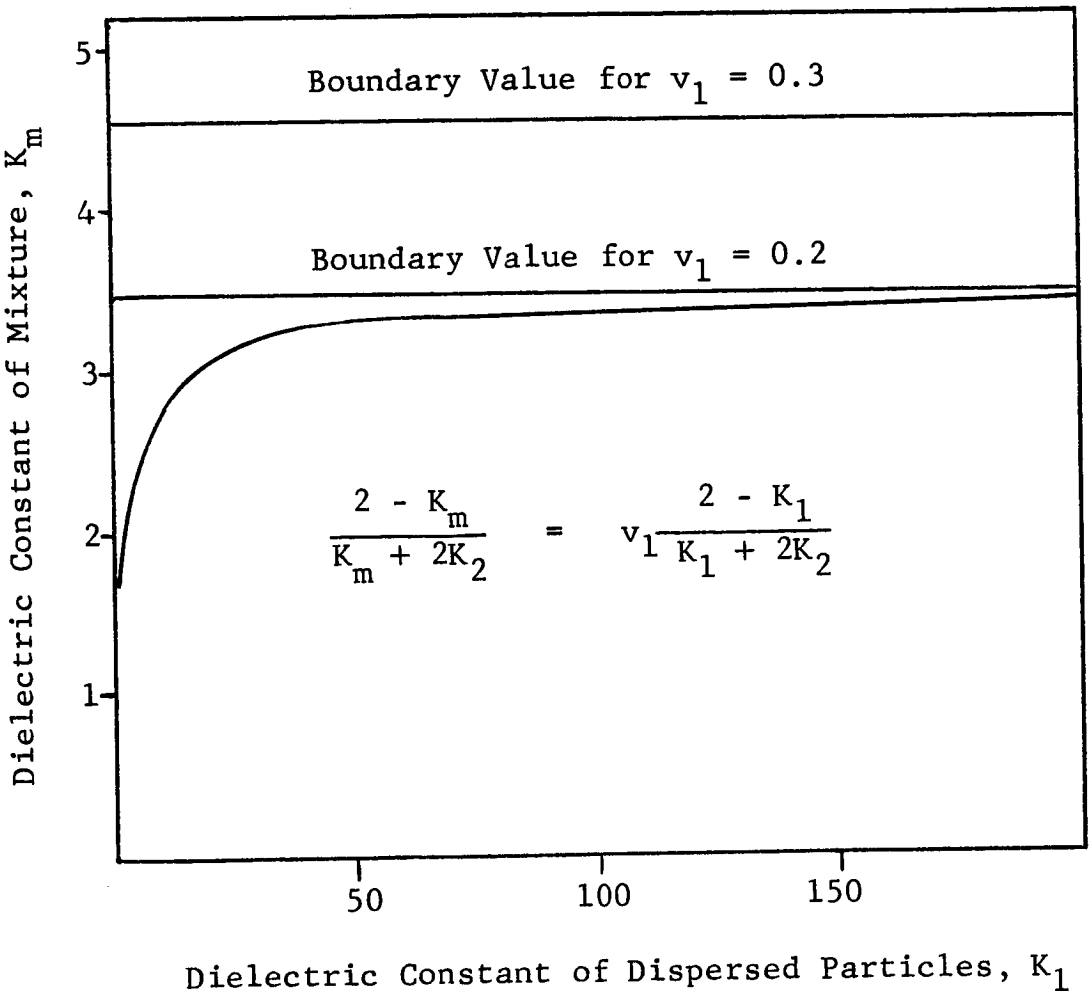

Fig. 20 - EFFECTIVE DIELECTRIC CONSTANT OF TWO-PHASE MIXTURE AS A FUNCTION OF DISPERSED $BaTiO_3$ PARTICLES

loss tangent have also been obtained, in situ, under a vacuum of about 10^{-5} torr and after prolonged exposure to the atmosphere.

In addition, the dielectric behavior of the samples has also been obtained under dc conditions.

For materials D, B, and 60D/40B, three different states of packing have been investigated. In all cases, Sample 1 refers to cold-compacted specimens, which have a density of about 47% of the theoretical value; Sample 2 refers to specimens which have been subjected to a maximum sintering temperature of 1250°C and have been densified to 88% of theoretical; and Sample 3 refers to specimens sintered at 1325°C and have a density of 96% of theoretical. The absolute values of the densities are not significant because we are examining the effects of relative changes in the microstructure on the dielectric behavior.

Figures 21 to 32 show the frequency dispersions of the dielectric constant (K') and loss tangent (tan δ) for the above-mentioned samples. The frequency dispersion of dielectric measurements indicates the nature of the surface layer in relation to that of the grain. Based on interfacial polarization effects, if the surface layer or grain boundary in the $BaTiO_3$ specimens has a conductance higher than the grain, a relatively small amplitude of the tan δ peak should be observed, along with a small capacitance dispersion and a large conductance dispersion. On the other hand, if the boundary layer is lower in conductance than the bulk, a large dispersion of tan δ should be expected.

The frequency dispersions of the dielectric properties measured in air at temperatures corresponding to 27°, 45°, 70°, 100°, 130°, and 160°C are shown in Figs. 21 to 28.

The results indicate that cold-compacted specimens, where the density is only 47% of theoretical, exhibit a larger frequency dispersion of K' and tan δ than the sintered specimens, which have a density $\geq$ 90% of theoretical. However, well-defined peak functions for the frequency dispersion of K' and tan δ are not evident for these specimens in the frequency range 10^2-10^4 cps. Because of the

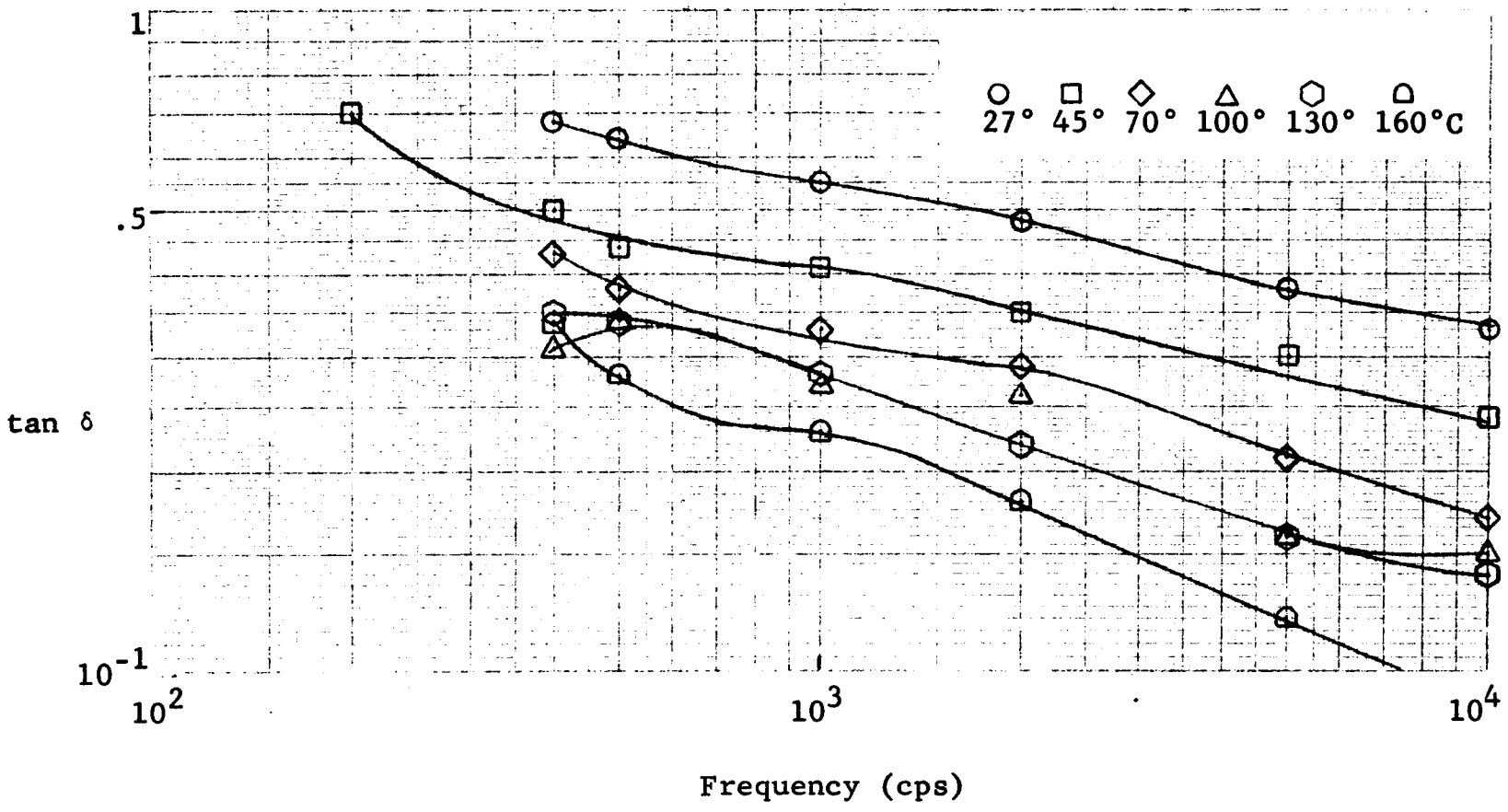

Fig. 21(a) - FREQUENCY DISPERSION OF TAN δ OF $BaTiO_3$
SAMPLE D1 (COLD COMPACTED)

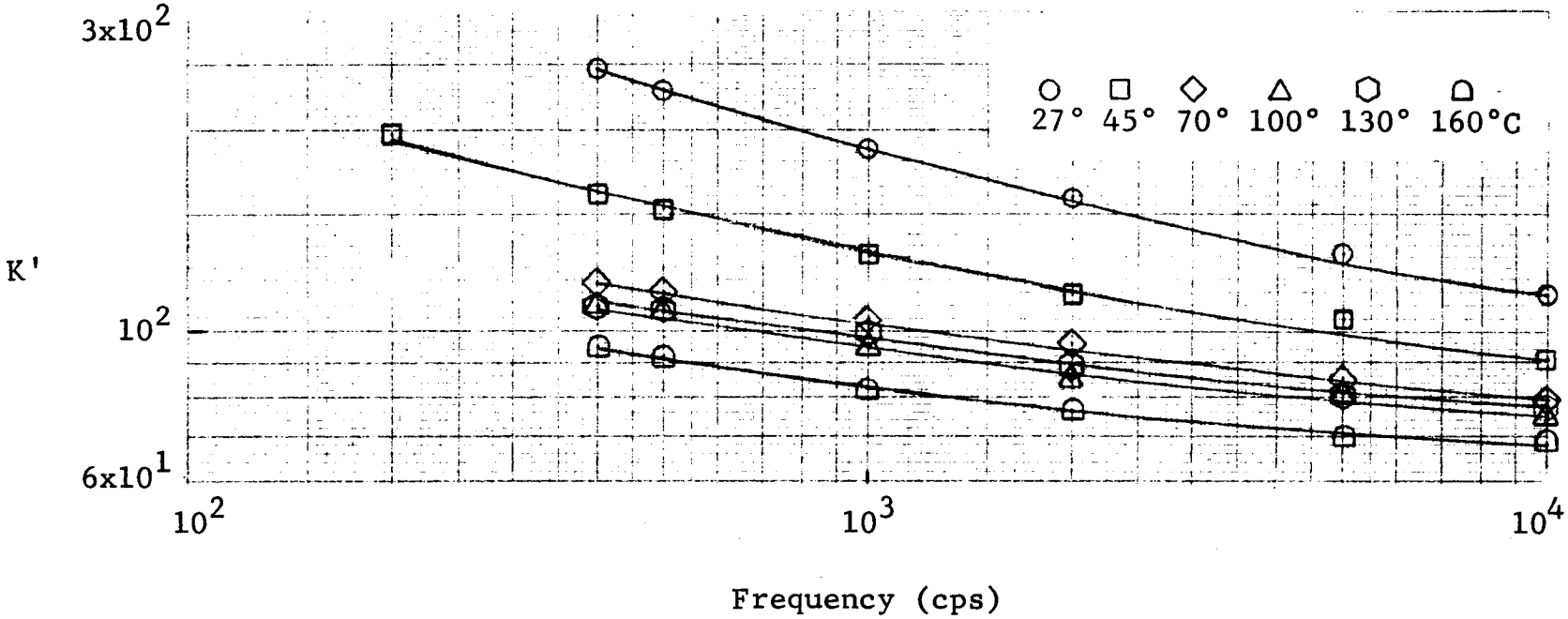

Fig. 21(b) - FREQUENCY DISPERSION OF RELATIVE DIELECTRIC CONSTANT K' OF $BaTiO_3$ SAMPLE D1 (COLD COMPACTED)

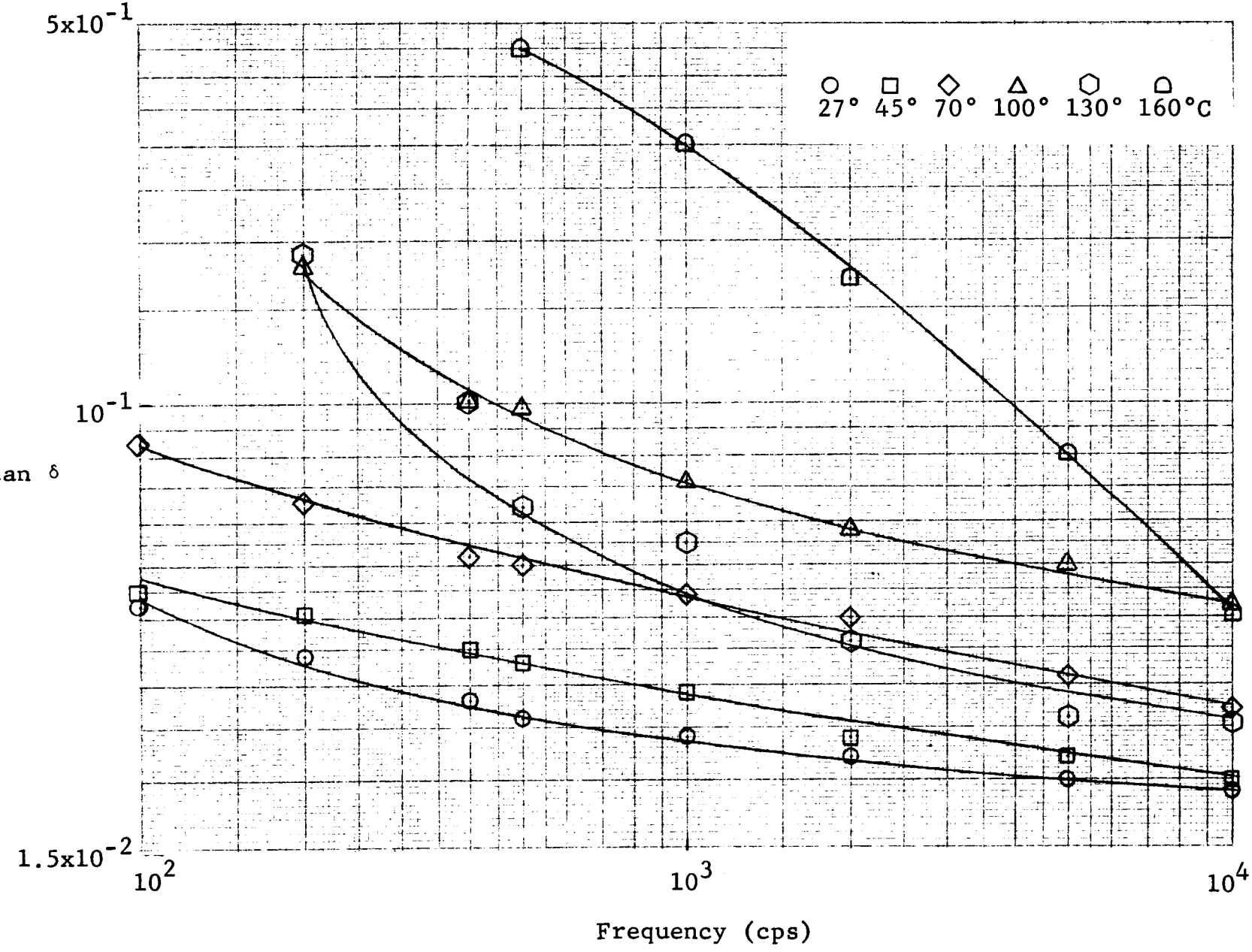

Fig. 22(a) - FREQUENCY DISPERSION OF TAN δ OF $BaTiO_3$
SAMPLE D2 (SINT. 1250°C)

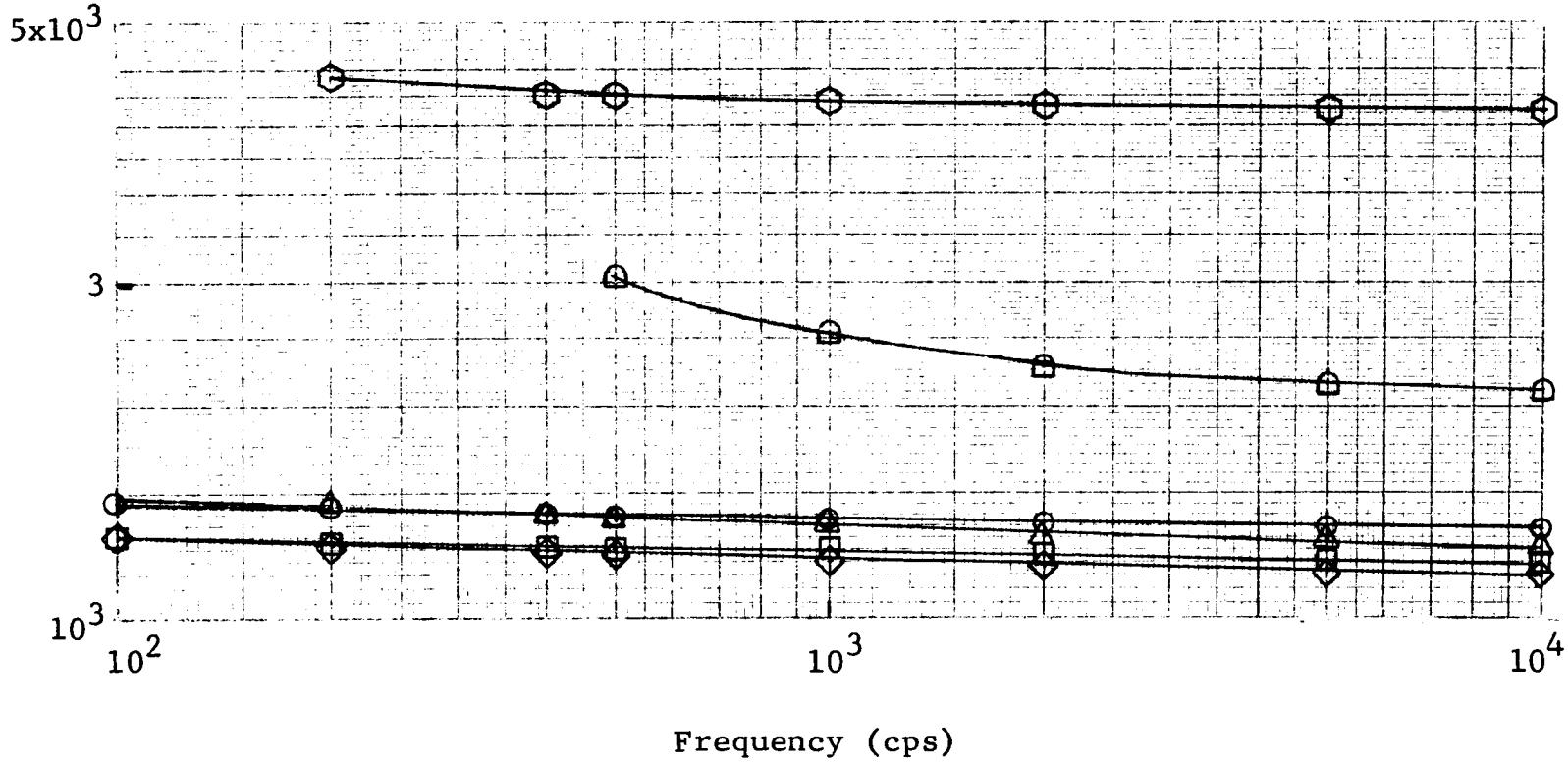

Fig. 22(b) - FREQUENCY DISPERSION OF RELATIVE DIELECTRIC CONSTANT K' OF $BaTiO_3$ SAMPLE D2 (SINT. 1250°C)

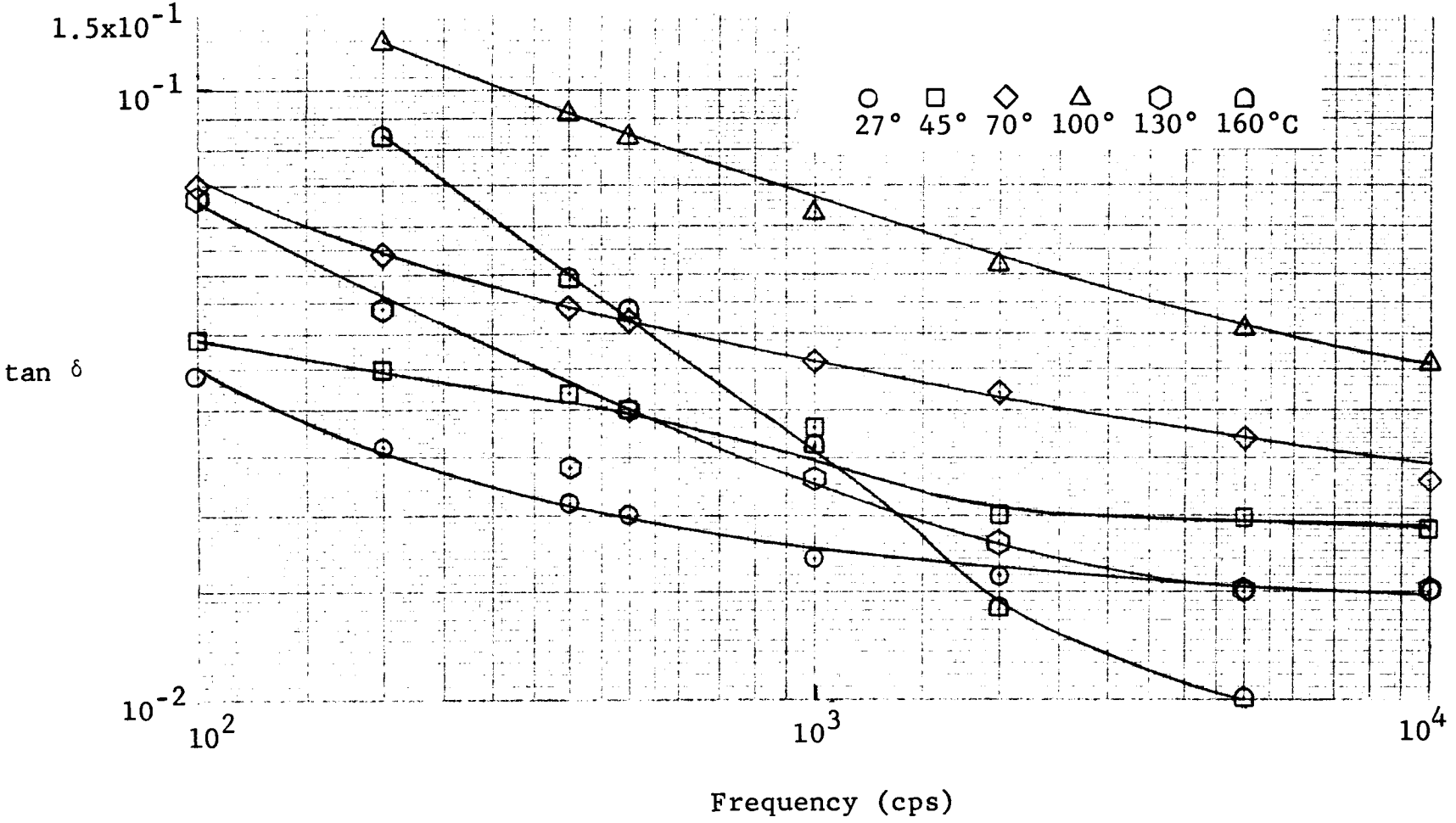

Fig. 23(a) - FREQUENCY DISPERSION OF TAN δ OF $BaTiO_3$
SAMPLE D3 (SINT. 1320°C)

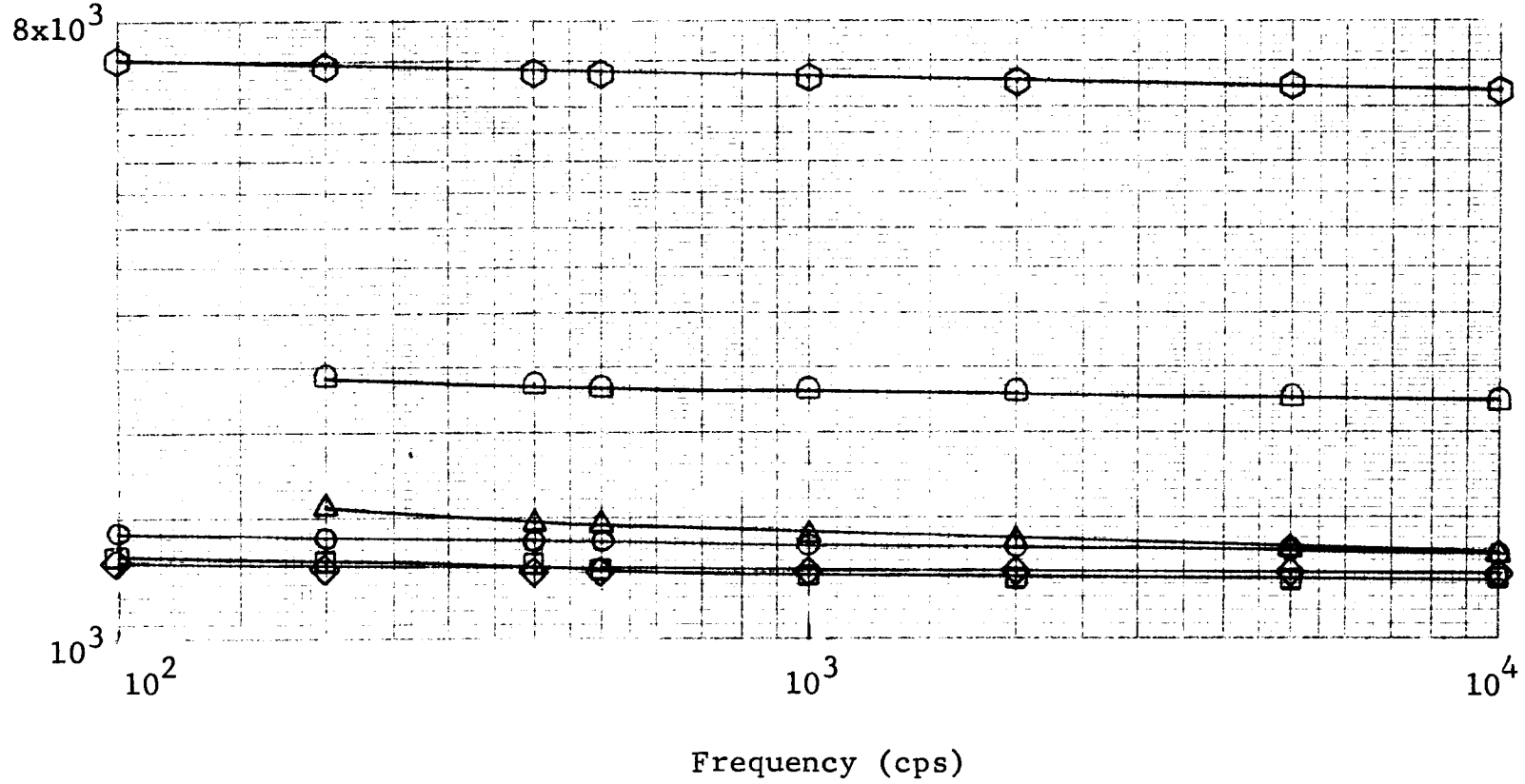

Fig. 23(b) - FREQUENCY DISPERSION OF RELATIVE DIELECTRIC CONSTANT K' OF $BaTiO_3$ SAMPLE D3 (SINT. 1320°C)

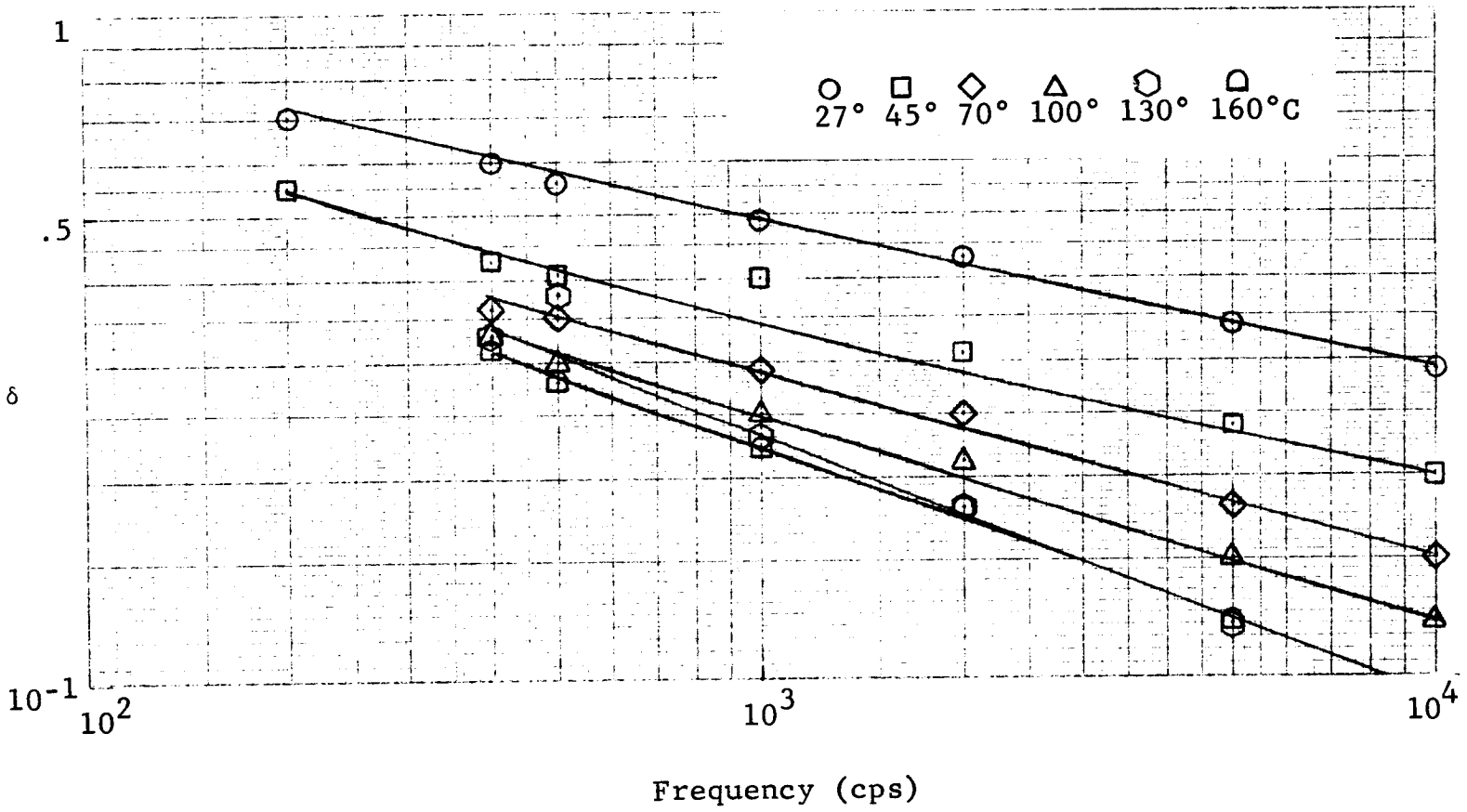

Fig. 24(a) - FREQUENCY DISPERSION OF TAN δ OF $BaTiO_3$
SAMPLE B1 (COLD COMPACTED)

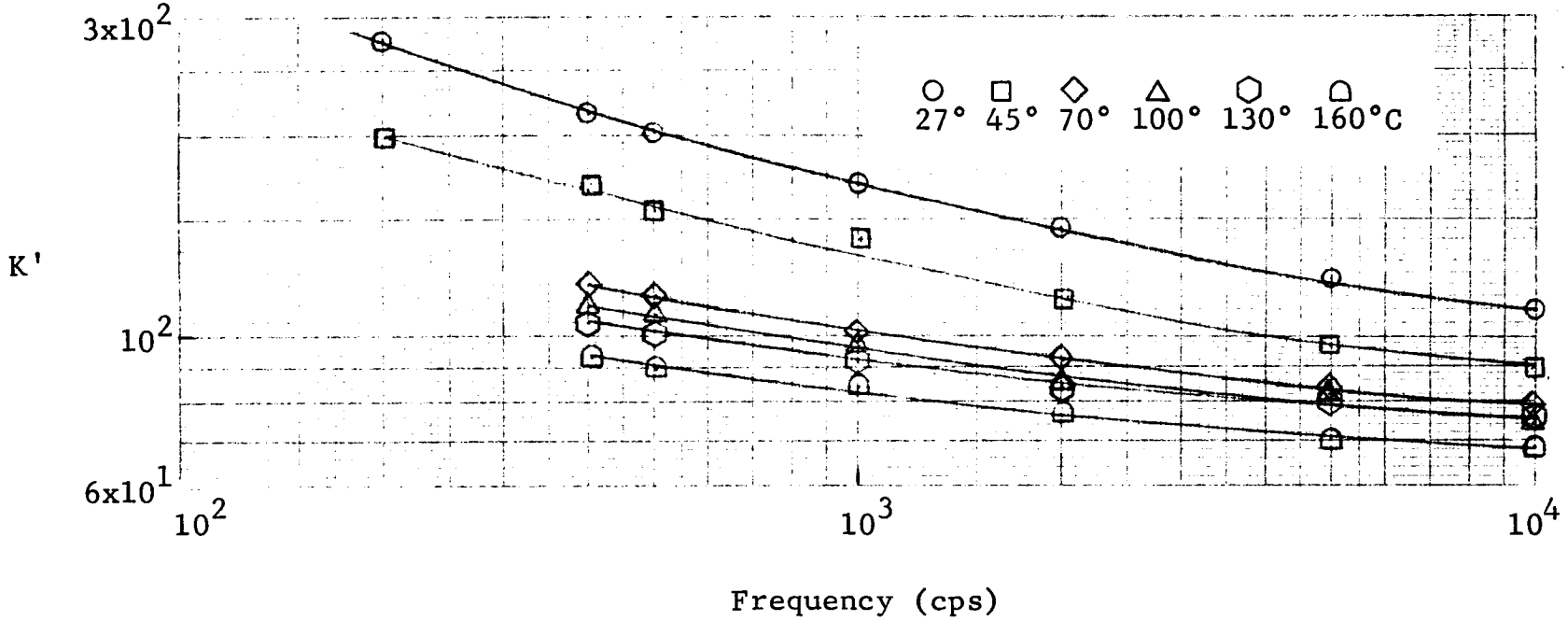

Fig. 24(b) - FREQUENCY DISPERSION OF RELATIVE DIELECTRIC CONSTANT K' OF $BaTiO_3$ SAMPLE B1 (COLD COMPACTED)

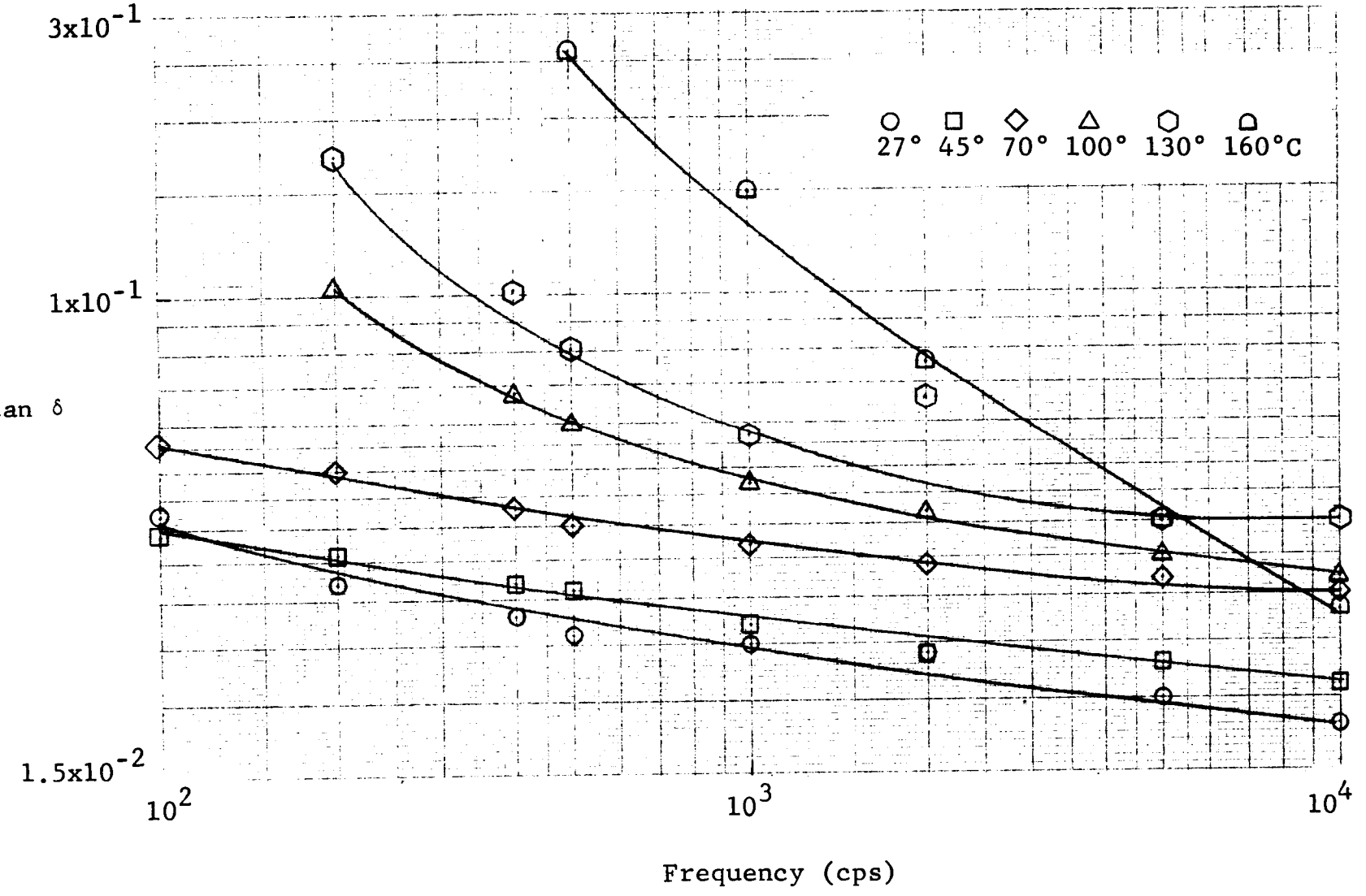

Fig. 25(a) - FREQUENCY DISPERSION OF TAN δ OF $BaTiO_3$
SAMPLE B2 (SINT. 1250°C)

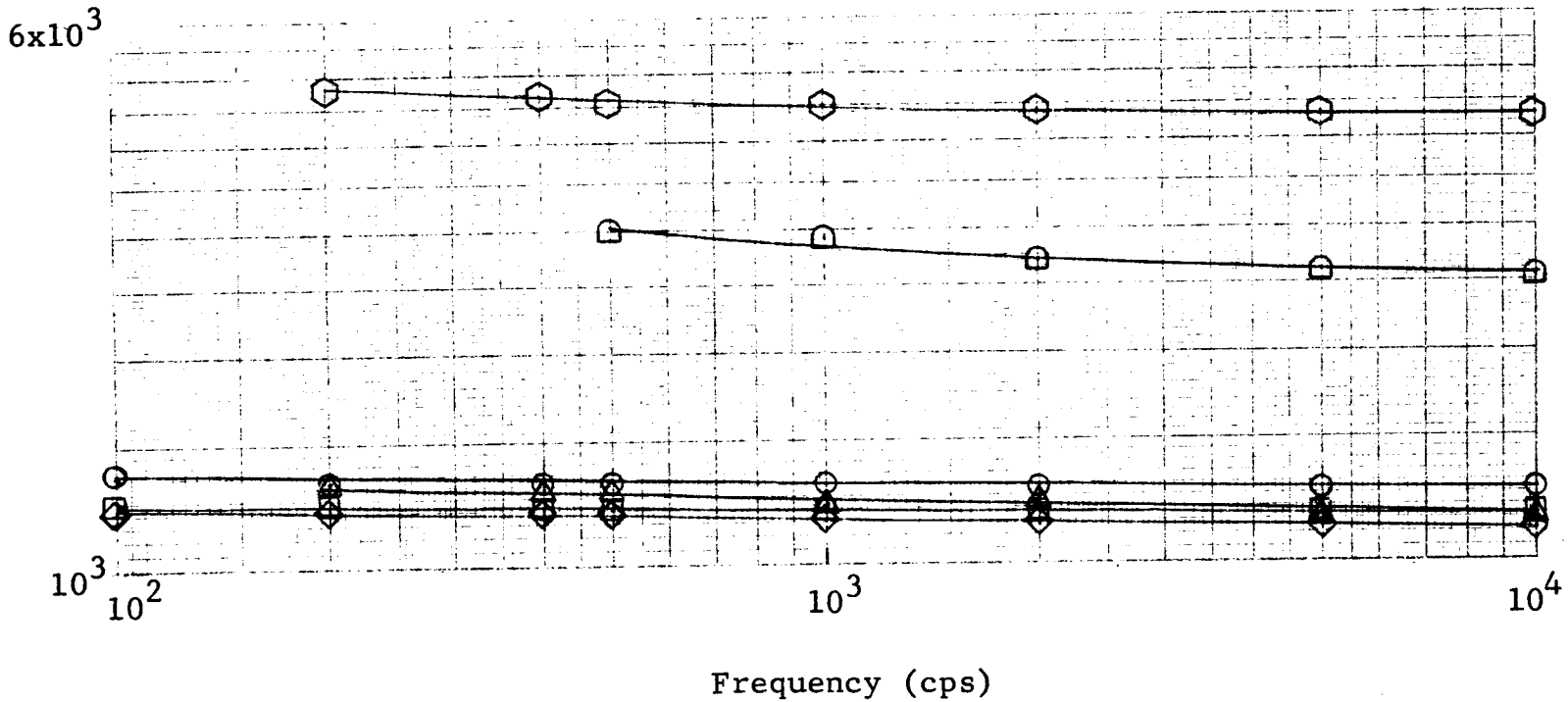

Fig. 25(b) - FREQUENCY DISPERSION OF RELATIVE DIELECTRIC CONSTANT K' OF $BaTiO_3$ SAMPLE B2 (SINT. 1250°C)

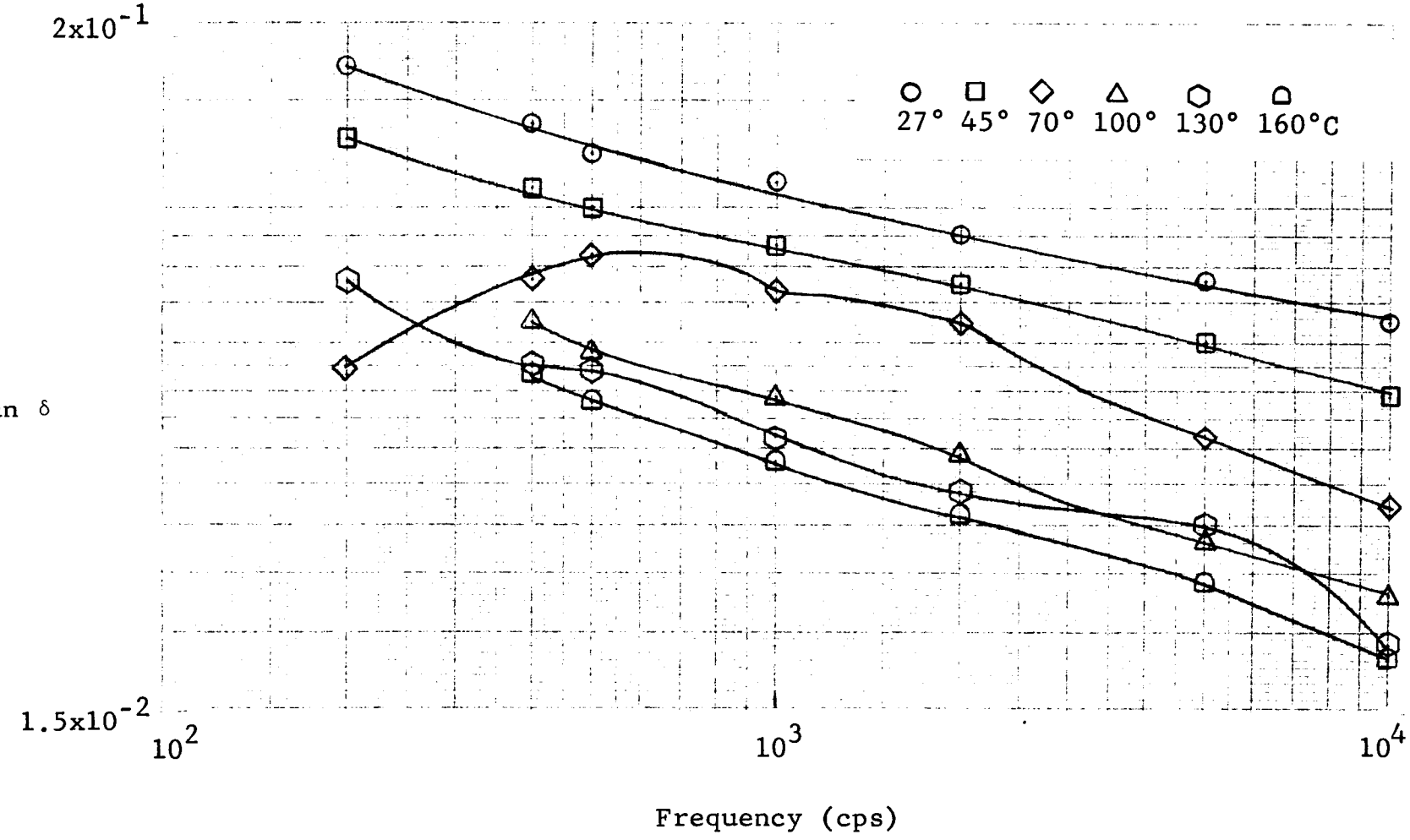

Fig. 26(a) - FREQUENCY DISPERSION OF TAN δ OF $BaTiO_3$
SAMPLE 60D/40B-1 (COLD COMPACTED)

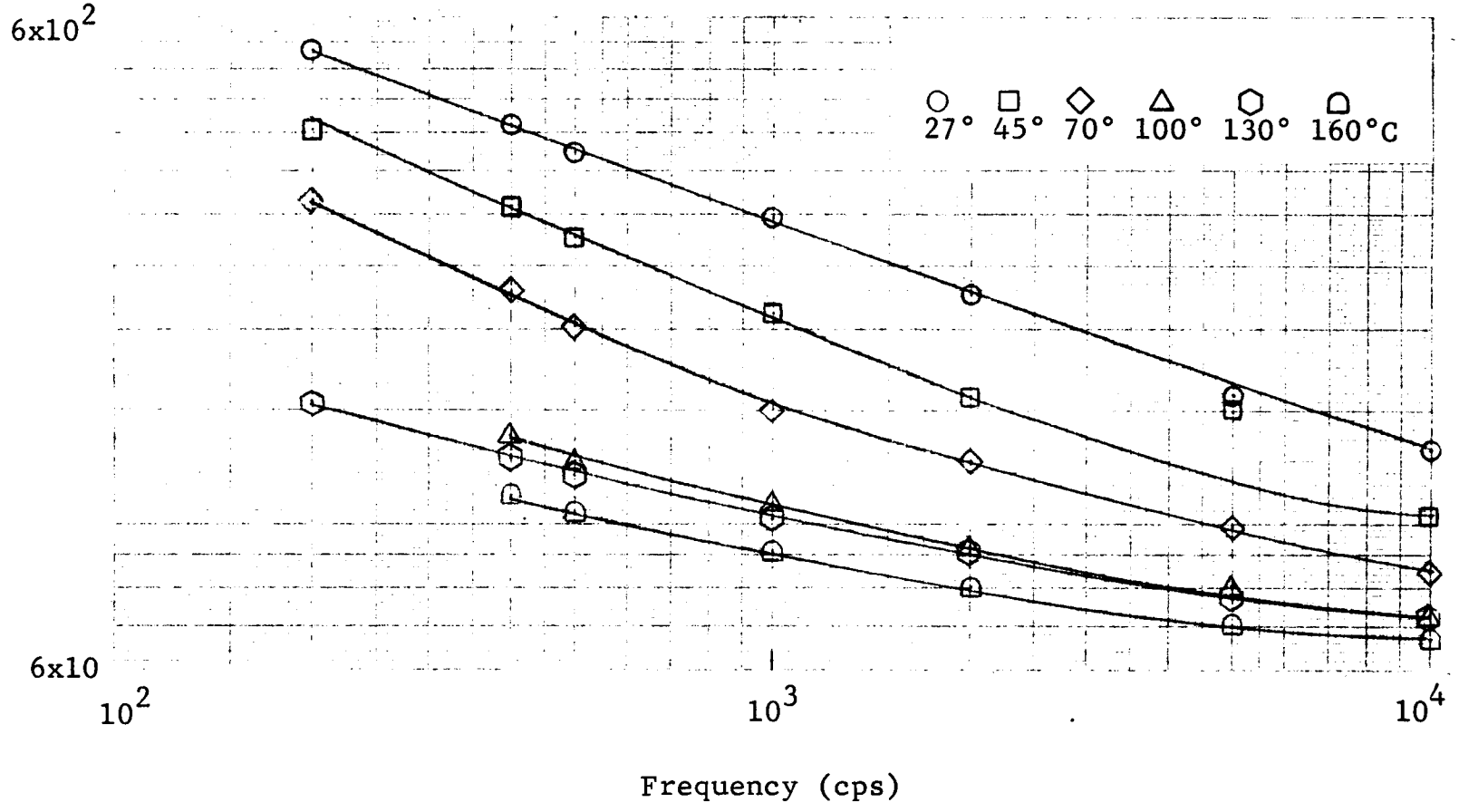

Fig. 26(b) - FREQUENCY DISPERSION OF RELATIVE DIELECTRIC CONSTANT K' OF $BaTiO_3$ SAMPLE 60D/40B-1 (COLD COMPACTED)

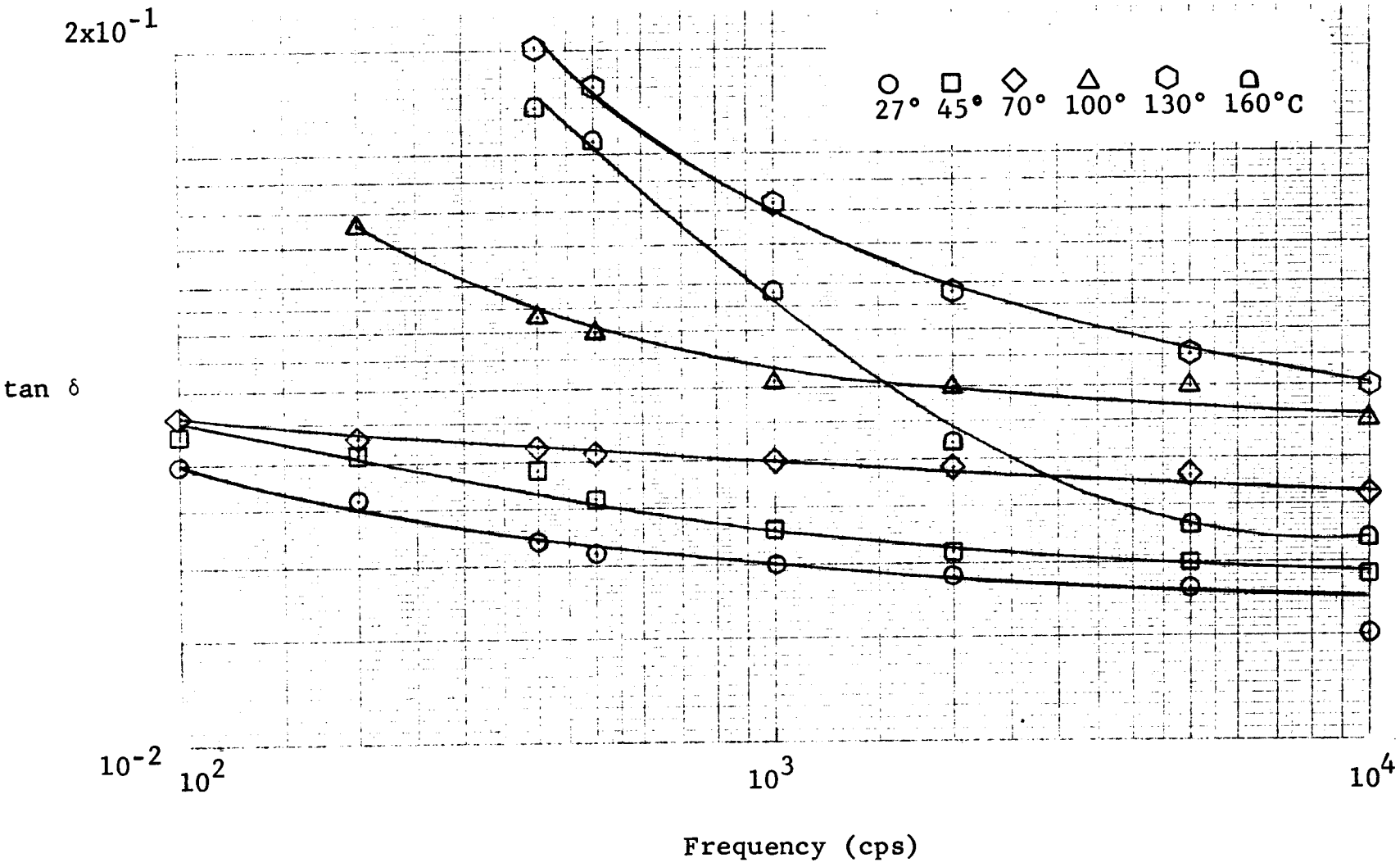

Fig. 27(a) - FREQUENCY DISPERSION OF TAN δ OF $BaTiO_3$
SAMPLE 60D/40B-2 (SINT. 1250°C)

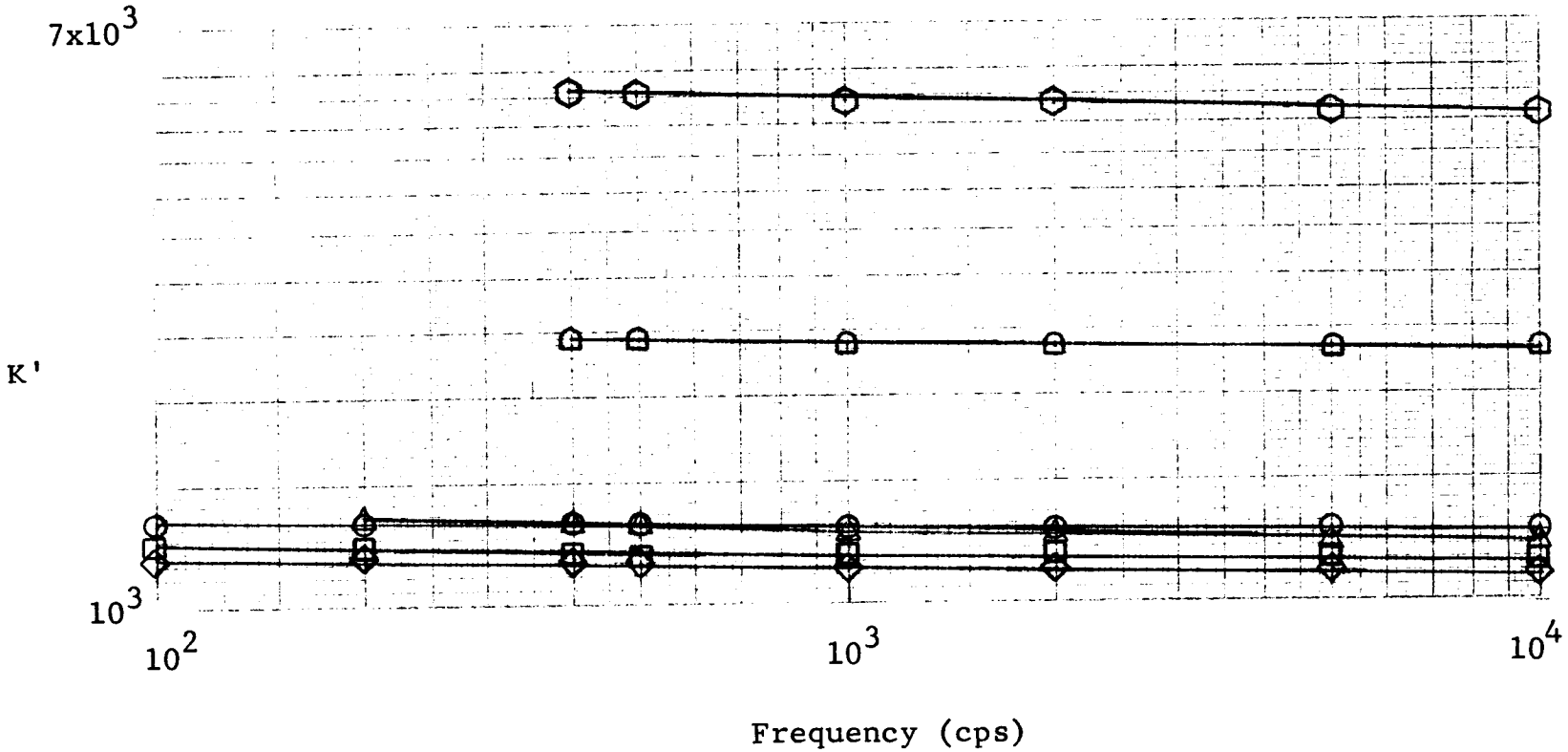

Fig. 27(b) - FREQUENCY DISPERSION OF RELATIVE DIELECTRIC CONSTANT K' OF $BaTiO_3$ SAMPLE 60D/40B-2 (SINT. 1250°C)

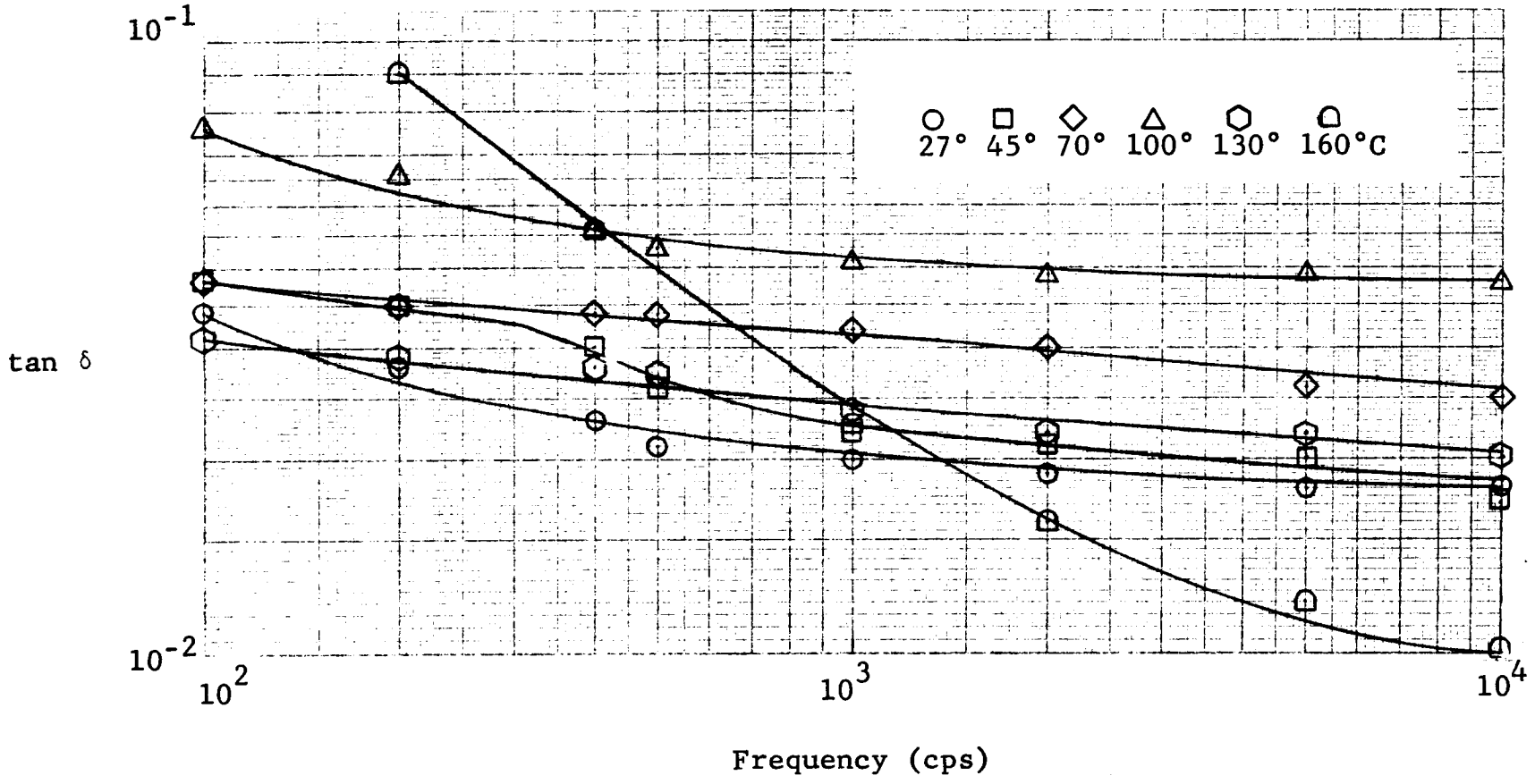

Fig. 28(a) - FREQUENCY DISPERSION OF TAN δ OF $BaTiO_3$
SAMPLE 60D/40B-3 (SINT. 1320°C)

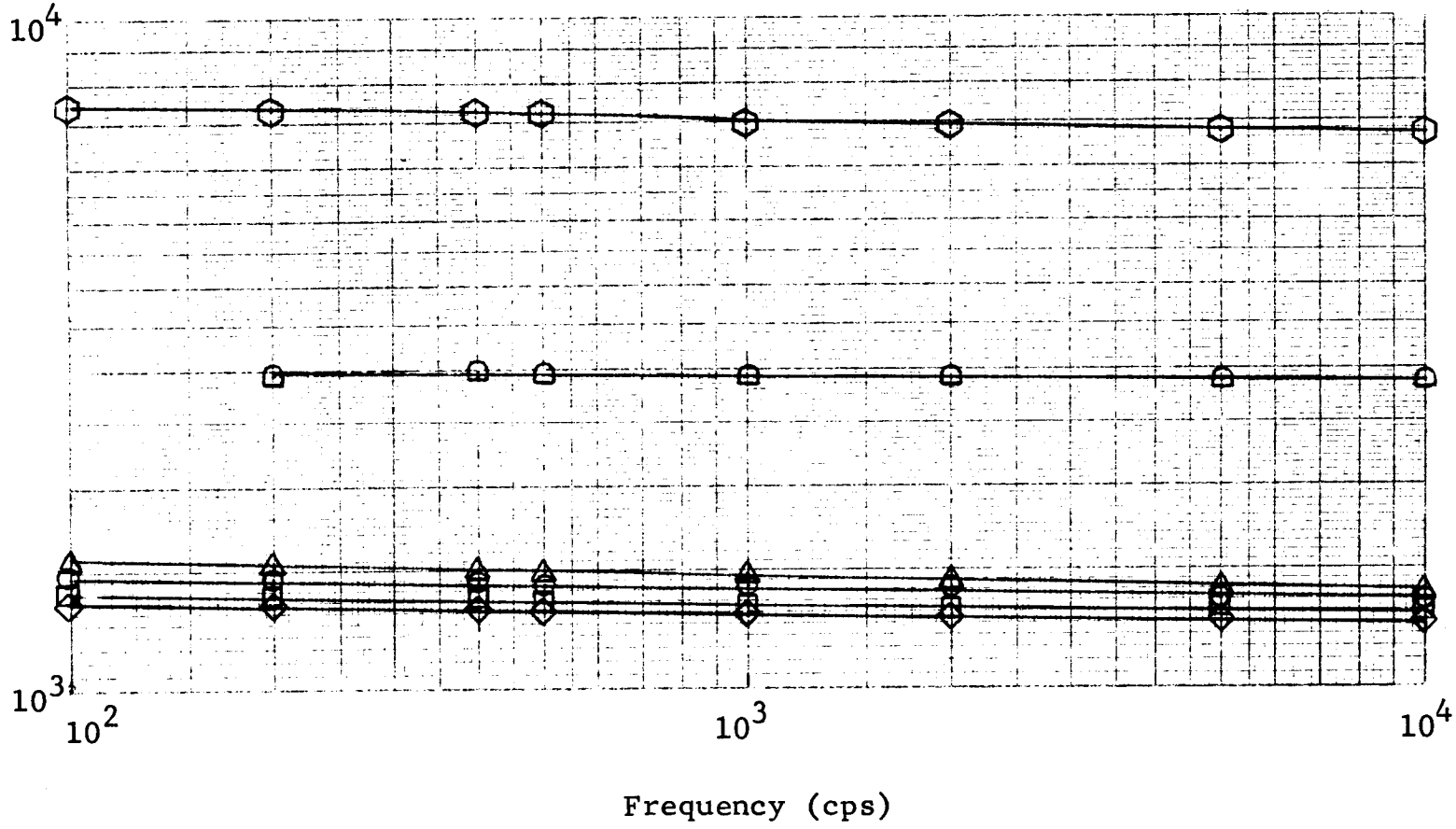

Fig. 28(b) - FREQUENCY DISPERSION OF RELATIVE DIELECTRIC CONSTANT K' OF $BaTiO_3$ SAMPLE 60D/40B-3 (SINT. 1320°C)

broad dispersion that is obtained, it is essential to make measurements at frequencies less than 10^2 cps and, further, to separate the dc and ac losses. For instance, an increase in temperature may increase the dc conductivity to an extent that tan δ peaks for relaxation losses are hidden.

Some interesting trends can be pointed out in the present results. In all cases, the cold-compacted specimens show a decrease in K' and especially tan δ with increasing temperature, whereas the reverse is true for sintered specimens. The temperature coefficient characteristics of K' and tan δ in cold-compacted, highly porous specimens is probably due to the depletion of free charge carriers from the adsorption of water and the effects of $(OH)^-$ ions, or a more complex defect mechanism associated with the formation of cationic vacancies due to injection of protons. The significant role of adsorbed $(OH)^-$ ions has been shown in subsequent results.

Materials D and B, although having different particle sizes, do not show any significant differences in dielectric properties in either the cold-compacted or the sintered specimens, as indicated by the data in Figures 21 to 25. However, the mixture of 60D/40B does show some interesting trends. Specimens prepared from this material have different dielectric characteristics from either D or B since its properties do not lie between those of its constituent powders. Among the cold-compacted specimens, the 60D/40B sample has a higher K' and lower tan δ than samples from materials D or B; but as the material sintered, this difference tends to diminish. Dielectric properties of 60D/40B (different from those of D and B in the cold-compacted state) are probably due to a change in contact area between particles, rather than absolute porosity or particle size. Further experimentation is necessary to establish these results.

Frequency dispersions of the loss tangent of nonferroelectric cubic $BaTiO_3$ material (shown by values obtained at 160°C) may be compared with that obtained for the ferroelectric tetragonal $BaTiO_3$ material (shown by values obtained below the Curie temperature,

such as 75°C). The nonferroelectric material has a larger frequency dispersion of tan δ in the 10^2 to 10^3 cps frequency range. However, its loss tangent is significantly reduced between 10^3 to 10^4 cps. The slope of the frequency dispersion of tan δ of nonferroelectric $BaTiO_3$ at 160°C changes more rapidly as a function of the state of compaction and densification, than in the case of the ferroelectric $BaTiO_3$. This indicates the differences in dielectric relaxations. Results show that dielectric behavior of $BaTiO_3$ ceramics can be followed with a change in grain size, porosity, contact area of grains, and internal stress.

Figures 29 and 30 show the change in the dielectric properties of $BaTiO_3$ specimens under vacuum (after storage in a desiccator) and on prolonged exposure to the atmosphere. These results indicate the effects of gaseous environments on the surface layer characteristics in $BaTiO_3$ as a function of its microstructure.

The cold-compacted, porous sample (D-1), as reported previously, has a large frequency dispersion of K' and tan δ. This specimen was exposed to air for a number of days after preparation and then measured for its dielectric properties. Subsequently, when the same specimen was stored in a desiccator for a few days and its dielectric properties measured under a vacuum of 5×10^{-5} torr, a significant difference was found in the frequency dispersion and the measured absolute values of K' and tan δ. The results are shown in Fig. 29. The measurement in vacuum, on the desiccated sample, did not show any marked frequency dispersion of K' and tan δ. The capacitance of the sample was reduced from a value of about 1650 pF to about 450 pF at 200 cps. Similarly, there was a marked reduction in the value of tan δ over the entire frequency range (40 to 10^4 cps), with the tan δ values approaching a constant value of about 0.025 at 10^4 cps, for both types of environmental exposures. The calculated ac conductivity of the sample was changed from a value of 3.3×10^{-10} mho-cm in vacuum to 3×10^{-8} mho-cm, on prolonged exposure to air, at 1 kc.

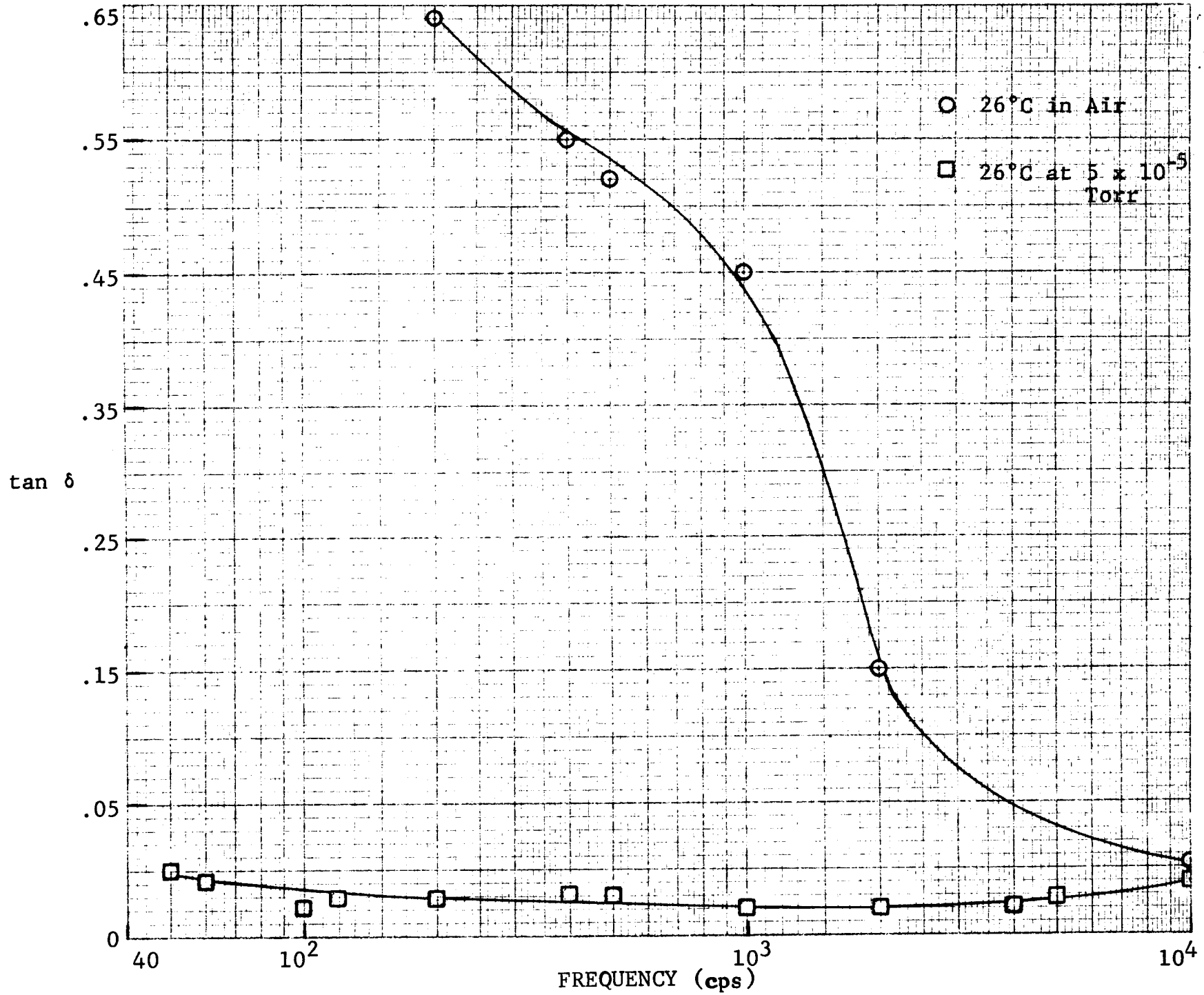

Fig. 29(a) - FREQUENCY DISPERSION OF TAN δ
SAMPLE D1 (COLD COMPACTED)

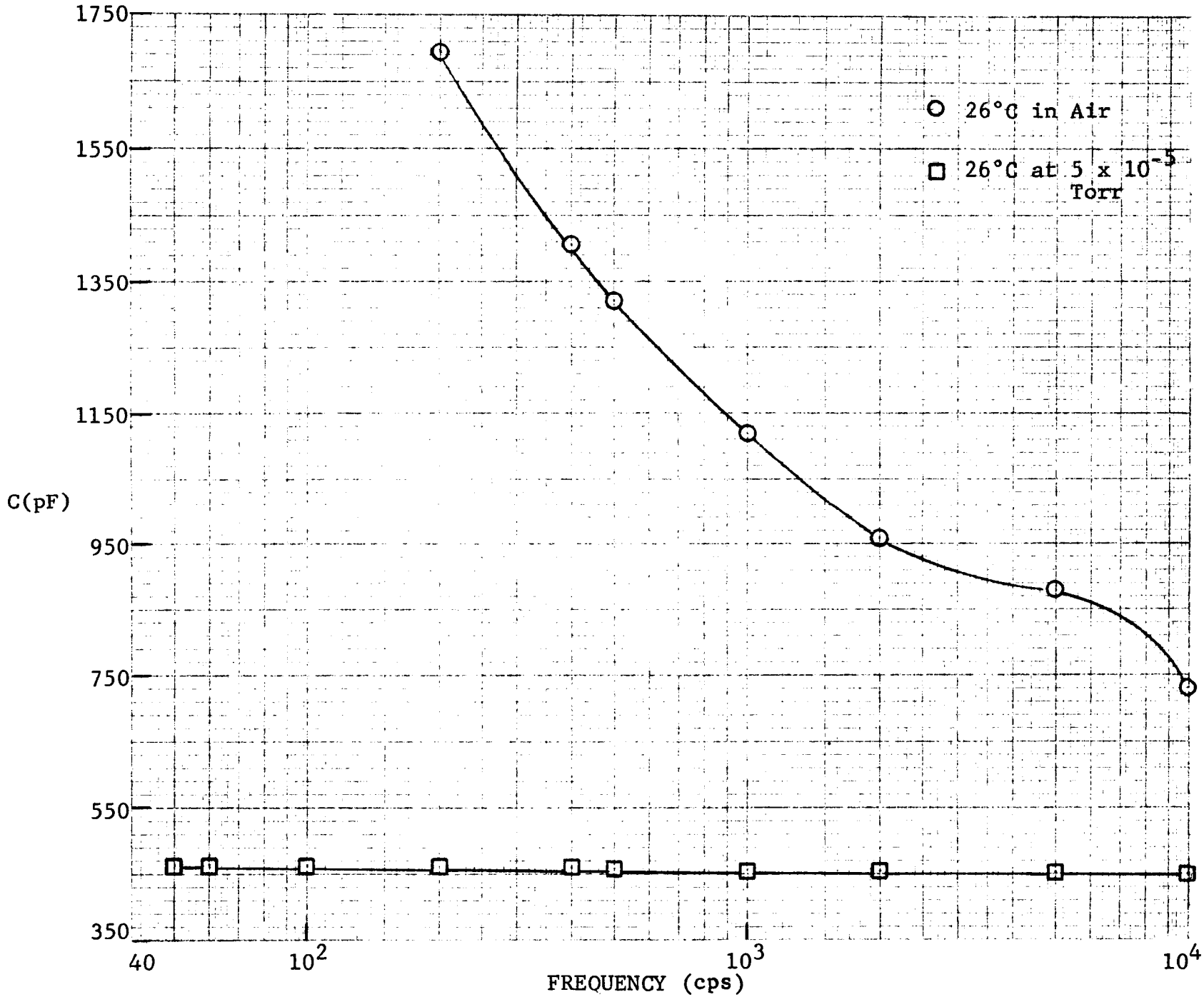

Fig. 29(b) - FREQUENCY DISPERSION OF CAPACITANCE C
SAMPLE D1 (COLD COMPACTED)

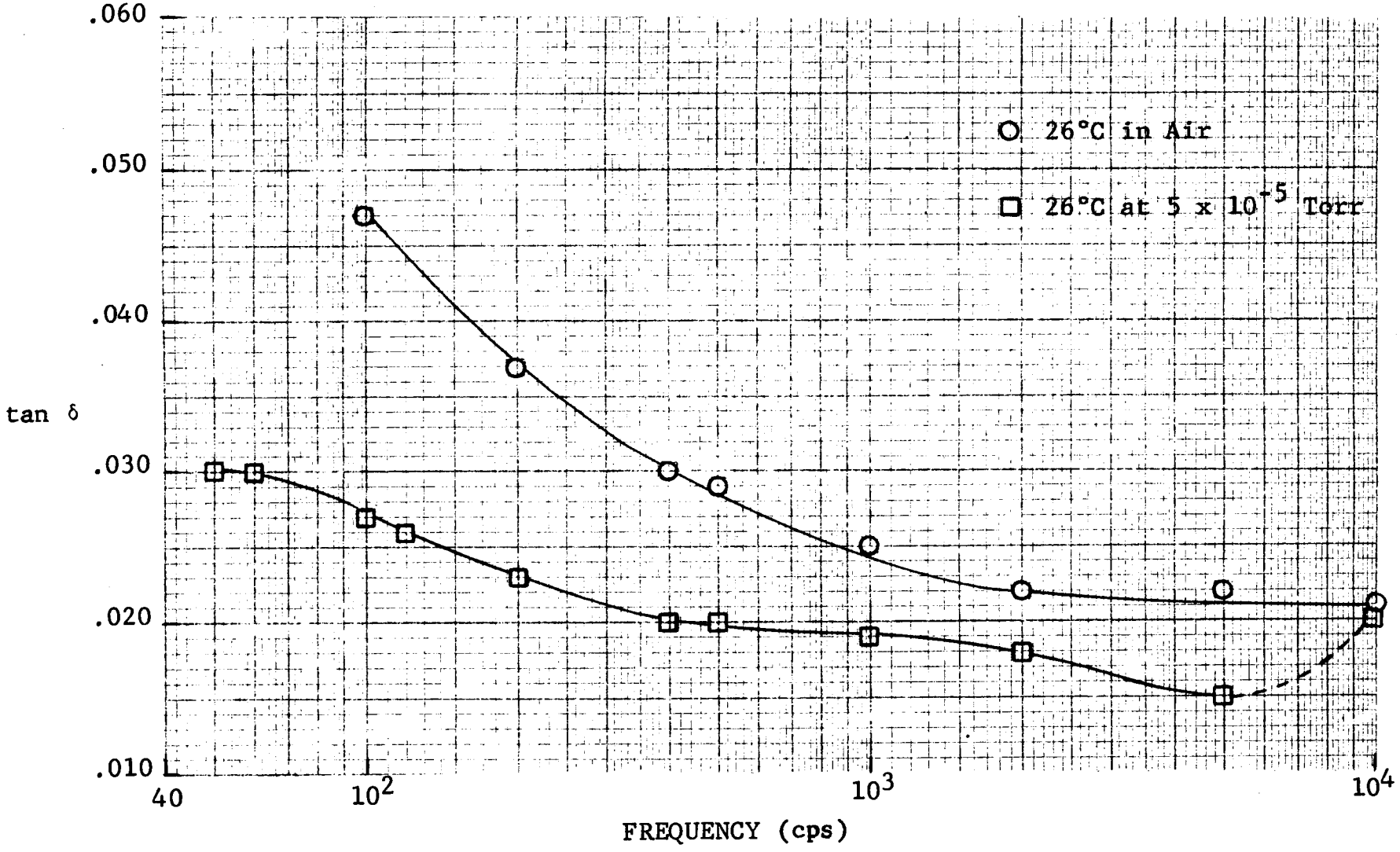

Fig. 30(a) - FREQUENCY DISPERSION OF TAN δ
SAMPLE D2 (SINT. 1250°C)

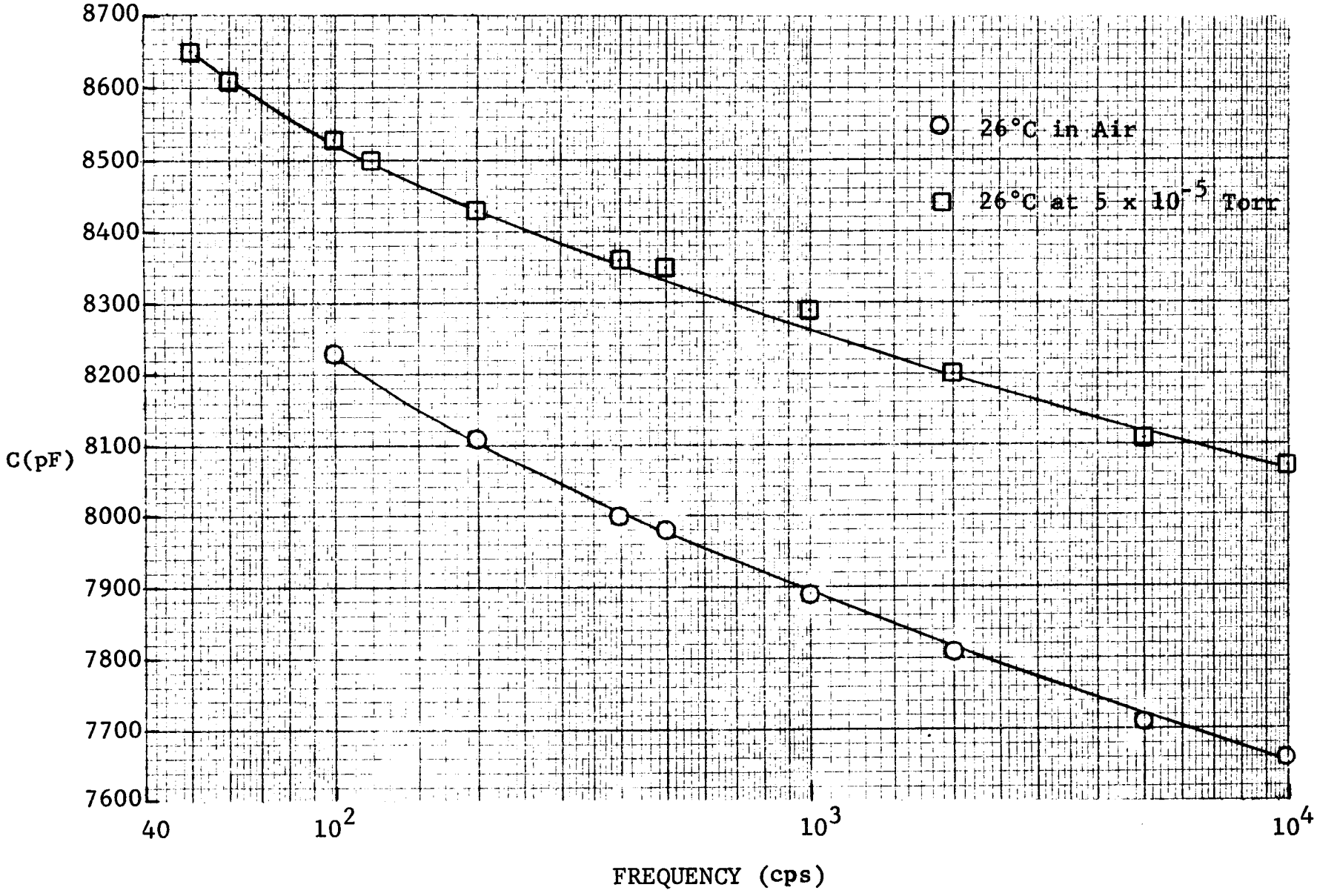

Fig. 30(b) - FREQUENCY DISPERSION OF CAPACITANCE C
SAMPLE D2 (SINT. 1250°C)

However, the dense sintered $BaTiO_3$ sample (D2) did not show as significant a change in its dielectric properties after storage under vacuum and on exposure to air. This is shown in Fig. 30. Its ac conductivity in vacuum and on prolonged exposure to air was found to be 1.5×10^{-8} mho-cm and 1.8×10^{-8} mho-cm, respectively, at 1 kc.

It should be noted that the specimens measured under vacuum, did not regain the K' and tan δ values of the exposed specimens, when air was let into the vacuum system even after 2 to 3 hours exposure. This indicates that the dielectric loss was independent of the oxidizing atmosphere, as no change in properties was observed on introducing air into the system. The controlling factor seems to be the partial pressure of water vapor.

The results indicate that these effects are due to a slow adsorption type process, confined to the surface or one that diffuses into the lattice very slowly. The fact that the effect is significant for the porous specimens and not for the sintered ones, may be due to the large surface-to-volume ratio of the former type of specimens, and to the penetration by water in depth.

The controlling mechanism(s) is probably not confined to the formation of surface (OH) groups. Such a defect would result in the formation of a high resistivity depletion layer. The probable mechanism seems to be an anodic type process where the migrating species are protons $(H)^+$ injected from the adsorbed water film. This results in the reduction of Ti^{+4} to Ti^{+3} ions. The injection of the protons would bring along electrons to maintain electroneutrality. These electrons would be in localized orbitals of the Ti^{+4} ions, near the $(OH)^-$ group and bonded to them by small energies of about 0. 1 to 0.2 ev. Only a small thermal activation is needed to move these electrons into the narrow 3d-conduction band. This results in an increase in the carrier concentration and conductivity of the material. Our results in vacuum and on prolonged exposure to the atmosphere for porous $BaTiO_3$

samples, does indicate such an increase in the ac conductivity.

Data on the change in the dielectric properties as a function of the partial pressure of water-vapor could further elucidate the kinetics of the controlling mechanism. For instance, a $p_{H_2O}^{1/3}$ dependence of σ would indicate that three species are produced from H_2O sorption. Measurements of dc conductivity in vacuum and in air will be carried out to further characterize the nature of the surface layers.

The results on the effects of water-vapor on the dielectric properties of $BaTiO_3$ are important to the processing and performance of microcapacitors. The porosity in some of these microcapacitors, along with the reduced thickness, would make the adsorbed surface layer effects very significant.

The results on the frequency dispersion of the dielectric constant, loss tangent and resistivity of powder compacts and sintered $BaTiO_3$ ceramics, enables us to obtain a more realistic check on the applicability of the equivalent circuit model.

From the dispersion relationships shown in Fig. 19, one obtains the following:

$$\frac{\epsilon - \epsilon_\infty}{\sigma - \sigma_\infty} = - \frac{(\epsilon_s - \epsilon_\infty)}{(\sigma_\infty - \sigma_s)} \quad , \text{ and } \epsilon = - \sigma \frac{\epsilon_s - \epsilon_\infty}{\sigma_\infty - \sigma_o} + C$$

with

$$C = \epsilon_\infty - \sigma_\infty \left(\frac{\epsilon_s - \epsilon_\infty}{\sigma_\infty - \sigma_s}\right) ;$$

it follows:

$$\left(\frac{d\epsilon}{d\sigma}\right)_f = - \frac{(\epsilon_s - \epsilon_\infty)}{(\sigma_\infty - \sigma_s)}$$

or, with the relaxation time

$$\tau = \frac{1}{4\pi} \frac{\epsilon_s - \epsilon_\infty}{\sigma_\infty - \sigma_o}$$

$$\left(\frac{d\epsilon}{d\sigma}\right)_f = - 4\pi\tau$$

This means that the effective dielectric constant ϵ and the effective conductivity σ must be linearly related; the slope of this relationship represents the relaxation time τ.

The relationships between the effective dielectric constant (K') and the ac conductivity (σ), for the porous, cold-compacted sample D1 and the sintered sample D2, under various environmental conditions, have been shown in Figs. 31 to 33. The ac conductivities were calculated from the measured values of parallel capacitance (C_p) and the loss tangent (tan δ).

Figure 31 shows the relationship between K' and σ, in air, for sample D1, as a function of temperature. The plot at 26°C has two distinct slopes, at high frequency and low frequency. As the temperature is increased to 45° and 70°C, the plots tend towards a single linearity and one distinct slope. In contrast, the relationship between K' and σ, at 26°C, in vacuum, is linear over the entire measured frequency range and significantly different from that in air. This is shown in Fig. 32.

Figure 33 shows the plots for K' vs σ for the sintered sample D2, under vacuum and exposure to air, at 26°C.

The relaxation times (τ) calculated from the plots of K' and σ are as follows:

Sample #	Atmosphere	T°C	Relaxation Time (τ) (secs)
D1' (Cold Compacted)	Exposed to Air	26	4.2×10^{-4} (low f); 1.5×10^{-5} (high f)
	" "	45	9.1×10^{-5}
	" "	70	1.8×10^{-4}
	Vacuum	26	2.7×10^{-5}
D2 (Sint. at 1250°C)	Exposed to Air	26	5.9×10^{-5}
	Vacuum	26	(3.5×10^{-5})

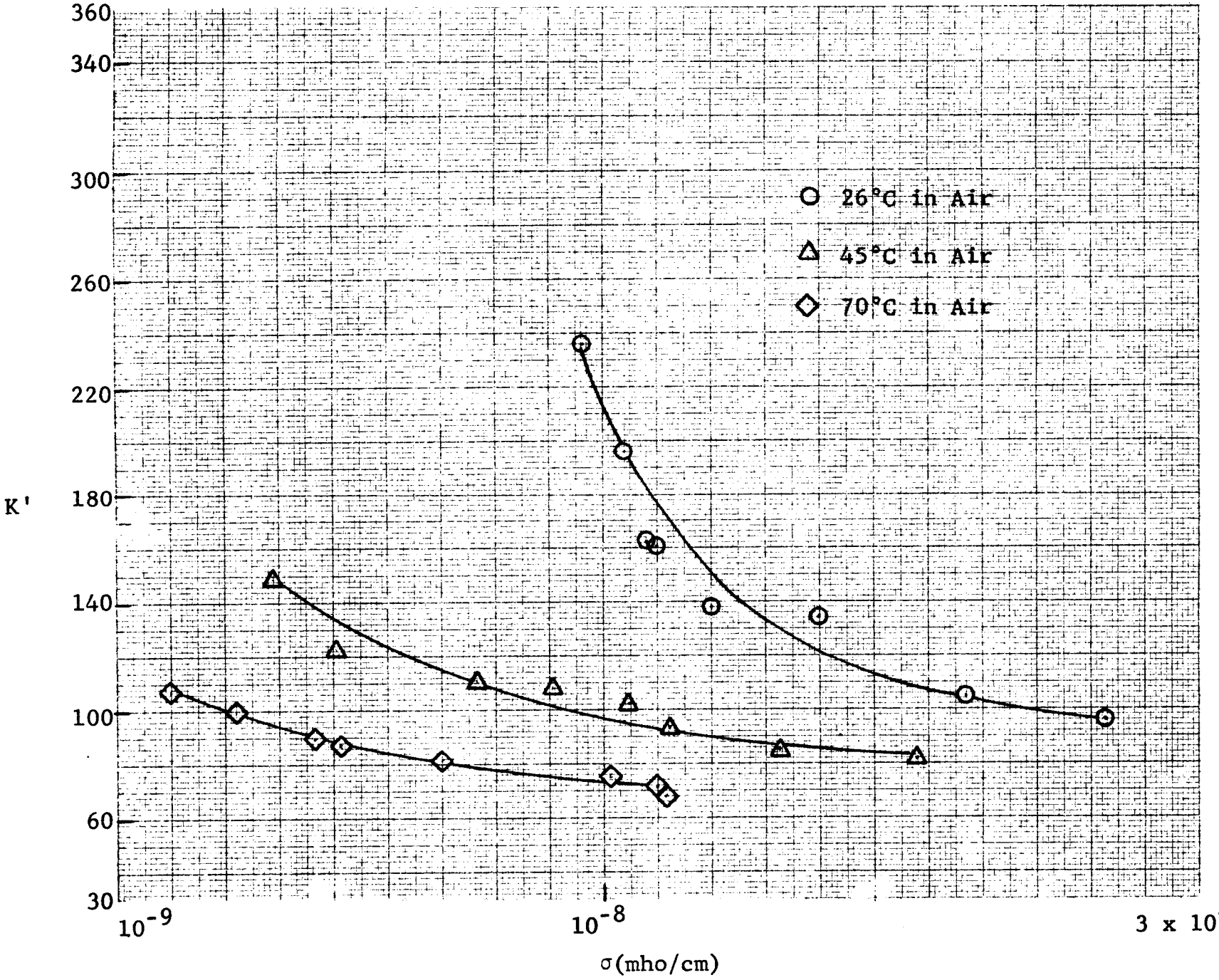

Fig. 31 - RELATIVE DIELECTRIC CONSTANT K' VS ELECTRICAL CONDUCTIVITY σ - SAMPLE D1' (COLD COMPACTED)

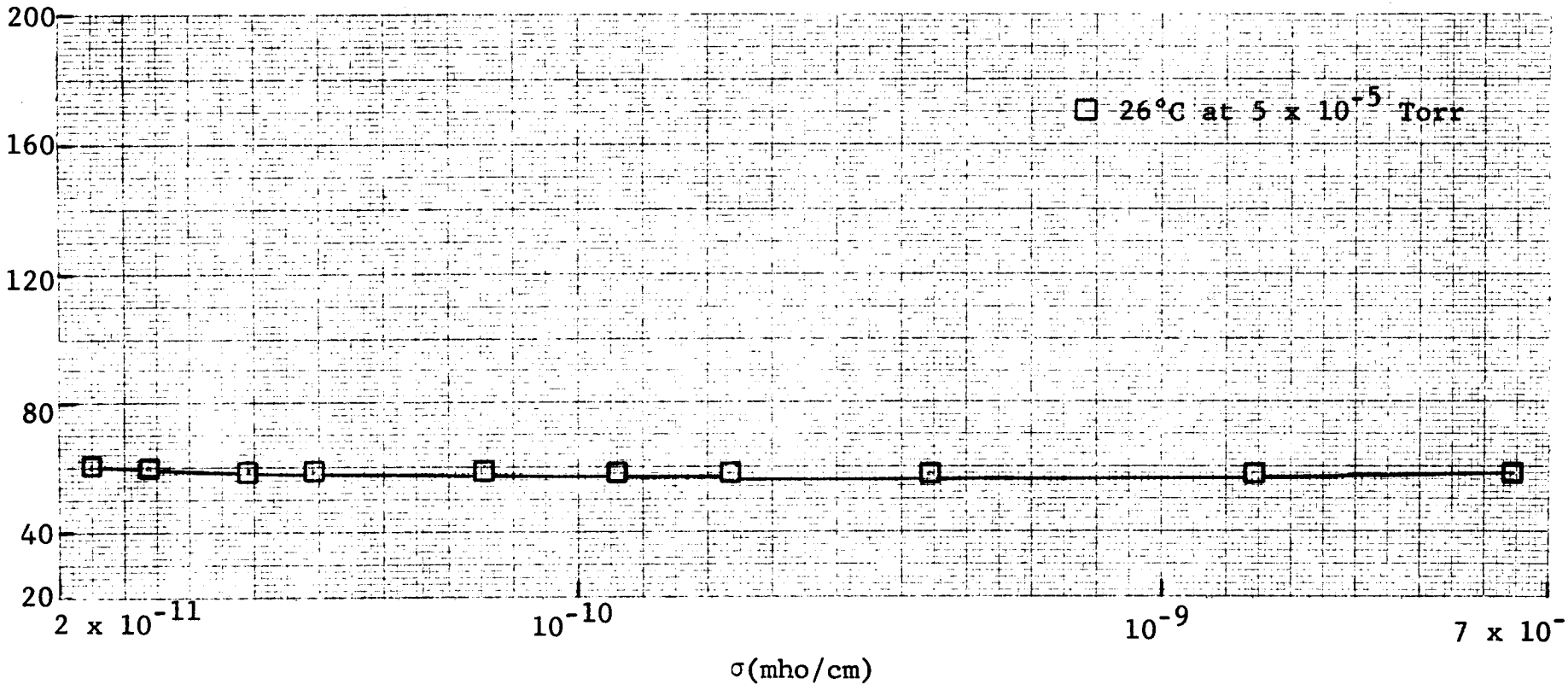

Fig. 32 - RELATIVE DIELECTRIC CONSTANT K' VS ELECTRICAL CONDUCTIVITY σ - SAMPLE D1' (COLD COMPACTED)

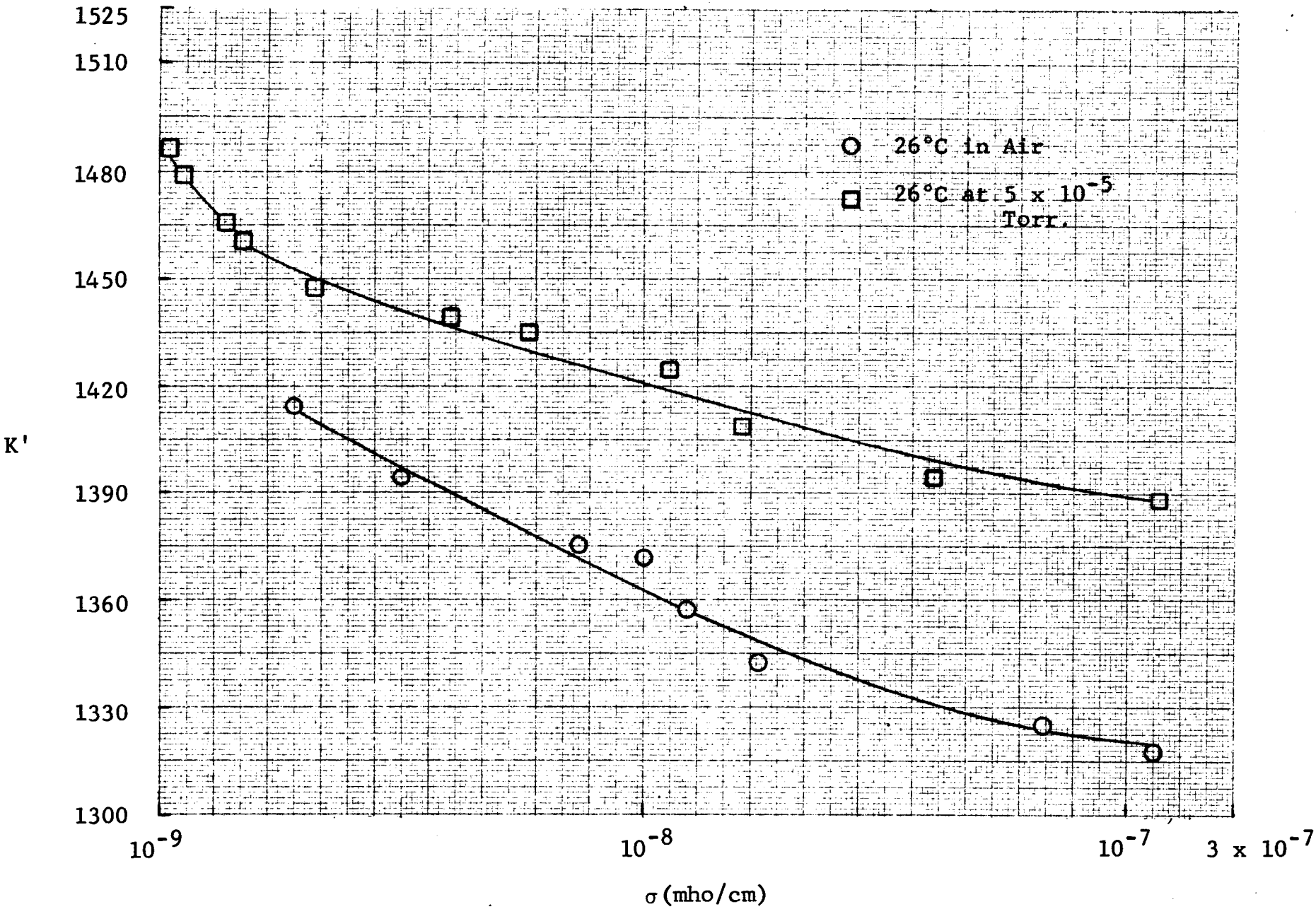

Fig. 33 - RELATIVE DIELECTRIC CONSTANT K' VS ELECTRICAL CONDUCTIVITY σ - SAMPLE D2 (SINT. 1250°C)

The results indicate a distribution of relaxation times, rather than an unique, single value. The changes in the relaxation time is due to the variations in conduction in the surface layer due to the adsorption and desorption of gases at surfaces. The relaxation times, obtained under dc conditions, must also be considered.

In order to study the dielectric characteristics of $BaTiO_3$ specimens under dc conditions, preliminary experiments have been carried out. In these experiments, the electrical response of the specimens to a voltage gate was measured. This provides an independent time constant measurement of the equivalent circuit, used to identify the grain and grain-boundary regions.

In these measurements, a battery, switch, and oscilloscope were connected in series. The switch was a mercury-wetted relay, triggered by the main sweep gate output of a Tektronic 545 oscilloscope and operated in a single sweep mode. The oscilloscope then displayed the voltage developed across its input impedance, which was 10^6 ohms shunted by about 100 pF (including cable capacitance). Considering the specimen as a resistor and capacitor in parallel, the experimental circuit then was:

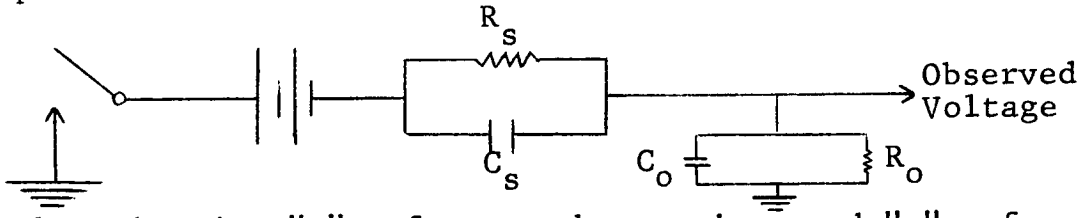

where the subscript "s" refers to the specimen and "o" refers to the oscilloscope. The instrumental time constant for this circuit is:

$$\tau_i = \frac{R_s R_o}{R_s + R_o} \quad (C_s + C_o)$$

which is usually much shorter than the specimen conductivity time constant, as given by Volger[2], i.e.

$$\tau_\sigma = \epsilon_o \frac{\epsilon_1 d_2 + \epsilon_2 d_1}{\sigma_1 d_2 + \sigma_2 d_1}$$

where subscript "1" refers to the grains and subscript "2" to the interface region between grains. (τ_i and τ_σ are actually identical, mathematically, since the experimental arrangement shown above is a realization of the network used to describe the specimens.)

The observed oscilloscope display is resolvable into the sum of two exponential decays, the first being the instrumental decay and the second reflecting the specimen time constant. This can be represented as follows:

$$V = Ae^{-t/\tau_i} + Be^{-t/\tau_\sigma}$$

The component representing the specimen is:

$$V' = Be^{-t/\tau_\sigma}$$

or

$$\ln V' = \ln B - \frac{t}{\tau_\sigma}$$

Therefore,

$$\tau_\sigma = \frac{-\Delta t}{\Delta \ln V'}$$

This means that, from the slope of the decay curve (representing the sample), it is possible to calculate the relaxation time, τ_σ.

Figures 34 to 36 show the dc charging curves for $BaTiO_3$ samples, prepared from material D and obtained on the oscilloscope. The samples were exposed to the atmosphere prior to and during evaluation. In all the oscilloscope traces, the horizontal scale represents time (each large division equals 20 milli sec), and the vertical scale represents the voltage. In Figs. 34a, 34b, 36a and 36b, each large division on the vertical scale represents 0.2 volts, while in Figs. 34c, 35a and 35b, it represents 0.05 volts.

The observed oscilloscope traces, as shown in Figs. 34 to 36 were magnified to obtain the exact values on the decay curve. From this we have calculated the relaxation time constant (τ_σ) for the specimens, it being the reciprocal of the slope of the specimen decay curve. In future experiments, the decay curve will be obtained for longer times, so as to obtain a more exact value for the relaxation time constants.

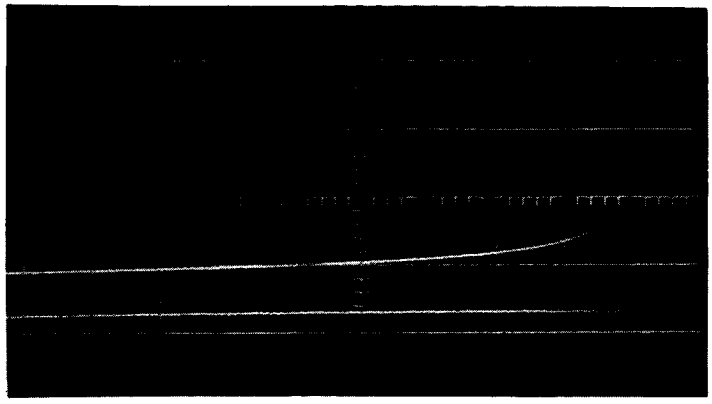

(a) Virgin Sample

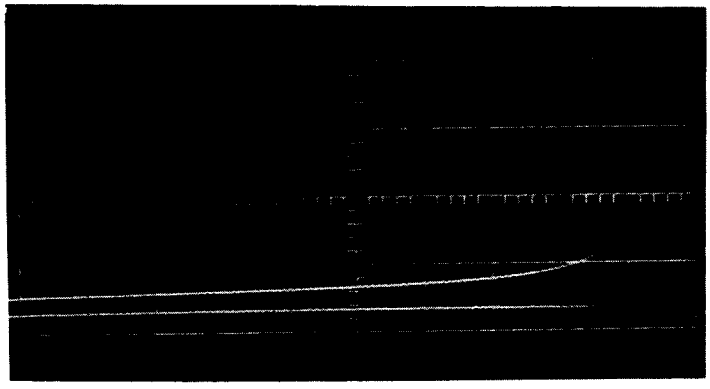

(b) Sample Shorted Before Run

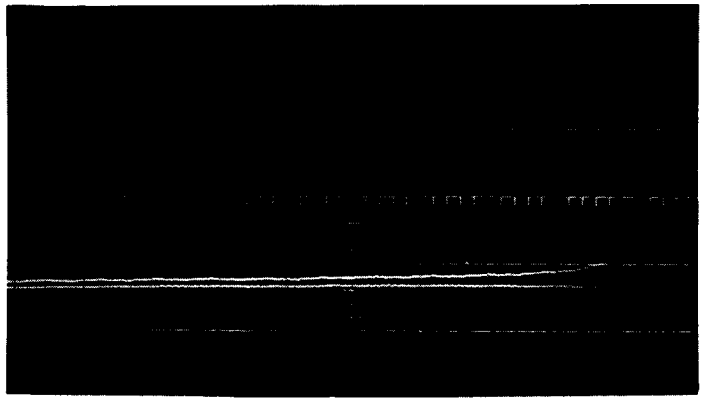

(c) Voltage Applied Ten Times Before Run

Fig. 34 - CHARGING CURVES (DC) FOR $BaTiO_3$ SAMPLE D1 (COLD COMPACTED)

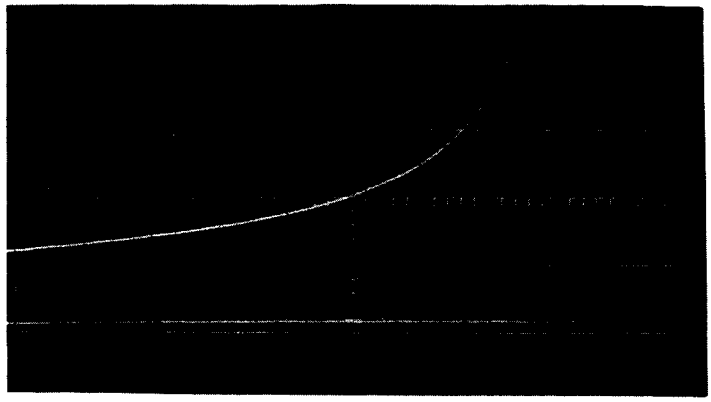

(a) Sample Shorted Before Run

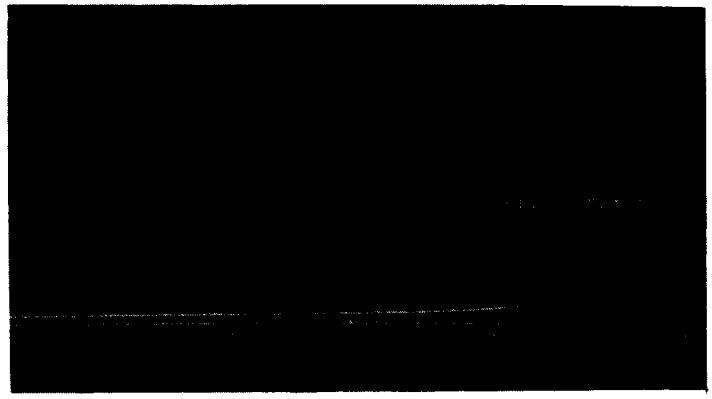

(b) Voltage Applied Ten Times Before Run

Fig. 35 - CHARGING CURVES (DC) FOR $BaTiO_3$ SAMPLE D2 (SINT. 1250°C)

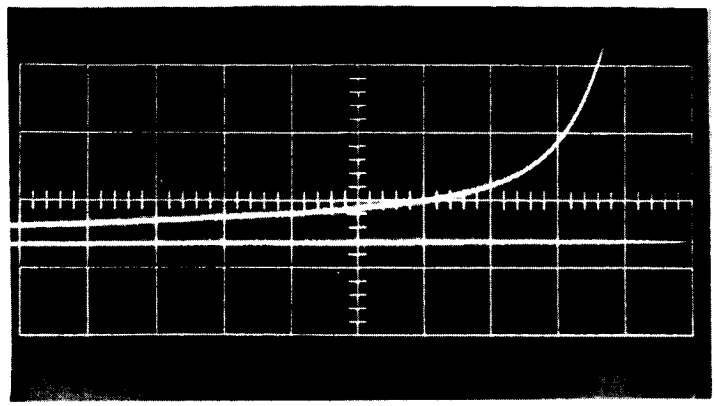

(a) Sample Shorted Before Run

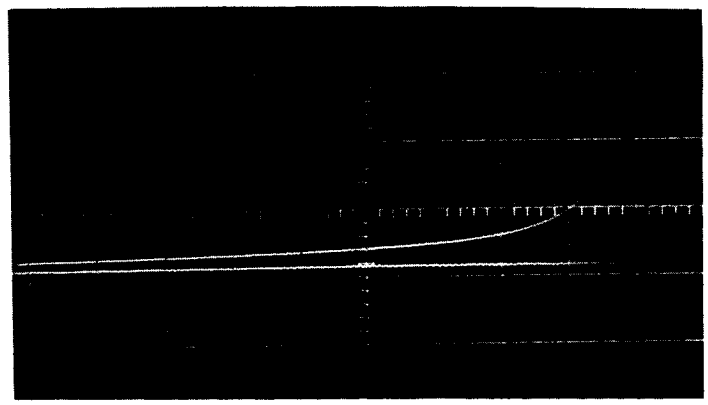

(b) Voltage Applied Ten Times Before Run

Fig. 36 - CHARGING CURVES (DC) FOR $BaTiO_3$ SAMPLE D3 (SINT. 1320°C)

The relaxation time constant (τ_σ) has been obtained, in air, for the samples, where the voltage was applied ten times before the run. The results are as follows:

Sample #	Relaxation Time (τ_σ) (secs)
D1 (Cold-Compacted)	~ 0.73
D2 (Sint. at 1250°C)	~ 0.44
D3 (Sint. at 1320°C)	~ 0.17

The data indicates that the relaxation time constant, τ_σ, decreases as the state of packing and bonding of the samples increases, as shown above.

These relaxation time values are for $BaTiO_3$ samples, exposed to the atmosphere and, therefore, the effects of adsorbed (OH) groups must be taken into consideration along with dc conduction losses. The very high values for τ, are characteristic of hindered molecular rotation, such as that of (OH) groups. The dc charging curves under vacuum will be obtained in a later phase of our program.

The dc results indicate that the cold-compacted specimen, D-1, which has the highest tan δ value under ac measurements, has the least dc loss. Also, the ratio of the resistances of the surface layer to that of the grain, is higher in the cold-compacted specimen (D-1) than in the sintered ones (D-2, D-3), under dc conditions. However, these deductions are based on our preliminary results. Further evaluation of the dielectric behavior of $BaTiO_3$ under dc conditions will be done to substantiate these results.

In order to fully understand the dielectric characteristics of the boundary phase and the bulk phase, measurements should be carried out under dc and ac conditions. The distinct differences in the values of K' and σ, for the bulk and boundary phases in $BaTiO_3$, would produce an accumulation of charge at the phase interfaces, when a field is applied, resulting in a net polarization.

However, if both phases have an unequal but high resistivity, the loss associated with the relaxation of this polarization would be observed only at very low frequencies. If one of the phases is comparitively conductive and the other is not, then the loss mechanism would be observed in the rf range. We have seen how varying degrees of compaction and bonding alter the surface layer characteristics due to adsorption processes, thereby superimposing the loss mechanisms due to these complex defects on the intrinsic characteristics of the boundary phase.

The equivalent circuit used to characterize the ceramic consisting of a capacitance (C_v) and parallel resistance (R_v) representing the grain, in series with a capacitance (C_b) and parallel resistance (R_b) representing the grain-boundary, is

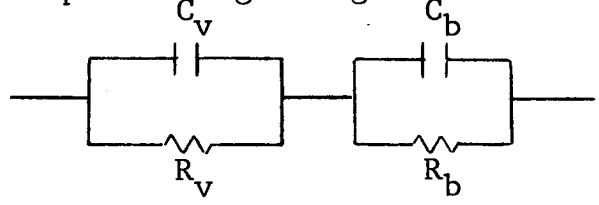

This should be modified, to account for adsorbed surface layer properties, due to exposure to specific atmospheres, by a shunt resistance (R_s) which may well be frequency dependent, affected by the nature of the adsorbed species and the complex defects formed therein. The modified equivalent circuit would now be

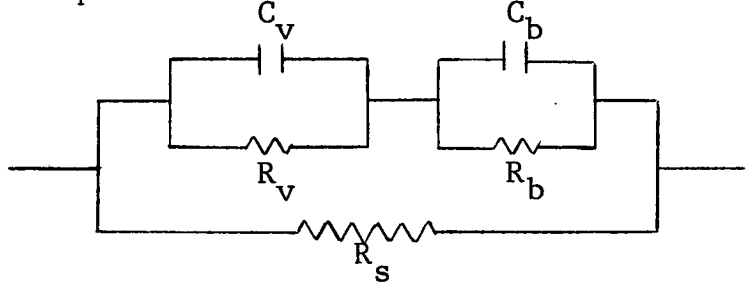

Further experimental results will substantiate the extent to which the equivalent circuit model is applicable. Its applicability, will give valuable information regarding the nature of the boundary layer and of the processes which result in energy dissipation, and simplify the interpretation of the dielectric properties of a ceramic for device applications.

VI. LOGBOOK RECORDS

All data pertaining to work done in this period are recorded in IITRI logbooks C 16491, C 16498 and C 16499.

VII. PERSONNEL

Major contributions to this report were made by S. L. Blum, A. J. Mountvala, A. G. Pincus and G. A. Rubin.

Respectfully submitted,

IIT RESEARCH INSTITUTE

A. J. Mountvala

A. J. Mountvala
Senior Scientist
Ceramics Research

APPROVED BY:

S. L. Blum
Director
Ceramics Research

ACKNOWLEDGEMENTS

This work was sponsored by the National Aeronautics and Space Administration, Langley Research Center, Hampton, Virginia, under NASA Contract NAS 1-4870.

REFERENCES

1. Jona, F. and Shirane, G., Ferroelectric Crystals, MacMillan: New York (1962).
2. Volger, J., Progress in Semiconductors, Vol. 4, Ed. by A. F. Gibson, Heywood:London (1960) pp. 206-36.
3. Marntake, M., J. Phys. Soc. Japan 11 807 (1956).
4. Marntake, M., Ibid. 11 814 (1956).
5. Bruggeman, D. A. G., Z. Phys. 92 561 (1934).
6. Bruggeman, D. A. G., Ann. D. Phys. 24 636 (1935).
7. Rushman, D. F. and Strivens, M. A., Proc. Phys. Soc. (London) 59 1011 (1947).
8. Stadelmaier, H. H., Contribution to Materials Science Research, Vol. V, Plenum:New York, in print.
9. Kanzig, W., Phys. Rev. 98 549 (1955).
10. Subbarao, E. C., McQuarrie, M. C. and Buessen, W. R., J. Appl. Phys. 28 1194 (1957).
11. Fatuzzo, E. and Merz, W. J., J. Appl. Phys. 32 1685 (1961).
12. Merz, W. J., J. Appl. Phys. 27 938 (1956).
13. Drougard, M. E. and Landauer, R., J. Appl. Phys. 30 1663 (1959).
14. Kniepkamp, H. and Heywang, W., Z. Angew, Physit. 6 410 (1954).
15. Minomura, S., Jap. J. Appl. Phys. 3 562 (1964).
16. Jonker, G. H. and Noorlander, W., Science of Ceramics, Vol. 1, Academic:New York (1962) p. 255.
17. Gerthsen, P. and Hardtl, K. H., Z. Naturforsch 18a 423 (1963).
18. Stadelmaier, H. H. and Derbyshire, S. W., Materials Science Research, Vol. I, Plenum:New York (1963) pp. 57-65.
19. Frohlich, H., Theory of Dielectrics, Clarendon:Oxford (1949).
20. Fricke, H., J. Phys. Chem. 57 934 (1953).
21. Reimerov, L. I., Soviet Phys.-Tech. Phys. 4 229 (1959).

22. Muller, R. K., J. Appl. Phys. 30 546 (1959).

23. Abe, R., Jap. J. Appl. Phys. 3 243 (1964).

24. Heywang, W., J. Am. Ceram. Soc. 47 484 (1964).

25. Heywang, W., Z. Naturforsch 20a 981 (1965).

26. Anliker, M., Brugger, H. R., and Känzig, W., Helv. Phys. Acta 27 99 (1954).

27. Schoijet, M., Brit. J. Appl. Phys. 15 719 (1964).

28. Saburi, O., J. Phys. Soc. Jap. 14 1159 (1959).

29. Carnahan, R. D. and Brittain, J. O., J. Am. Ceram. Soc. 48 365 (1965).

30. Rase, D. E. and Roy, R., J. Am. Ceram. Soc. 38 102 (1955).

31. Hellicar, N. J. and Parnell, M. W., "Controlling Mechanisms in Reduced - Reoxidized Ceramic Capacitors," Presented at Conf. on Dielectric and Insulating Materials, (May 1964).

32. Gruver, R. M., Buessen, W. R., Dickey, C. W., et al., "State-of-the-Art Review on Ferroelectric Ceramic Materials," Technical Report AFML-TR-66-164, (May 1966).

33. Brandmayr, R. J. et al., "Evaluation of Fine Particle $BaTiO_3$ Prepared from Alcoholic Solution," USAERDL Tech. Report 2326 (Jan. 1963).

NASA CR-66253

DISTRIBUTION LIST

NAS1-4870

	Copies
NASA Langley Research Center Langley Station Hampton, Virginia 23365	
Attention: Contracting Officer, Mail Stop 126	1
Charles H. Husson, Mail Stop 470	25
Library, Mail Stop 185	1
R. L. Zavasky, Mail Stop 117	1
NASA Ames Research Center Moffett Field, California 94035	
Attention: Library	1
Thomas Fryer	1
NASA Flight Research Center P. O. Box 273 Edwards, California 93523	
Attention: Library	1
D. Veatch	1
NASA Goddard Space Flight Center Greenbelt, Maryland 20771	
Attention: Library	1
A. Franta, Code 722	1
Jet Propulsion Laboratory 4800 Oak Grove Drive Pasadena. California 91103	
Attention: Library	1
B. Martin	1
NASA Manned Spacecraft Center Houston, Texas 77001	
Attention: Library	1
Ralph S. Sawyer, Code EE	1
D. Hickman	1
NASA Marshall Space Flight Center Huntsville, Alabama 35812	
Attention: Library	1
R. E. Currie, Jr.	1
D. Anderson	1
Alvin Holliday	1
NASA Western Operations 150 Pico Boulevard Santa Monica, California 90406	
Attention: Library	1

NASA CR-66253

DISTRIBUTION LIST

NAS1-4870

	Copies
NASA Wallops Station Wallops Island, Virginia 23337 Attention: Library	1
NASA Electronics Research Center 575 Technology Square Cambridge, Massachusetts 02139 Attention: Library W. C. Dunlap	1 2
NASA Lewis Research Center 2100 Brookpark Road Cleveland, Ohio 44135 Attention: Library, Mail Stop 3-7 John Sturman	1 1
NASA John F. Kennedy Space Center Kennedy Space Center, Florida 32899 Attention: Code ATS-132	1
NASA Michoud Assembly Facility P. O. Box 26078 New Orleans, Louisiana 70126 Attention: Mr. Henry Quintin, Code I-Mich-D	1
Franz Huber Defense Microelectronics RCA Defense Electronic Products Somerville, New Jersey 08876	1
Howard Martin, Mail Stop 415 Texas Instruments, Inc. P. O. Box 5303 Dallas, Texas 75222	1
Harold Sullivan, Secretary Advisory Group on Electron Devices Law Power Devices 346 Broadway, 8th Floor New York, New York 10013	1
National Aeronautics and Space Administration Washington, D. C. 20546 Attention: Library, Code USS-10 George Deustch, Code RRM James J. Gangler, Code RRM Robert Nash, Code RRM	1 1 1 1
NASA Scientific and Technical Information Facility P. O. Box 33 College Park, Maryland 20740	40 plus repro.